

https://dspace.org/

The Breakdown Mechanism Of Long Sparks In Air

Kritzinger, John Jacob

2015-05-22
http://hdl.handle.net/10539/17836

Downloaded from a DSpace repository. https://dspace.org/

I hereby declare that the thesis "The Breakdown Mechanism of Long Sparks in Air" is my own work and the work forming the basis of the thesis has not been incorporated in a thesis submitted for another degree.

J. Kotzinger.

THE BREAKDOWN MECHANISM OF LONG SPARKS IN AIR

A THESIS
PRESENTED TO
THE DEPARTMENT OF ELECTRICAL ENGINEERING
IN THE FACULTY OF ENGINEERING
UNIVERSITY OF THE WITWATERSRAND JOHANNESBURG

IN FULFILMENT
OF THE REQUIREMENTS FOR THE DEGREE
DOCTOR OF PHILOSOPHY

BY
JOHAN JACOB KRITZINGER
JANUARY 1962.

Thesis G. 2491

THE BREAKDOWN MECHANISM OF LONG SPARKS IN AIR.

S U M M A R Y

		Page
Chapter I.	INTRODUCTION:	1.
Chapter II.	APPARATUS:	
	2.1 Production of the Required Voltages.	5.
	2.2 Measuring Equipment.	11.
Chapter III.	THE VALIDITY AND MEANING OF THE MEASUREMENTS:	
	3.1 Relation between Ionisation and the Light Produced.	22.
	3.2 Recording of Light.	24.
	3.3 Ionisation Current.	26.
	3.4 Photographs of Ionisation.	27.
Chapter IV.	NOMENCLATURE AND MEASUREMENTS FROM OSCILLOGRAMS:	
	4.1 References to Graphs and Oscillograms.	28.
	4.2 Abbreviations used in the Results.	28.
	4.3 Measurements from Oscillograms.	29.
Chapter V.	CORONA:	
	5.1 Positive Corona.	
	(1) Oscillograms.	30.
	(2) Graphs.	36.
	(3) Summary.	44.
	5.2 Negative Corona.	
	(1) Oscillograms.	44.
	(2) Graphs.	46.
	(3) Slow rise of voltage.	49.
	5.3 Corona Currents.	53.
	5.4 Explanation of the Corona Mechanism.	
	(1) Electron Avalanche.	54.
	(2) Negative Corona.	58.
	(3) Positive Corona.	61.

cont'd....

			Page
	5.4	(4) Corona with a slowly rising voltage.	63.
		(5) Formation of Negative Ions.	63.
		(6) Return Ionisation.	64.
Chapter VI.	BREAKDOWN:		
	6.1	Transition to Breakdown.	65.
	6.2	Positive Breakdown.	66.
		Explanation.	75.
	6.3	Negative Breakdown.	77.
Chapter VII.	CONCLUSIONS:		85.
	References.		
	Graphs.		
	Plates.		

INDEX TO GRAPHS.

I.	G 1 - 3.	Positive Corona 150 kV.
II.	G 4 & 5.	Positive Corona 300 & 600 kV.
	G 6 (a).	Positive Corona size.
	G 6 (b).	Peak Corona Current with 3 μsec rise.
III.	G 7 - 10.	Negative Corona 150 - 600 kV.
IV.	G 11 & 12.	Negative Corona 3 μsec rise.
	G 13.	Peak Corona Currents.
V.	G 14 - 18.	Positive Leader 150 - 600 kV.

INDEX TO PLATES.

	PL 1.	Layout of Laboratory.
	PL 2.	(a) Resistance Divider Termination. (b) Layout in Screened Room.
I.	PL 3 - 5.	Positive Corona
II.	PL 6 - 10.	Negative Corona
III.	PL 11-13.	Positive Breakdown (Oscillograms).
IV.	PL 14-16.	Positive Breakdown (3 μsec rise and Photographic recordings).
V.	PL 17-19.	Negative Breakdown (Oscillograms). 300 & 600 kV.
VI.	PL 20-22.	Negative Breakdown (Oscillograms and Photographic recordings 600 kV).

SUMMARY

This concerns an investigation into the mechanism by which an ionised path is established in a non-uniform air gap to allow the full conduction of current when an impulse voltage is applied.

The effect of the following variables were investigated: polarity, voltage, risetime, electrode size and gap length. The mechanism was found to be basically that of balls of ionisation simultaneously moving into the gap from the smaller electrode, very shortly after the critical gradient had been exceeded. These balls carry a charge with them and the propagation has been shown to be due to photo-ionisation and a localised charge effect with speeds ranging from 1.5×10^7 cm/sec to 8×10^8 cm/sec. The movement is dependent on the variables for its speed, intensity and extent.

If breakdown is to occur the initial ionisation must traverse the gap and reach the opposite electrode with enough energy to be reflected back to the starting point. This up and down movement is continued with increasing intensity until enough electrons and positive ions have been produced to allow full conduction of the current. If the ionisation does not return to the starting point breakdown does not occur.

CHAPTER I.

1. INTRODUCTION:

Initially it is necessary to consider the factors of major importance before a full description of the investigation is started.

(a) The main difficulties are that the time taken for the ionising action before breakdown is in the range 1 - 20 microseconds and the light produced by the ionisation can occur at intensities as low as a hundreth of that recordable with the best photographic means at present available. Hence, if we could obtain a cine camera capable of taking at least 10^8 frames per second with a light sensitivity a hundred times of that presently available, we would be able to record the full process of ionisation. It is also important to obtain as much information as possible from one spark since even if external conditions are identical there can still be considerable time and amplitude differences between consecutive sparks which cause uncertainties in the investigation.

(b) However, since this is not possible at present, it was necessary to turn to other ways and means of obtaining this information. Even the rotating lens camera is of little use as the smallest time differences measurable is just less than 1 μsec. For the measurement of small time differences which are not regular, the oscilloscope leads the field by a long way, since with those presently available, the measurement of time differences of 5 nanoseconds (5×10^{-9} sec.) is possible.

To transform the light variation into an electrical variation for display on an oscilloscope a photomultiplier is the best device since it can transmit time differences of approximately 5 nsec when operated suitably and even for this operation provides a light sensitivity approximately 100 times that photographically recordable [5]. There are, however, certain difficulties to consider. First of all the amplification stability is very sensitive to voltage changes and although the voltages were stabilised, the overall

CHAPTER I.

1. INTRODUCTION:

Initially it is necessary to consider the factors of major importance before a full description of the investigation is started.

(a) The main difficulties are that the time taken for the ionising action before breakdown is in the range 1 - 20 microseconds and the light produced by the ionisation can occur at intensities as low as a hundreth of that recordable with the best photographic means at present available. Hence, if we could obtain a cine camera capable of taking at least 10^8 frames per second with a light sensitivity a hundred times of that presently available, we would be able to record the full process of ionisation. It is also important to obtain as much information as possible from one spark since even if external conditions are identical there can still be considerable time and amplitude differences between consecutive sparks which cause uncertainties in the investigation.

(b) However, since this is not possible at present, it was necessary to turn to other ways and means of obtaining this information. Even the rotating lens camera is of little use as the smallest time differences measurable is just less than 1 μsec. For the measurement of small time differences which are not regular, the oscilloscope leads the field by a long way, since with those presently available, the measurement of time differences of 5 nanoseconds (5×10^{-9} sec.) is possible.

To transform the light variation into an electrical variation for display on an oscilloscope a photomultiplier is the best device since it can transmit time differences of approximately 5 nsec when operated suitably and even for this operation provides a light sensitivity approximately 100 times that photographically recordable [5]. There are, however, certain difficulties to consider. First of all the amplification stability is very sensitive to voltage changes and although the voltages were stabilised, the overall

accuracy in amplitude is probably not better than 20%, but then light amplitude measurements photographically are even less accurate. Secondly, there is the possibility of noise and secondary pulses being generated in the photo-multiplier. By careful checking and comparison it has, however, been shown that these do not occur.

The main limitation is that this technique does not give an overall picture but only shows the light variation with time at a plane, perpendicular to the direction of travel of the ionisation. Although the position of this scanning plane could be altered to cover the whole gap it only allows one recording per applied voltage pulse.

Ideally, a few photo-multiplier and oscilloscope combinations, each scanning at a different level, will enable more accurate results to be taken, but by the use of simultaneous recordings of the ionisation current, photo-multiplier recordings and actual photographs of the ionisation, it has been possible to overcome most of these difficulties.

Propagation speeds are measured by noting the average time from the start until the light reaches the scanning plane. By altering the position of the scanning plane, the speed of propagation across the gap can be obtained.

(c) The most basic requirement for this investigation was a voltage pulse of the required shape and amplitude. Ideally, a pulse is required with an infinitely short risetime and subsequently a constant amplitude in order that the ionisation can take place under constant voltage conditions.

The apparatus supplying this pulse was 1 M.V. impulse generator and due to practical limitations the normal risetime was .25 μsec with a decay time to half value of 100 μsec. For the lower voltages a risetime of .07 μsec was obtainable which allowed conditions to be used where the voltage had reached the maximum before the ionisation started.

(d) The following are the controlled variables which were combined in such a way as to show the importance and influence of each.

(1) POLARITY:	Positive and negative.
(2) VOLTAGE:	150, 300 and 600 kV.
(3) RISETIME:	.07, .25, 3.0 μsec.
(4) ELECTRODE SIZE AND SHAPE:	Point, ½", 2" and 5" diameter sphere.
(5) GAP LENGTH:	8 - 120 cm.

The variables which could not be controlled but were measured and stayed approximately constant through the investigation are given in table 1.

UNCONTROLLED VARIABLES

Table 1.

Voltage kV.	Barometric Pressure inches-Hg.	Temperature °K.	Humidity %.
150	24.65	290	30
300	24.65	295	25
600	24.65	298	25

Extremes:

	Max.	Min.
Barometric pressure	24.81 "Hg.	24.50 "Hg.
Temperature	301 °K.	286 °K.
Humidity	45%.	20%.

(e) The non-uniform field distribution was used because the ionisation starts at the point of highest stress and thus the start was always at the point, growing across towards the plane. In addition, the speeds of growth are slower than in a uniform field and the effect of polarity on the propagation is brought out.

(f) The results are divided into two groups, the first dealing with

CORONA:

This is considered as the growth of ionisation into air that is free from existing ionisation. This process determines whether breakdown is going to occur or not.

and the second,

IONISATION LEADING TO BREAKDOWN:

This is ionisation occurring along previously ionised paths and which by consecutively travelling along the same path produce enough electrons and positive ions to allow the full conduction of current.

In both cases a division is made between positive and negative polarities since the speeds, amplitudes and extent of ionisation are different although the basic propagation mechanism is the same.

CHAPTER II.

APPARATUS

2.1. PRODUCTION OF THE REQUIRED VOLTAGES:

2.1.1. Impulse Generator

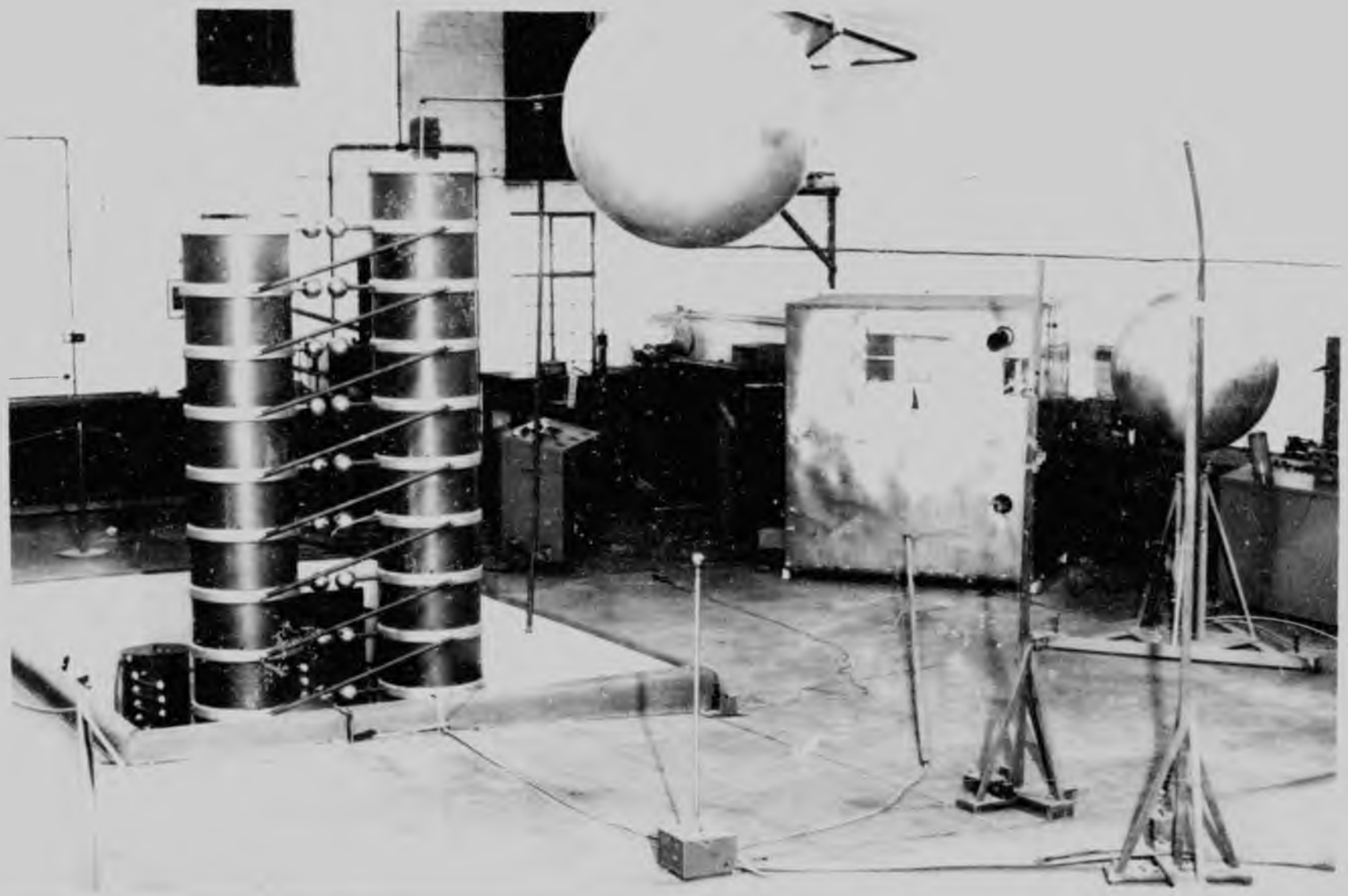
The 1 million volt Marx type Impulse Generator used for the investigation consisted of twelve condenser sections, each with a capacitance of .055 microfarad giving a total output capacitance of .0045 microfarad and maximum energy of 2.25 kilojoules. The layout of the equipment as used for the investigation is shown in figures 1 and 2 and also by the photograph. (PL.1)

For the production of the 600 kV voltage, the impulse generator was used normally but for the 150 kV and 300 kV voltages a series parallel connection was used in which the condensers were paralleled in pairs, thus giving six stages. These connections are shown in figures 3 and 4 (D .2) respectively.

The reason for the latter connection was that the output capacitance is increased four times while the voltage is still sufficient and hence much lower resistances, giving faster rise-times, could be used without causing an undesirably short decay time. The resistance R is a 120 kΩ resistance forming part of the impulse generator charging circuit, but which has to withstand the full output voltage.

2.1.2. Oscillations and Waveshape

One of the main difficulties in producing a voltage with a short rise-time is that overshoot occurs causing oscillations on the voltage wave. Normally these oscillations are damped out by an $R_s C_{sh}$ circuit which is required to give the standard rise-time of 1 μsec. The steepest rise (.1 - .2 μsec.) was obtained from the impulse generator when the series resistance and the shunt capacitance was a minimum; however, for this condition the overshoot was as high as 50 - 80% which could not be used for the investigation.



PL. I.

LAYOUT OF EQUIPMENT. D.I.

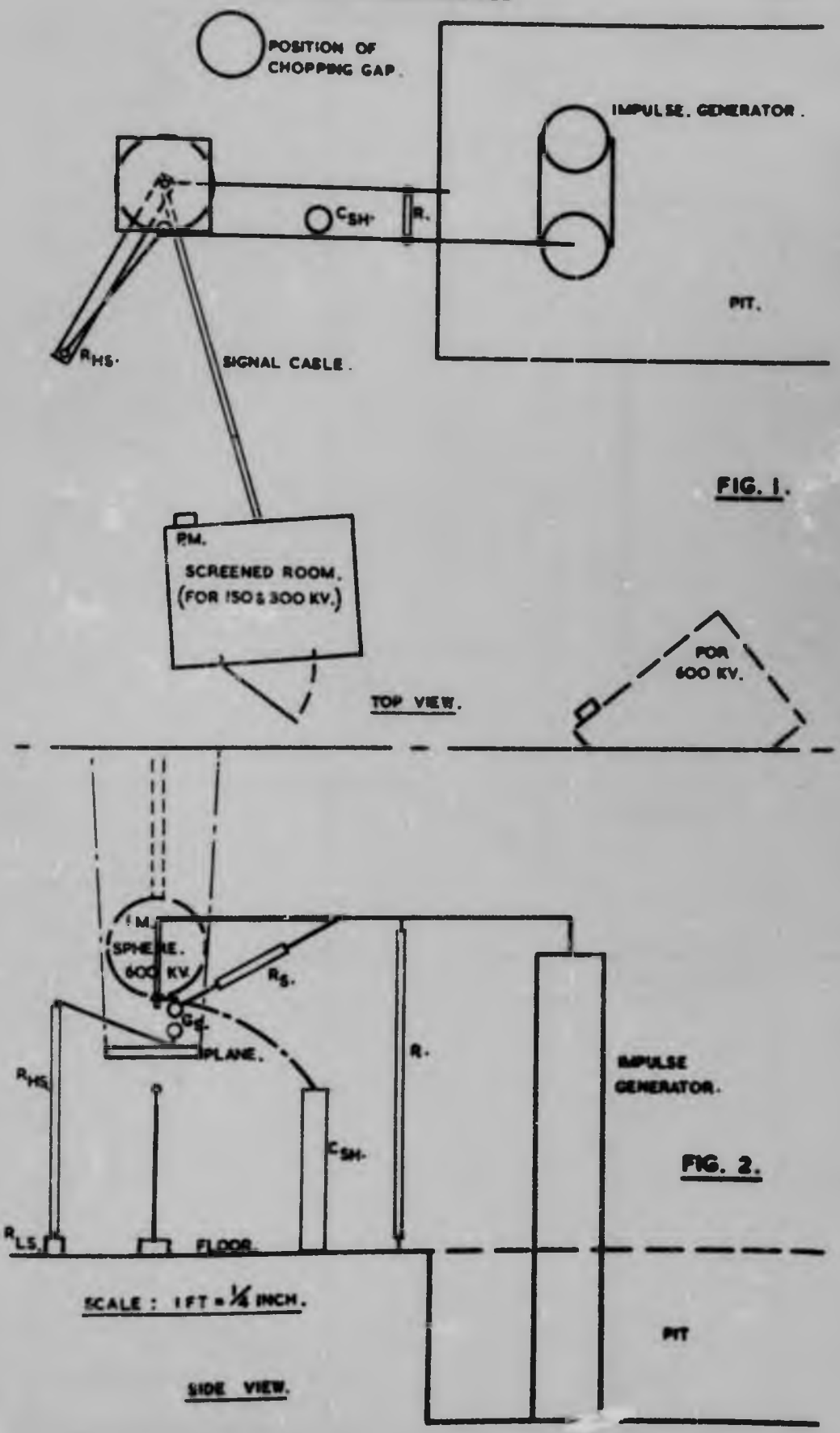


FIG. 1.

FIG. 2.

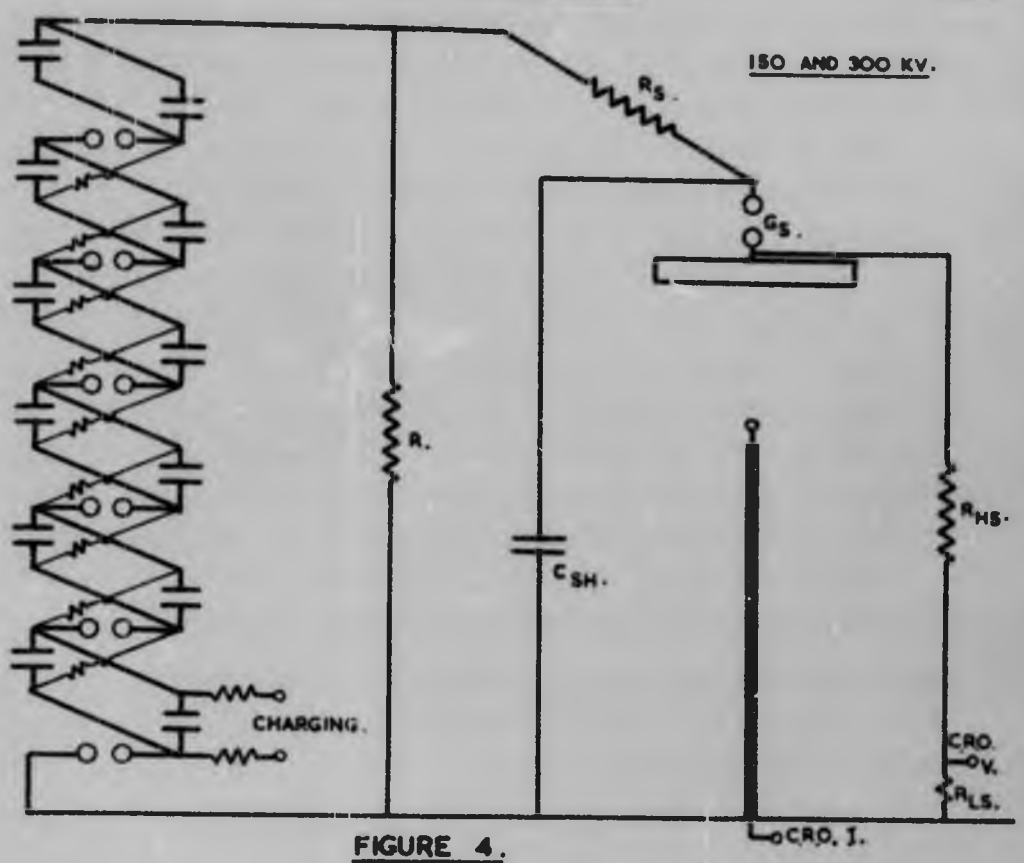


FIGURE 4.

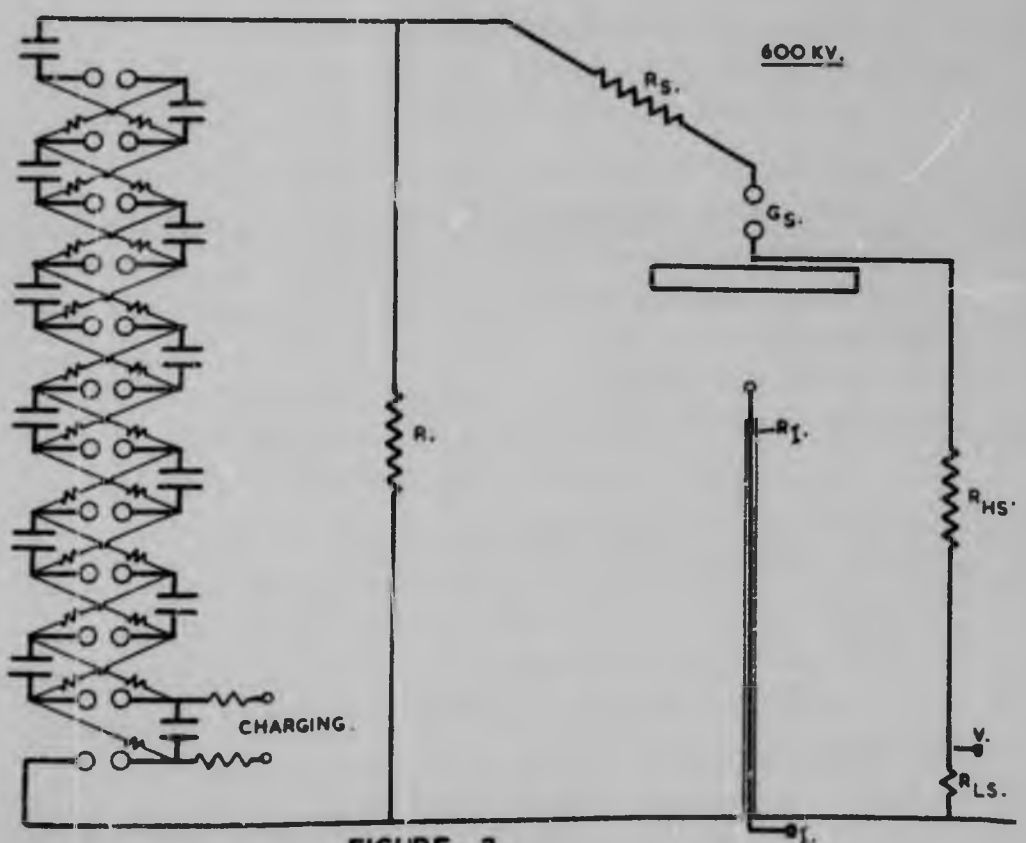


FIGURE 3.

By means of a series gap G_s close to the test gap electrodes[1] the rise-time can be reduced if a low resistance R_{HS} is used, and what is even more important, the oscillations can be almost eliminated by using the optimum gap distance. The action of this series gap is not quite clear. The rapid rise-time is caused by and depends on the rate of rise of ionisation current in the series gap, which produces a voltage across the Resistance R_{HS}, which is also the voltage applied to the test electrodes. The oscillations are normally caused by travelling waves which are reflected between the test gap and the Impulse Generator. When the series gap is introduced, it acts essentially as a variable resistance which probably provides the correct termination when the voltage wave reaches it (when the gap is at the optimum setting), and thus damps out the oscillations.

Even when a relatively high R_{HS} is used which gives a rise-time equal to that without the series gap (.2 μsec.), the gap still retains the property of damping out oscillations at the optimum gap distance. This condition allows a reasonably long wave tail of 100 μsec to be obtained, and for the biggest part of the investigation this compromise was used. The optimum gap was obtained by trial and error, observing the output voltage on the oscilloscope and determining the gap setting which produced minimum oscillations or overshoot.

Oscillations are also reduced by resistances in series with the gaps of the impulse generator. Throughout the investigation five resistances of 45 Ω each were used in five gaps of the generator. For the connection of figure 3 it was in every second gap and for the connection of figure 4 in every gap except the first. 45 Ω was used as a compromise between damping and not producing too high a voltage drop.

For all the investigations the amplitude of oscillations was less than ± 5% except for the .07 μsec rise at 150 kV and for the 600 kV conditions where they were less than ± 10%. Representative voltage wave-shapes are shown in the oscillographic results.

The .07 μsec rise at 150 kV was produced by R_{HS} = 1000 Ω in conjunction with a series gap. This

enabled the voltage to reach the maximum before the ionisation growth started.

The circuit constants providing the required voltage magnitudes and shapes are listed in table 2.

For the investigations with the slow 3 μsec rise the connections were as shown in figure 5, where the series gap G_S was short circuited and the high voltage condenser C_{SH} was added to provide the slow rise in conjunction with R_S.

2.1.3. Voltage Chopping

In order to make photographic recordings of the actual ionisation it is necessary to switch off the voltage before the full breakdown occurs, since on a photograph of a full breakdown the ionisation produced prior to breakdown is obscured by the halo due to the bright spark. For the condition of the "chopped" voltage, ionisation develops normally until the voltage is switched off and then stops. (Neglecting secondary effects which are discussed later). The photograph then shows the ionisation from the start until the time of chopping. This is the method which has been most extensively used up to-date for obtaining information on ionisation leading to breakdown[1,2,3,4]. By varying the time of chopping a series of pictures can be obtained which give a reasonably good overall picture of what happens. The limitations are that weak ionisation is not recorded, that time measurements are indirect, only one recording is obtained per spark and quantitative amplitude measurements are difficult.

In this investigation these recordings are used to give overall and supplementary information about ionisation and are used to confirm the results obtained from the photomultiplier recordings.

The chopping can be very easily obtained by having a gap in parallel with the test electrodes - if this gap is shorter than the test gap it will break down first and thus produce the required voltage. By varying the length of the chopping gap the required voltage pulse can be obtained.

One limitation of this type of chopping is that the time length of the voltage pulse varies as the time to

TABLE 2.

VOLTAGE kV	RISE TIME μsec.	DECAY TIME μsec.	R_{HS} Ω	R_{IB} Ω	R_S Ω	C_S cm.	C_{SH} pf.	OSCILLOSCOPE Volts/cm.
150 kV	.07	12	1,055	1.08	0 + 225	5 cm	600	50
150	.22	100	8,200	8.84	900 + 225	3.5	0	50
150	3	100	8.200	8.84	900 + 225	0	1200	50
- 300 kV	.25	100	8,200	8.84	900 + 225	5.8	0	100
+ 300	.25	100	8,200	8.84	900 + 225	6 - 6.5	0	100
- 300	3	100	8,200	8.84	900 + 225	0	1200	100
- 600 kV	.25	40	11,800	8.84	900 + 225	7	0	100/200
+ 600	.25	40	11,800	8.84	900 + 225	10	0	100/200

CIRCUIT DIAGRAM FOR 3 μSEC RISETIME. D.3.

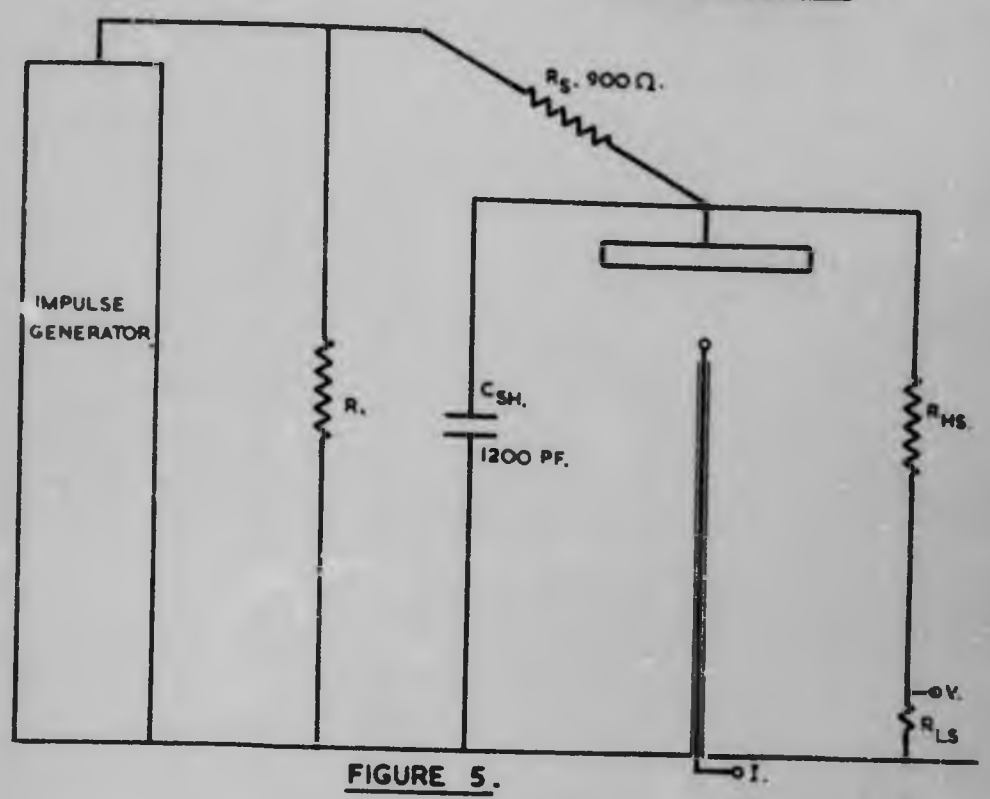


FIGURE 5.

ARRANGEMENT OF THE SMALL ELECTRODES.

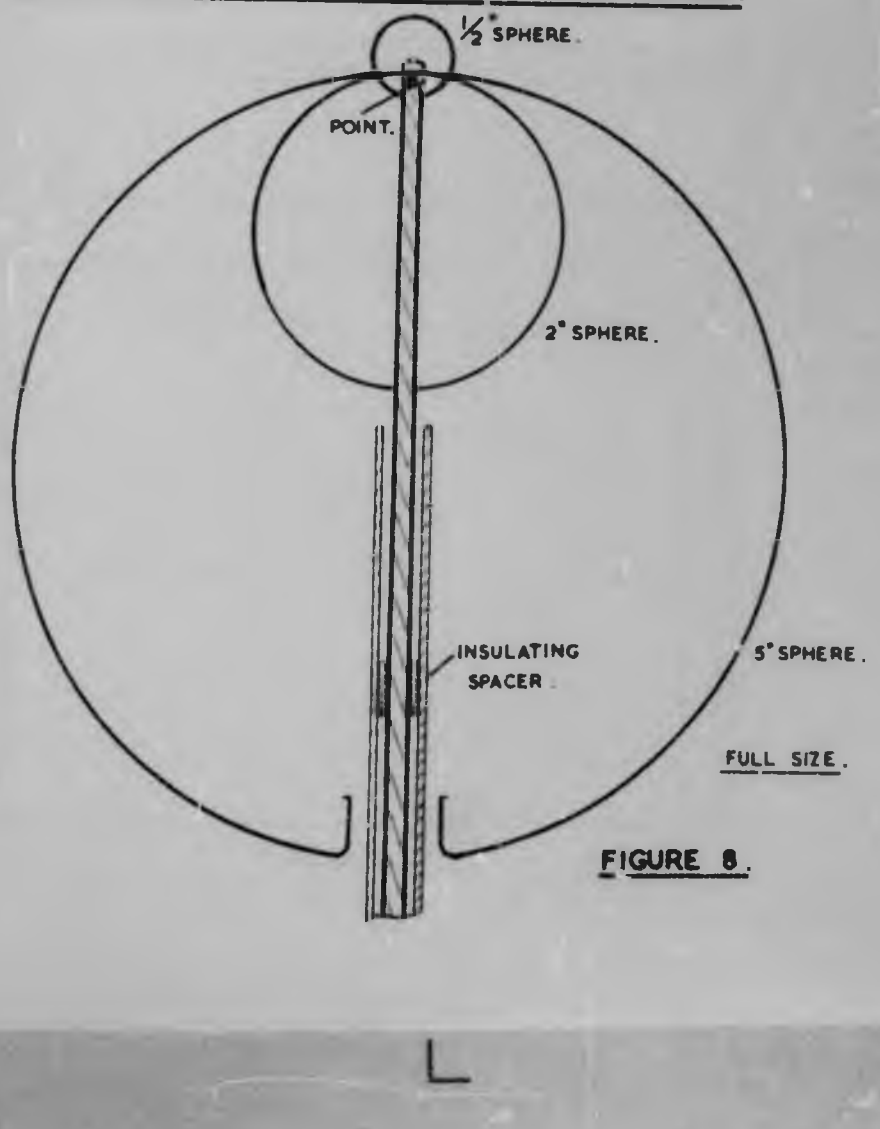


FIGURE 8.

DIAGRAM OF THE VOLTAGE CHOPPING CIRCUIT FOR 300 KV.

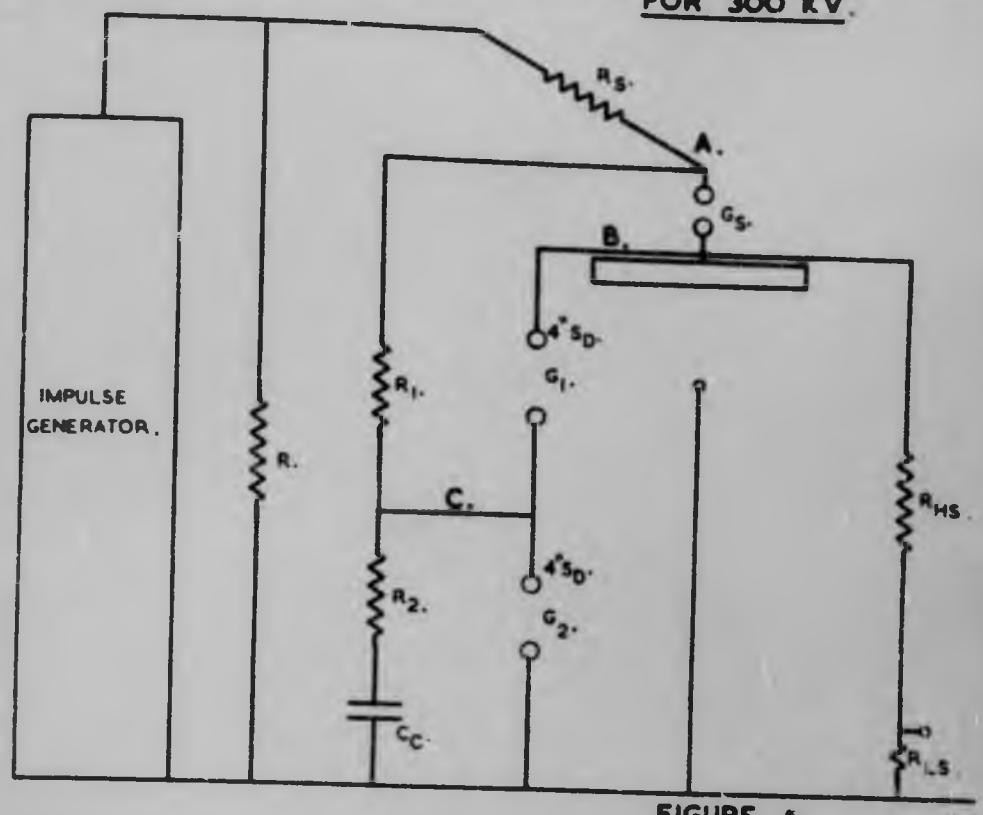


FIGURE 6.

VOLTAGE VARIATIONS AT POINTS A, B & C.

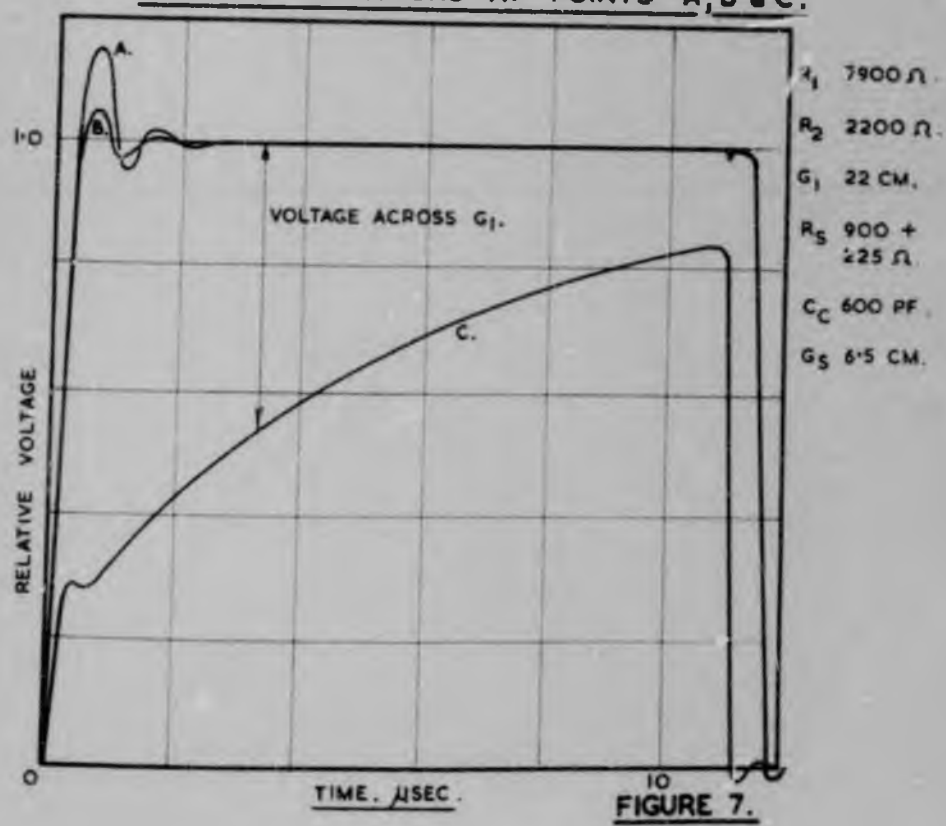
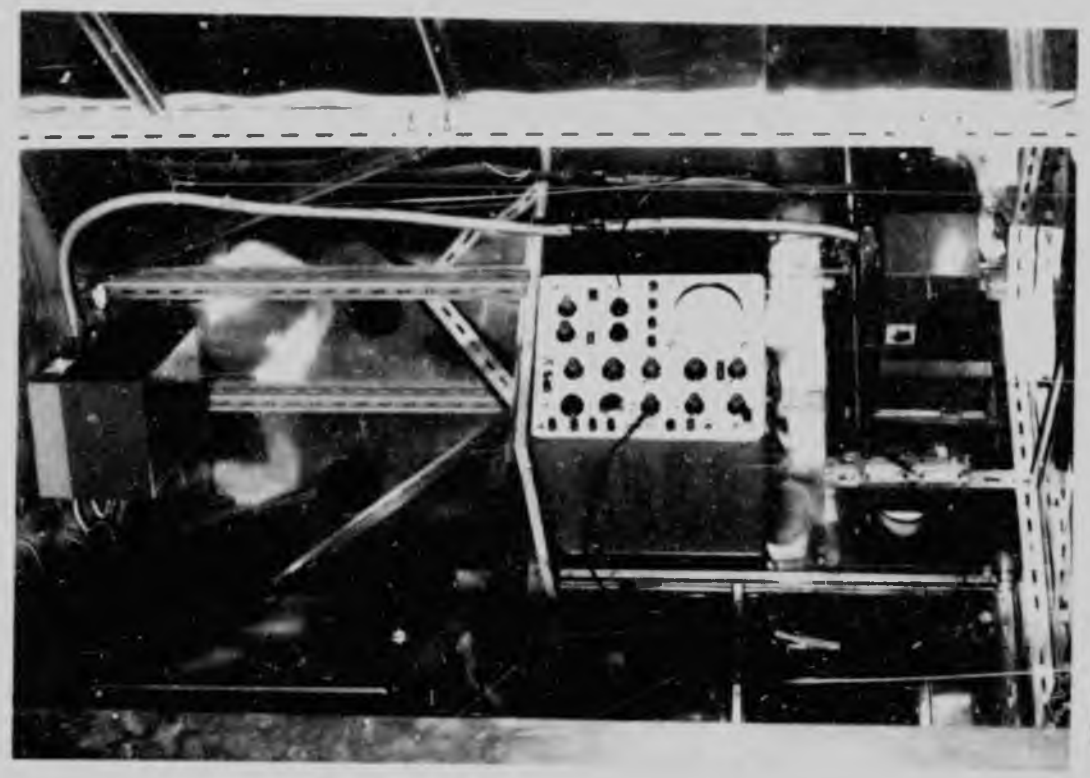


FIGURE 7.



b.



a.

PL 2.

breakdown varies for the same setting of the chopping gap, and may be as much as 20%.

A circuit developed by Johnson and also used by Park and Cones[1] is shown in figure 6 and was used to produce voltage pulses chopped at an accurately predetermined time. The voltages at the different points indicated are shown in figure 7.

Basically the voltage across gap G_2 rises slowly, after the initial jump caused by R_2, and gap G_2 breaks down at a definite instant just after the critical voltage has been exceeded. By varying the length of the gap G_2, different accurate breakdown times are obtained for gap G_2.

Gap G_1 is set such that when the voltage is applied and while the potential of point C rises, it just does not breakdown. However, when gap G_2 is short-circuited, G_1 receives the full voltage and also breaks down, thus short-circuiting the test gap at the time determined by the setting of G_2.

One difficulty arises at high voltages when the time of breakdown for gap G_1 becomes so long that it does not produce a sharp drop of voltage. Since the breakdown of the test gap is so variable, this arrangement does not offer any real advantages because it gives fixed times after the start but not before the breakdown of the test gap, which is what is required but is impossible to obtain without full knowledge of the breakdown mechanism.

For relatively long chopping times as required for the positive breakdown the accurate chopping technique was used and for the negative breakdown which required voltage pulses of less than 2 μsec duration, the simple shunt gap was used.

2.1.4. Electrodes

The electrodes were arranged in such a way that the plane electrode was at the top and the adjustable small electrode at the bottom as shown in the layout of figures 1 and 2. The following shapes were used for the small electrode.

(1) $\frac{1}{8}$" diameter rod with a pointed conical end tapering at a 30° angle.

(2) ½" and 5" diameter copper spheres.

(3) 2" diameter chromium plated sphere.

The reason why the smaller electrode is at the bottom is that the capacitive current is much smaller and the ionisation current bigger at the small electrode than at the plate. To measure the currents flowing through the small electrode if it is at a high potential is almost impossible. If it is at the bottom and at earth potential the current can very easily be measured by connecting the small electrode through a known low resistance to earth. The voltage produced across this resistance by the ionisation current can then be displayed on an oscilloscope. This arrangement was used by Meek and Craggs and also by Park and Cones[1,5].

The bottom part of the 1/8" rod providing the connection from the small electrode was shielded by a larger telescopic tube 3/8" diameter for the inner top portion and 3/4" diameter for the outer bottom portion, as shown in figure 8. This formed a coaxial cable connection and together with a short piece of flexible 50 Ω coaxial cable the connection was brought down to floor level. From that point it was connected by the normal 50 Ω signal cable to the oscilloscopes. The minimum height of the small electrode above the floor was 130 cms.

The top electrode consisted of a 3' x 3', 1/8" thick aluminium plate mounted on a frame for rigidity and suspended from the ceiling by asbestos tapes at fixed heights. Two settings were used; for ± 150 kV and -300 kV: the bottom surface was 190 cm above the floor and for +300 kV it was 210 cm above the floor.

For the investigation at 600 kV it was necessary to use a 1 metre diameter sphere as the top electrode, since discharges at this voltage were initiated at the edges of the plane electrode. For -600 kV the bottom of the sphere was 250 cm above floor level and for +600 kV it was 210 cm. In order to prevent confusion this 1 metre sphere is referred to as plane(s) for the results of the 600 kV investigation.

2.1.5. Triggering.

The charging voltage on the first stage of the impulse generator was measured by an Abrahams Electrostatic voltmeter and the necessary charging voltage for the required output voltage, as measured on the oscilloscope, was obtained by triggering at slowly increasing charging voltage steps until the necessary deflection on the oscilloscope was obtained. This charging voltage was then used as the indication for the manual tripping, operated by breaking the circuit of an ignition coil which was connected to the bottom gap. By superimposition of this voltage pulse on the charging voltage existing across the bottom gap, the impulse generator was triggered. The charging supply was set such that the charging time to the triggering point was in the range 20 to 30 seconds.

The output voltage shapes and magnitudes were checked at regular intervals to ensure that conditions had not changed.

2.2 MEASURING EQUIPMENT.

2.2.1. Oscilloscopes.

Oscilloscope Details:

For the investigation two high speed oscilloscopes were used.

(a) The one was specially constructed in the laboratory for high voltage pulse recordings. It is capable of producing recordable single sweep traces at sweep speeds of .1 μsec/cm. with fixed controllable sweep speeds from .015 μsec/cm - 1 m sec/cm. and with sensitive variable delay triggering.

The vertical input is directly to the deflecting plates through an input attenuator which also forms the terminating impedance of the 50 Ω coaxial signal cable, giving calibrated vertical deflection sensitivities of 16.7, 20, 30, 50, 100 and 200 volts/cm.

This oscilloscope was used mainly for recordings of either voltage waveshape or ionisation current in the investigation, and is referred to as the

lab oscilloscope. The recording area is 10 x 4 cm., cut-off occuring above and below this area although the graticule extends further.

(b) The other oscilloscope is a Tektronix Model 545 which is a general purpose oscilloscope but also capable of single sweep traces at .1 µsec/cm sweep speeds with fixed controllable sweep speeds ranging from .02 usec/cm to 10 secs/cm and with sensitive variable delay triggering.

The vertical deflection is obtained through an amplifier with a 40 mc bandwidth and a rise time response of 12 nsec. The vertical input sensitivities used were .05, .1, .2, .5, 1, 2 and 5 volts/cm. In addition it has a vertical signal delay of .2 µsec which allows the front of the triggering pulse to be displayed.

This oscilloscope was used mainly for the amplification and display of the pulses produced by the photomultiplier which were in the range .02 - 2 volts depending on the intensity of ionisation.

Voltage and current measurements were also made on it by connecting a wide band probe with 50 times reduction across the terminating attenuator impedance of the signal cable.

The recording area is also 10 x 4 cm.

Comparison of Oscillograms:

In order to facilitate time and amplitude comparisons between the recordings on the two oscilloscopes, the vertical and horizontal calibrations of the lab oscilloscope were adjusted until they corresponded to within 1% over the centre 8 cm of horizontal deflection and to within 3% for the vertical deflection with those on the Tektronix oscilloscopes. These adjustments were done with the aid of a 20 nsec rise time 1 mc. square wave generator by displaying the wave on the two oscilloscopes simultaneously. The adjustments were done for sweep speeds of .1, .2, .5, 1, 2 and 5 µsec/cm.

The calibration was checked and remained accurate during the investigation. Oscillograms 1 (a and b) on plate (PL21) is the best example to show this comparison.

Triggering of Oscilloscopes:

Triggering of the oscilloscopes was obtained by means of aerials approximately six inches long, which picked up a large enough voltage pulse when the first gap of the impulse generator flashed over to provide reliable triggering. Reliable triggering was obtained by careful adjustment of the trigger controls on both oscilloscopes and had to be changed when the I.G. polarity was changed.

Here a difficulty arose in that the position of the waveshapes with regard to the graticule was different horizontally due to the signal delay in the Tektronix oscilloscope. The difference was between .2 and .3 μsec. The obvious solution was to use the trigger delay on the Tektronix but although it reduced the difference, exact correspondence could not be obtained because the minimum trigger delay was just more than .3 μsec. This was the condition used for the major part of the investigation with a time difference from the starting point of less than .1 μsec existing between the two oscillograms. This time difference was measured for each set of recordings and allowed for in the final results. The trigger jitter between the two oscilloscopes was found to be less than 10 nsecs.

Screening (Interference).

The major difficulty in obtaining the results for this investigation was the elimination of interference. When the impulse generator is triggered and switches to the series connection, strong electromagnetic fields are propagated covering the frequency spectrum from 100 kc/sec to 200 mc/sec. The lab oscilloscope was specially constructed to produce oscillograms free from interference without additional screening. However, the Tektronix oscilloscope is not shielded against such strong interference and even with the input short-circuited, more than full scale interference deflection was obtained, lasting 5 to 10 μsecs. This interference is produced mainly through the 220 volt mains supply.

Hence it was necessary to construct a screened room with a 6' x 4'6" floor and 6'3" high of 24 S.W.G. copper, to house the oscilloscopes and the photomultiplier. The mains supply to the room is taken through a capacitance-inductance high frequency

filter and a shielded isolating transformer to prevent interference entering the copper room by that means. With the door closed the interference was practically zero at 150 kV and 300 kV. At 600 kV the peak-to-peak interference was less than 2 mm., lasting less than 1 μsec. With the door open the interference rose to approximately 1 cm peak-to-peak. The room was mounted on wheels and could be moved to the most suitable position for recording, where it was lifted on blocks to ensure stability during a set of recordings. Only two positions were used for the investigation, as shown in the layout figure 1 and 2.

The earth point used for measurements was either at the bottom of the connection from the small electrode or the bottom of the potential divider. These two points were 6 ft. apart and joined by a copper busbar of cross-section 3" x 1/8" and can practically be regarded as the same point electrically.

The signal was transmitted through a double screened coaxial cable. The inner portion was a normal 50 Ω polythene insulated coaxial cable with insulation over the outer screen. Over this heavy flexible braiding was slipped to form an outside screen. The two screens were connected together at the earth point while at the other end the outer screen was connected at the entrance of the cable to the screened room and the inner screen was connected to the oscilloscope chassis at the signal input plug.

At the earth point the signal wire was connected across the appropriate resistance, while at the other end, in the oscilloscope, it went to the input attenuator which formed the terminating impedance of the cable and thus ensured that the cable was correctly terminated at the one end in order to prevent reflections in the signal cable.

2.2.2. Measurement of Voltage:

In order to display the high voltage waveshape of 150, 300 or 600 kV on the oscilloscope, it is necessary to reduce it in amplitude to about

50 volts but keeping the waveshape unchanged. For this use, resistive potential dividers (R_{HS} and R_{LS}) were used with reduction ratios of approximately 1000 : 1 as shown in figures 3 & 4. Further reduction in voltage amplitude was obtained by means of the input attenuator. Three different high voltage resistances R_{HS} were used.

(1) The first of total value 1055 Ω was made up of two tubular Dubilier high voltage resistances. The construction is simply a thin layer of carbon on a ceramic tube. This has the property of small change in resistance with increase in frequency. The resistance remains practically constant up to at least 30 mc (from specifications) and this was the resistance used for the production and recording of the fast .07 μsec rise-time for which it gave accurate recordings. This resistance could only operate at 150 kV.

(2) The second and third of values 8,200 Ω and 11,800 Ω respectively were made up of a string of 5 watt carbon resistances which are suitable for pulse work. By immersion of the string in an oil filled insulating tube, each resistance string could withstand the 600 kV impulse. With the slower rise-times of .25 and 3 μsecs for which these resistances were used, they also gave undistorted waveshapes.

The low voltage resistances R_{LS} of the potential divider were specially constructed from Brightray resistance tape .003" x .05" in cross-section. They were made up in small plug-in units by folding the tape back on itself in zig-zag fashion every two inches, with thin insulating material (.004" leatheroid) between the adjacent sides of the tape. The unit was clamped between two insulating boards and each side of the resistance tape was connected to a pin [1].

A special termination was constructed to allow the connection of the signal cable and the low voltage resistances to ensure that minimum inductance was introduced. The whole unit with one of the resistances, but without the shielding cover, is shown in plate 2(a).

Only two resistances were used, the one 1.08 Ω and the other 8.84 Ω. From R.F. bridge measurements these resistances are constant up to 10 mc. with 20% increase of impedance at 20 mc. The time constant $\frac{L}{R}$ was 5×10^{-9}.

By means of the input attenuator, suitable deflection amplitudes were obtained on the oscilloscope.

2.2.3. Measurement of Current.

For current measurements from .2 amps up to 16 amps maximum, the terminating impedance of the 50 Ω cable was used as the resistance across which the voltage proportional to the ionisation current was developed. This simply meant that the inner conductor was left isolated at the small electrode side and terminated as usual in the oscilloscope. This gave very satisfactory results with no reflections and no inductance effects even at rise-times as short as 10 nsecs. This arrangement was used for the 150 kV and 300 kV voltages and with the input attenuator, sensitivities of .34, .4, .6, 1, 2 and 4 A/cm were obtained.

For the 600 kV investigation the early ionisation currents were higher than 16 amps and it was necessary to use a resistance lower than 50 Ω. The only position where it could be placed electrically was right at the electrode, at the input to the coaxial cable. When the resistance was tried at the base, where the connection is made to the signal cable, readings were impossible due to the reflections in the cable between the electrode and the base. It was just possible to fit a resistance R_I of 1.5 Ω in the airspace between the inner conductor and the outer tube, just below the small electrode (see figure 3). The resistance was of the same type as that used for the low voltage resistance R_{IS} but with the clamping boards and the pins removed. The resistance tape was clamped by P.V.C. tape and pressed into the air space with the connections made directly on to the inner conductor and the outer tube.

Due to inductance effects at high rates of change, the resistance did give overshoot (to be discussed in the results) but gave satisfactory recordings. With this resistance, currents in the range 10 - 600 amps could be recorded in conjunction with the input attenuator which gave sensitivities of 11, 14, 21, 35, 70 and 140 amps/cm.

2.2.4. Recording of Light with the Photomultiplier and Amplifier.

Photomultiplier and Amplifier:

The photomultiplier used throughout the investigation was a Philips P A 11, No. A3, the equivalent of the Philips 50 AVP, with a sensitivity of 36 μA/lumen.

The overall current amplification depends on the applied potentials and for the normal operating condition of 120 volts per dynode for the eleven dynodes it is 1×10^6 while at 103 volts per dynode it is 2×10^5.

The photomultiplier was operated with supply voltages of approximately 1100 volts at the photocathode and +300 volts at the plate. The dynode voltages were obtained by means of a resistance divider. The supply voltages were stabilised with voltage regulating circuits which allowed adjustment of the voltages. It was calibrated to provide 100, 110 and 120 volts per dynode. The 120 volt operation was most often used in the investigation and in the results all the readings are referred back to that amplification.

The load resistance in the plate of the photomultiplier was 300 Ω which allowed a maximum voltage of approximately 1 volt with a maximum rise time of 15 nsec. In order to retain the rise time through the coaxial cable feeding the signal to the oscilloscope, one stage of amplification was built next to the photomultiplier which only had a gain of 2 but kept the rise time better than 20 nsecs at the input to the oscilloscope.

The voltage pulses produced by the photo-

multiplier and amplifier were then further amplified by the oscilloscope amplifier before display. By using the stepped attenuator, sensitivities of .05, .1, .2 and .5 volts/cm were obtained. Since the accuracy of this attenuator is 3% this was normally used for changing the light recording sensitivity and only when sensitivities outside this range were needed, were the other conditions, altering sensitivity, changed, because they could not be calibrated so accurately.

Lens and Screen:

The light recordings with the photomultiplier were achieved by focusing the image of the ionisation through an 18 cm, f 4.5 Wollensak lens on an opaque screen. This screen had a single slit .010" wide and 2" long in it, perpendicular to the direction of the growth of ionisation [5]. The photocathode of the photomultiplier was placed directly behind this slit and when the ionisation image fell on the slit, it passed through, and on reaching the photo-cathode it produced a pulse on the oscilloscope. Due to the length of the slit and the depth of field given by the lens, a plane was scanned in the actual ionisation volume which was 12" wide, at least 12" long (depending on the lens opening) and .06" high, lying parallel to the plane electrode. At 600 kV these dimensions were doubled. Any light variations in this plane were recorded vs. time on the oscilloscope and it was thus possible to determine at which instant after the start of the voltage, ionisation occurred in the scanning plane, to an accuracy of approximately 10 nsec.

The amount of light coming through the lens could be controlled by a diaphragm, which was originally calibrated from f 4.5 to f 64. It was re-calibrated by means of a steady light source and a micro-ammeter in the plate of the photomultiplier to give a linear amplitude relation starting at a value of 1 with the diaphragm full open and ending at 80 with the diaphragm fully closed. The intermediate calibrated positions used were 2, 4, 8, 16, 32 and 64. Final checking

showed the accuracy of the calibration to be within 10% for an 8 to 1 change in setting, while the ratio between 1 and 80 was within 20%. The unit used for the measurement of the light pulses was taken as the voltage sensitivity of the oscilloscope in volts/cm multiplied by the lens opening, for dynode voltages of 120 volts and a slit width of .01", giving L units/cm.

Scanning Arrangement:

The photomultiplier camera, its power supply and the recording oscilloscope were all placed together in the copper room as shown in plate 2(b). The power supply was at the bottom, the oscilloscope in the centre and the photomultiplier camera at the top. The photomultiplier camera scanned the test gap through a 6" diameter hole in the top of the copper room.

At this level the photomultiplier was very close to the horizontal plane of the vertical centre of the test gap. Different scanning heights covering the distance from the smaller electrode to the plane were obtained by tilting the photomultiplier camera. The whole range could be covered by tilting the camera less than 5^{o} up or down, and hence the added complication of moving the whole camera up and down to keep the scanning plane absolutely horizontal was not considered necessary.

The required position of the scanning plane was obtained by adjusting the tilting mechanism to the calibrated position. The calibration was done by placing a point source of light, 1 mm diameter, at a known distance from the plane and then moving the camera until a peak deflection on the micro-ammeter in the plate circuit was obtained and marking the appropriate position. The calibration was checked throughout the investigation and for the 150 kV and 300 kV tests, was accurate to within 1 mm of actual height and for 600 kV within 2 mm, which represented, even for the shortest gaps used, an accuracy of better than 1% of the total gap distance.

2.2.5. Camera and Arrangement used for Photographing the ionisation.

The camera used for photographing the ionisation was a Futura with an f 3.5 lens. The special feature of the lens was that it had transparency to the ultra violet light of the ionisation, which produced recordings equal to that obtained with a normal f 1.5 lens and with a much greater depth of field. The film used for this recording was either Ilford HP3 (200 ASA) or Kodak TRI - X. (400 ASA) overdeveloped three times in order to obtain maximum sensitivity.

Due to the fact that the camera had to be close to the high voltage plane for recording, it was necessary to mount it on an insulated stand with remote and insulated tripping and winding control. This allowed the film to be wound on and the shutter tripped from inside the copper room. For the recordings, the laboratory was darkened and the shutter was opened for approximately 1 second, during which time the impulse generator was triggered.

Recording of Oscillograms:

Because each spark only produced a single sweep recording on each oscilloscope, it was necessary to photograph the traces to enable comparisons to be made. The two cameras which had f 1.5 and f 2.0 lenses respectively were placed at such distances from the cathode ray tube faces, that the image size of the centimeter graticules were identical on the negatives of the two cameras. This enabled time comparisons to be made by superimposition of the negatives or by placing the one print below the other as shown in the results.

By means of a ganged remote tripping control, the shutters on the two oscilloscope cameras and the one photographing ionisation could be opened and closed simultaneously by the operation of one lever. While the shutters were open the impulse generator was triggered and the recording made by each respective camera.

2.2.7. Preparation of Results.

Results of ionisation current, ionisation light variation and sometimes photographs of the actual ionisation were taken in sets of approximately 40 recordings for different combinations of the controlled variables. 40 recordings were the maximum that could be taken per camera on one loading of film. The conditions of the controlled variables for each recording were noted on special results sheets. Contact prints were made of all the film recordings on paper, allowing 32 oscillograms per page, special care being taken to keep the simultaneous recordings of the same spark together. On these sheets the conditions of the variables were noted and then the information for plotting the graphs and the explanation of the ionisation mechanism were extracted. The most representative oscillograms and photographs to illustrate the mechanisms were then selected and reproduced for this thesis. During the whole investigation, approximately 8,000 different oscillograms and photographs were taken.

CHAPTER III

THE VALIDITY AND MEANING OF THE MEASUREMENTS

In this investigation it is extremely important to know what is being measured and what these measurements mean.

3.1. RELATION BETWEEN IONISATION AND THE LIGHT PRODUCED:

The ionisation was recorded by the visible light produced in the test gap. The first point to consider is the relation between the light given off and the actual amount of ionisation occurring.

Ionisation is the process by which accelerated electrons or positive ions smash into neutral atoms with enough energy to knock one or more of the orbiting electrons out of the influence of the respective nucleus. This causes the production of free electrons. The nucleus is left with a deficit of electrons and is called a positive ion.

In a volume where ionisation is occurring there are some electrons that have energies less than that required for ionisation at the instant of collision. This is due to differences in path length before a collision occurs. In these collisions one or more of the orbiting electrons are forced into larger orbits but are not set free. The larger orbits are normally unstable and the electrons fall back to their original orbits in one or more steps, taking less than 1×10^{-8} second for each step for excitations in air[10]. (p.390 and 391). Due to the reduction of energy level, energy must be released during the fall-back process and this is done by the production of quanta of light. The frequency of the light depends on the energy released in one fall-back process and the relation is given by

$$\Delta E = h f$$

where ΔE is the energy released, h is Planck's Constant and f is the frequency of the light. If the energy of the photon is measured in electron-volts -

$$E_{ph} = 4.13 \times 10^{-15} f \qquad \text{(Ref:10, p.393)}$$

where f is the frequency in cycles per second.

The following energies have been obtained by previous investigators[9] (p.10) as the first Excitation potentials and the Ionisation potentials for the constituent gases of air.

Gas	First Excitation Potential (EV).	Ionisation Potential (EV) I	II
N	6.3	14.5	29.6
O	9.1	13.6	35.2
CO_2	10.0	13.7	-
H	10.2	13.6	-

The light recorded by the photomultiplier was mostly in the ultra-violet region lying in the visible spectrum and seems to have been produced by multiple step fall-backs because the energy associated with the highest light frequency recordable is about 3 EV, while the minimum excitation potential is 6.5 EV.

It seems likely that a large amount of light is produced deep in the ultra-violet region, associated with energies of the order of the excitation potential (14 EV.), but which were not recordable by the photo-multiplier.

Since the relation between the minimum excitation potential and the minimum ionisation potential is of the order of 1 : 2, it seems reasonable to assume a proportional relationship between the amount of light produced and the amount of ionisation taking place, when a large number of collisions are considered.

During recombination of electrons and positive ions, light is also produced but the proportion in comparison to the initial light produced by excitation appears to be small, as indicated by the results. The reason for this seems to be the longer time over which this action is spread. From the results and also confirmed by the time between Trichel pulses[9] (p. 150) it appears that substantial recombination, for the ionisations considered, only occurs in approximately 40 μsec. (See Ch. 5.2.3. Graph 12).

It is important to consider the time lags involved in the production of light when the collisions take place. By recording the instant of the ionisation current start and the start of the light pulse, with the

photomultiplier scanning the air adjacent to the small electrode, it was determined that the pulses occurred at exactly the same instant on the Tektronix oscilloscope. The time for the transmission of the pulses, where they travel along different paths, must however, be considered.

The time for the transmission of the current pulse along the signal cable was 40 nsec, as determined from the timing of reflections when the cable was not terminated correctly. For the light pulses there was a delay of 17 nsec through the eleven feet of air from the electrode to the photomultiplier and the delay in the photomultiplier. The delay in the probe connection to the oscilloscope and in the oscilloscope was the same for both measurements because the same oscilloscope was used for this comparison, and need not be considered. The delay time in the photomultiplier is not accurately known and also depends on the dynode voltages but the normal delay of that type of photomultiplier is in the range 20 - 30 nsec[6]. (p.276). Since the pulses reach the oscilloscope at the same time, the delay in the production of the light and the delay in the photomultiplier must be 23 nsec. This means that the time delay in light pro-duction can be a maximum of approximately 5 nsec and probably is less than that. In relation to the time scales used, it can be considered instantaneous[10] (p. 390).

The production of light is thus taken as an instantaneous indication of ionisation that is taking place. If the light produced at a certain position disappears it does not mean that the electrons and positive ions have disappeared or re-combined, but it means that the field strength existing at that time is not high enough to produce new ionisation.

3.2. RECORDING OF LIGHT:

In most of the previous investigations, photographic recording of the light has been used to investigate the breakdown mechanism. This has two basic drawbacks in that the light sensitivity is not high

enough to record the faint ionisation and also because return ionisation may be produced due to space charge effects when the voltage is chopped, making interpretation difficult.

The corona propagation, which occurs at extremely fast speeds when photographically visible, was recorded by Park and Cones[1] who obtained speeds of 5×10^8 cm/sec for negative corona and 8×10^8 cm/sec for positive corona. By means of the photomultiplier it was found that the speeds can be as low as 1.5×10^7 cm/sec for the weak ionisation and the recordings are free from space charge effects because the ionisation is not interfered with electrically.

To prove the validity of the photomultiplier recordings the photomultiplier lens was covered and when the impulse generator was triggered, the oscillo - scope trace was a straight line, even on maximum amplification, when the door of the screened room was closed. This indicated that the recordings are free from electrical interference. To show that secondary pulses were not generated the chopped voltage technique was used and after the voltage was chopped, no further light pulses occurred. At the chopping of voltage a light pulse occurred in some cases, which led to the discovery of return ionisation on chopping.

The best proof of the accuracy of the recordings is the comparison of light and current pulses. When the light recordings at the small electrode and the ionisation currents are compared, the correspondence in time of occurrence and relative amplitudes are so convincing that it does not leave room for any doubt.

For the corona the start of ionisation is so consistent for .07 and .25 μsec risetimes, that it was possible to use the start of the oscilloscope sweep as a reference. By taking an average of 4 to 8 recordings of the same condition, it was possible to make time measurements to the accuracy of measurement, which is 5 nsec.

The use of a double or multiple slit technique appears very attractive because it provides simultaneous readings with no need for an additional

time reference. The corona pulse does not lend itself very well to this technique and the subsequent ionisation even less. It must be realised that the corona is not one single uniform volume of light but is made up of a number of balls of light which start almost simultaneously at the small electrode and move towards the plane along the field lines. Those travelling along the shortest lines are the brightest and fastest and reach the flat scanning plane before those moving along the longer lines, which in addition to having a longer length are also slower and weaker. Thus the shape of the corona pulse is that of a sharp rise with a comparatively slow and roughly exponential decay. The decay is however, not very smooth due to the different discreet balls of light.

When the corona was observed with a double slit screen it was found that the start of the second pulse can be confused with the last pulses from the first slit, especially because the intensity at the second slit is less than at the first. By using a wider second slit this can be corrected for but for each different scanning position and combination of the investigated variables, a different slit-width ratio would be required. Since this becomes so cumbersome, this method was only used in a few cases to check the validity of the described method of propagation measurement.

By using a short slit, the ratio of bright to weak pulses can be increased, thus giving a pulse with a shorter decay time - but it is never possible to scan a small cubic volume to look at a single ball because the depth of field of the lens always produce a flat scanning plane at least 12 inches long. In applying the short slit to the double slit scanning some improvement can be obtained but the possibility of balls of ionisation passing the one slit and not the other, leads to uncertainties.

3.3. IONISATION CURRENT:

The ionisation current has been recorded because it provides a measurement of the amount of charge supplied to the gap and mainly because the major part of the current recorded is due to electrons or

positive ions (depending on the polarity) flowing into the electrode. The induced current due to the movement of charge at a distance from the electrode seems to be small in comparison, because when the photomultiplier indicates ionisation at the plane, no current pulses are recorded but when the ionisation occurs at the small electrode, a current pulse occurs at the same time. The current thus gives an indication of the ionisation occurring in the immediate vicinity of the small electrode, and can be used instead of a photo-multiplier scanning at that level.

By scanning close to the plane with the photomultiplier the up and down movement of the balls of ionisation can be observed by noting the times of occurrence of the light pulses at the plane and the current pulses at the small electrode. This comparison forms the basis of the explanation of the breakdown mechanism when the small electrode is negative and is also important for the positive breakdown.

3.4. PHOTOGRAPHS OF IONISATION:

Photographs of the ionisation have been taken to obtain an overall three-dimensional picture of the paths taken to provide supplementary information of the processes and to indicate the limitations, in comparison to the photomultiplier technique, to which this method is subjected. (As referred to in Ch. 3 - 2 and discussed later).

C H A P T E R IV

NOMENCLATURE AND MEASUREMENTS FROM OSCILLOGRAMS

4.1 REFERENCES:

1. Graphs. Graphs are numbered (G1), (G2) ---- . A summary of the variables on each graph and its reference number is given in the index.

2. Oscillograms. The oscillograms are reproduced on plates denoted by(PL 3)(PL 4) ---- .

   Oscillograms on each page are numbered with one number for each set of simultaneous recordings. The number of each set is marked in white in the top left hand corner of the top oscillogram of a set. If there is only one oscillogram per spark, each oscillogram is marked with a different number, as in the oscillograms of corona. The top oscillogram is usually that of the current (on the 6 x 10 graticule) and is referred to as (a) (not marked).

   The bottom oscillogram is normally that of light recorded by the photomultiplier (4 x 10 graticule) denoted by (b) (not marked).

   If there is a simultaneous photograph of the ionisation it is placed directly below the two oscillograms and is referred to as (c). A list of the conditions for the plates is also given in the index.

4.2 ABBREVIATIONS USED IN THE RESULTS:

1. Variables. Due to the large number of oscillograms it was necessary to use the following abbreviations to indicate the values of the variables.

   (N) indicates the value of the variable in the units given.

   G (N) = Gap length in cm.

   S (N) = Scanning level as measured from the small electrode in cm.

   (N) S_D = Small electrode sphere diameter, measured in inches.

2. Scales.

(a) Time: The horizontal time scale is indicated in white by showing the starting point and one convenient reference time in μsec, opposite a graticule line (normally the last).

(b) Amplitude: The vertical scale is marked in units per division (4 divisions being the maximum recordable).

Light - (N) L = (N) Light units per division
see end of 2 - 2 - 4 (b)
Current - (N) A = (N) Amperes per division.
Voltage - (N) V = (N) Volts per division.
The scale is indicated next to each oscillogram or a set of oscillograms using the same scale.

4.3 MEASUREMENTS FROM OSCILLOGRAMS:

1. Time Measurements. Time measurements indicated on the graphs were measured as starting from the first graticule line from the left, on the light amplitude oscillograms, except for the positive breakdown at 100 kV where the second graticule line from the left was used as the starting point (PL 13).

The light amplitude and current oscillograms were placed such that points lying on a vertical line through both oscillograms are coincident in time. Due to the difference in triggering of the oscilloscopes, the vertical graticule lines do not correspond for this condition. The left hand graticule line of the Tektronix oscilloscope (4 x 10 graticule) was always taken as the starting point of time measurement.

The time difference between the occurrence of a current pulse and the corresponding light pulse at the scanning plane was measured as the horizontal distance between vertical lines drawn through the respective peaks of the pulses.

2. Amplitude Measurements. The zero line for amplitude measurements was taken at the horizontal level of the spot on the oscillogram, which normally coincided with one of the graticule lines. The amplitude was measured as the vertical distance above or below the zero level.

C H A P T E R V

CORONA

5.1 POSITIVE CORONA:

5.1.1. Discussion of Oscillograms.

Before discussing the results on the graphs it is advisable to consider a representative set of oscillographic results, to see the general waveshapes obtained and the readings which were taken for plotting the graphs.

This is best shown by oscillograms 1 - 8 and 17 on PL 3, which represent the positive corona recordings for an 80 cm gap at 300 kV for a 2" diameter sphere with a rise-time of .25 μsec. No.17 indicates the voltage applied to the gap on a sweep speed of .1 μsec per division, i.e. 1 μsec for the full sweep. The voltage sensitivity was 100 volts per division, thus the actual voltage was 325 volts multiplied by the potential divider ratio. From table 2, the ratio is $\frac{8200}{8.84}$ = 925, which gives 325 x 925 = 300 kV. The rise-time taken from the start up to the full voltage is .25 μsec since the rise is practically linear.

These results are plotted on graph (G4) for G80, 2" SD. The voltage wave on (G4a) was plotted from PL 3 No. 17, using the same time starting instant.

The current flowing through the small electrode as measured on the Tektronix is shown in PL 3 No.1, where the capacitive current is seen to have an amplitude of approximately 1 amp with a peak value at about .1 μsec. At .27 μsec there is a sudden rise in current to 7 amps in .03 μsec, which decays practically to zero in .4 μsec. This is the ionisation current with a peak amplitude of 7 amps and a starting instant at .27 μsec.

The oscillograms of the light variation as recorded by the photomultiplier are shown in Nos 2 - 8, each recording being for a plane consecutively further away from the 2 inch sphere. The two measurements taken from each oscillogram are (1) the start of the rise of the light pulse, plotted on part (a) of the

graphs and (2) the peak amplitude of the pulse plotted in part (b) as the peak light amplitude.

A list of the readings from Nos 2 - 8 are given which can to be compared with the appropriate graphs on (G4) a and b.

No.	Dist. from 2 sphere	Starting instant	Peak Amplitude
2	15	.32	25
3	20	.37	8
4	30	.55	1.5
5	40	.80	1.2
6	50	1.1	.8
7	60	1.9	.5
8	70	2.4	.7

This shows that the light pulse occurs later in time and with diminishing amplitude as it moves from the sphere towards the plane. It is important to note that the rise-time of the pulse is approximately 20 nsec which is the rise-time of the recording apparatus and may indeed be faster. The time measurement was taken at the start of the rise since this measurement was easier and more accurate to make. The instant of the peak amplitude occurred 20 nsec later for amplitudes in excess of 1 L. so that the time of peak amplitude can be obtained by addition of a constant 20 nsec. For smaller amplitudes the rise-time became longer but was always less than the spread in time of occurrence between different breakdowns. Hence the measurement of the speed of the peak of the light can be taken as the speed of movement of the start of the light.

The speed of movement is obtained by taking the time difference to travel the distance between the two scanning planes, e.g. from S15 to S20 the time taken was .05 μsec for 5 cm., giving a speed of 1×10^8 cm/sec., and from S60 to S70 the time was .5 μsec for 10 cm, giving a speed of 2×10^7 cm/sec.

From PL 3 No.2, the duration of the light pulse is .15 μsec, which at a speed of 1×10^8 cm/sec, obtained above, would represent a light volume 15 cm long. However, the subsequent oscillograms show that the light pulse does not consist of a single pulse but

is made up of a number of separate light pulses, each seeming to be limited in rise and fall time by the response of the recording apparatus. If this time is taken (40 nsec for the rise and fall), this gives a maximum length of 5 cm for each light volume producing a pulse.

The photographic results by previous investigators[1,2,3,4] and also taken for this investigation (PL 16 No. 1c) show that the corona growth is not that of a large volume of light but consist of a number of streamers less than 1 mm diameter. From the photomultiplier recordings it can be seen that the streamers are not lines of light produced but are elongated balls of light not longer than 5 cm., moving at a high speed. It appears that they all start at almost the same instant but due to the fact that some travel along longer field paths, they are slower and weaker. Near the sphere they are still so close together in space and time that they cannot be distinguished as separate pulses by the recording apparatus, and produce an apparently single pulse, with a sharp rise and a slower decay as shown in PL 3, No.2. Further away from the point there is enough time difference between the light volumes reaching a horizontal plane to be recorded as separate pulses, best shown by Nos 4 and 5.

Later in the results, a more accurate determination of the lengths of these balls is given.

For 300 kV the critical gap spacing is 60 cm and although the corona light bridges the gap at a spacing of 80 cm, it does not lead to breakdown. The transition to breakdown is discussed in the second part of the results.

If a smaller electrode (½" diameter sphere) is used, with other variables remaining constant, a set of results as shown in PL 3, Nos 9 - 16 are obtained. These results show the same pattern as with the 2" sphere except that the current and light amplitudes are less, with a spread of about .1 μsec of the peak of the pulse. In this case the ionisation started while the voltage had only reached half the peak value, whereas with the 2" sphere the ionisation only started after the voltage had risen to the maximum value, so that the initial part

of the propagation occurs under increasing voltage conditions with the ½ inch sphere.

The ionisation also does not reach the plate but disappears at S55 as indicated by No. 15 and 16. For these measurements the maximum amplification was used and although there may still be some light produced, the rate of decay is so sharp that it is unlikely to extend much further. In the subsequent results it will also be seen that light of this amplitude does not represent ionisation of any importance.

For a 40 cm gap where breakdown does occur, representative recordings are shown in PL 3, Nos 18 to 22. The initial portion is still the same as before except that the amplitudes are much higher (120 L as compared to 20 - .5 L for the 80 cm gap), and the times are much shorter, representing higher propagation speeds. Additional pulses indicating that ionisation, which will lead to breakdown, is taking place, can be seen but will be discussed later. Important in this set of oscillograms is the coincidence in starting time of current and light from the photomultiplier (when it scans next to the small electrode) as shown by Nos 18 and 19. This coincidence occurred in all cases but is only shown for this condition.

The results with a 5" diameter sphere show that no corona or any ionisation occurs for gap spacings bigger than 38 cm (No. 30 and 31 on PL 3), for a voltage of 300 kV. For 36 cm gap length, corona pulses occur which lead to breakdown but with considerable jitter in the starting instant. For G32.5 the jitter is less and the propagation can be determined as shown by PL 3, Nos 27 - 29. Corona does not occur at gaps bigger than 38 cm because the critical gradient is not exceeded for these conditions due to the more uniform field produced by the 5" sphere. For the 2 inch and ½ inch spheres the critical gradient is exceeded in much longer gaps. When the corona does occur with the 5 inch sphere, it happens at a faster rate and is more intense than with a more non-uniform field as shown in graphs (G4) a and b.

From the shape of the light and the current pulses it seems that no ionisation takes place until a certain instant, which occurs shortly after the critical

gradient has been exceeded. The ionisation occurs by trigger action (which is even more noticeable with more uniform gaps than with a point) because a number of streamers start off from the small electrode almost simultaneously and move across to the plane. No further ionisation pulses occur at the small electrode even if the voltage rises after the start of ionisation (except for the slow rate of rise of voltage to be discussed later), and it appears that the steamers inhibit further ionisation from taking place behind them.

The best explanation is that the start of the corona depends on the presence of a free electron in the volume of air where the critical gradient is exceeded. Since the test gap was always illuminated by the spark gaps of the impulse generator, there were always some free electrons available. The free electron is accelerated to produce an ionising collision which produces more free electrons and hence forms an avalanche. This would, however, only produce one streamer since the electrons either move towards or directly away from the small electrode. Normally there are a few streamers starting simultaneously. This can be due to a number of free electrons being available to start avalanches, but it must also be kept in mind that if high energy photons are released in the first avalanche, they would be able to produce electrons in positions to the side of the original avalanche, since they are not affected by the field. These electrons would then be able to start streamers. Thus a single electron would be able to produce a few streamers if photo-ionisation is possible. (More details about photo-ionisation are discussed later). From the photographic recordings the number of streamers at the critical gap spacing is approximately ten, increasing as the gap length is reduced. Park and Cones[1] estimated an average of 50 streamers with positive corona at 60% of the critical gap spacing with .07 μsec rise of voltage.

The important point is that a number of corona streamers start almost simultaneously and prohibit further streamers from being formed until a change in conditions occurs as will be indicated later.

Pulses occurring .1 μsec and .3 μsec after the start, as seen on the oscillograms taken at maximum sensitivity, e.g. PL 3, Nos 6 - 8 and 13 - 16, are due mainly to reflections of the bright corona light at the small electrode and light from the spark gaps of the impulse generator. For most of the experiments a black cloth was suspended some distance behind the test gap, as viewed from the recording side, to reduce extraneous light pick-up.

The oscillogram No. 23 on PL 3 indicates these light pulses quite clearly with the corona pulse occurring at .58 μsec. For this condition the cloth was behind the gap and the amplitude of the light pulses are approximately .5% of the corona pulse at the small electrode. When the cloth was removed, leaving a black surface approximately 20 feet further back as background, oscillogram No. 24 PL 3 was obtained, giving a slight reduction in amplitude, but more important, occurring approximately 50 nsec later in time. The time difference for the extra distance that the reflected light has to travel is approximately 50 nsec. Thus it seems that one cause of these pulses is background reflections.

With a cloth in front of the small electrode, shielding the first 20 cm of the gap adjacent to the small electrode, the oscillogram PL 3, No. 26 was obtained, showing that the light pulses, occurring at the same time as the start of the corona (.3 μsec) have disappeared, indicating that the normal pulses must be due mainly to reflections in the lens and the lenscap. The first light pulse still occurs because it is produced by the light from the series gap and the gaps of the impulse generator, which were not shielded by the cloth. Excitation due to photons seems to be absent or not recordable at a distance of 30 cm from the point where the corona starts.

The reflections in the photomultiplier lens are thus the main cause of these light pulses, which increase in amplitude as the scanning level approaches the point of intense corona. However, when scanning close to the intense corona they are a small percentage of the corona light occurring at the scanning level and when they occur at the same amplitude there is enough time difference not to cause confusion.

The oscillograms on PL 4 show corona propagation at 600 kV. For the 110 and 85 cm gaps, simultaneous current recordings are also reproduced. The shape of the corona pulses are the same as for 300 kV. The critical gap giving 90% breakdown for 600 kV was 110 cm. These oscillograms have been included mainly to illustrate the transition to breakdown discussed in the second part of the results.

5.1.2. Discussion of Graphs.

Before a description of the method of corona propagation is given, it is necessary to consider the different speeds and amplitudes of the corona as supplied by the graphs for various conditions of the variables.

The graphs were plotted from oscillographic results as described in 5 - 1 - 1. To obtain the value of each point the average of at least four oscillograms were taken. In cases where a considerable spread occurred the range of values obtained are indicated by a line instead of a point. It was very seldom necessary to take more than eight recordings to obtain a reliable average.

Graph G1. This graph represents the corona propagation at 150 kV when the voltage rise-time is .22 μsec and the small electrode a point. In part (a) the distance from the point is plotted against the time of occurrence of the corona at that position, for different values of gap length. For this voltage and electrode shape 90% breakdown occurred at a gap spacing of 30 cm. The voltage applied to the test gap is shown on the same time scale.

In part (b) of the graph the amplitude of the corona pulse at different distances from the point for the corresponding gap lengths of part (a) are shown.

The first point of importance to notice is that the corona starts at practically the same instant on the voltage wave, independent of the gap spacing. This occurred when the voltage had only risen to 50 kV, and is due to the fact that the maximum gradient at the point is more dependent on the actual value of the voltage than the gap length.

In all cases only a single corona pulse occurred. As the gap spacing is reduced, it can be seen that the time to cover a certain length is reduced, which represents an increase inspeed. At the same time the peak amplitude of the corona is increased with reduction of gap length. For the 60 cm gap the speed is the lowest, starting at 4×10^7 cm/sec, and decreasing to approximately 1.5×10^7 cm/sec at 20 cm from the point. On part (b) the curve shows that the corona light is about 20 L at the start and disappears between 15 and 20 cm. from the point. As the gap is reduced the corona extends slightly further, at higher speeds and bigger amplitudes. It was never found to extend further than 35 cm from the point, with a minimum speed of 1.5×10^7 cm/sec occurring just before it disappears. This seems to be the minimum speed at which positive corona can occur.

For gap spacings of 30 cm and less, part (b) shows that the corona reaches the plate with some amplitude. The shorter the gap, the larger the amplitude. For gaps longer than 30 cm the amplitude decays gradually across the gap, while from 30 to 15 cm the amplitude tends to remain more constant in its movement across the gap. For the 10 cm gap the amplitude increases rapidly. Also important to notice for gaps less than 30 cm is the rise in amplitude over the last few cm before the plane is reached. Comparing part (b) with the fact that the critical gap is 30 cm, it seems that if the corona reaches the plate with an amplitude in excess of 1 L, breakdown is likely to occur.

At the critical gap spacing the speed is almost constant, being 5×10^7 cm/sec at the start and 4×10^7 cm/sec at the plate. For shorter spacings the speed increases as it moves across, especially over the last few cm, corresponding to the increase in light amplitude. The maximum speed recorded (for the 10 cm gap) was 2.5×10^8 cm/sec.

The propagation in this case is difficult to analyse theoretically because the sharp point makes the field distribution difficult to calculate and also

because the propagation occurs under increasing voltage conditions from the start at .3 μsec until .5 μsec. It must be kept in mind that the field intensity and distribution existing at the instant when the corona occurs at the point are the factors determining the starting speed and amplitude.

The electromagnetic field is propagated at the speed of light (3×10^{10} cm/sec) which is so much faster than the corona speeds that the field distribution can be taken to vary instantaneously with the voltage (neglecting space-charge effects). Hence, as the corona moves along into lower field strengths, the reduction in gradient is less than it would have been if the voltage remained constant after the start, instead of rising until .5 μsec.

In order to make conditions more calculable, it was necessary to obtain results for propagation under constant voltage conditions. This can be obtained either by using a more uniform field or by using a faster rise-time. A faster rise-time is the more desirable method since different field distributions can then be investigated, but it is more difficult to obtain.

A compromise between the two was the best solution, giving a small electrode of ½ inch diameter with a rise-time of .07 μsec. To show the influence of the more uniform field given by the ½ inch sphere, graph G2 has been included giving the corona propagation with .22 μsec voltage rise.

Graph G2. The general shapes of the curves are the same as on G1. The main differences are that the initial speeds and the speed at the critical gap spacing are higher although the maximum and minimum speeds are practically the same at 2.5×10^8 and 1.7×10^7 cm/sec respectively.

The critical gap spacing was found to be 31 cm, with the speed varying between 8×10^7 and 1×10^8 cm/sec. Because the field intensity at the sphere was more influenced by the gap spacing, the corona started earlier and at a lower voltage as the gap was reduced. For a 50 cm gap the corona started at 75 kV and for a 10 cm gap at 50 kV, so that for all the gaps shown the

corona started while the voltage was still increasing. When the gap was 60 cm the corona started after the voltage rise in the time rang 1 - 7 μsec with the same minimum speed as before.

The extent of the corona is slightly more than before, being recordable up to 40 cm from the point. The amplitudes are considerably higher, especially at the small electrode, for large spacings but they are about the same for a 15 cm gap and slightly less for the 10 cm gap.

Graph G3. With a risetime of .07 μsec it was possible to obtain conditions where the start of the corona, for the critical gap spacing, only occurred after the voltage had reached the maximum.

The shapes of the curves follow the same pattern as before, but with still higher speeds and amplitudes than for the previous conditions. The minimum speed at the extinction of the corona for 50 and 60 cm gaps is still the same at 1.5×10^7 cm/sec but at the critical gap spacing (31 cm) the speed is approximately 1.6×10^8 cm/sec, while the maximum speed for the 10 cm gap is 5×10^8 cm/sec.

The corona amplitude is considerably higher for all gap spacings as compared to the previous conditions and it is important to note that although the corona reaches the plate at spacings much larger than the critical (40 cm) it does not necessarily lead to breakdown.

The important points indicated by graphs G1, G2 and G3 are that the critical gap is almost the same at 30 to 31 cm, although the corona varies very widely. In all cases the corona bridges the critical gap length, so that this seems a necessity if breakdown is to occur. However, the corona can reach the plate with considerable amplitude and speed, but still not lead to breakdown.

In the second part of the results concerning breakdown it is shown that the transition to breakdown also depends on the rate of decay of corona amplitude in going from the small electrode to the plate.

All the recorded propagation speeds fall in the range 1.5×10^7 cm/sec to 5×10^8 cm/sec with the

amplitudes ranging from .05 L to 200 L.

Graph G4. The corona was investigated at 300 kV to determine whether any basic changes in the propagation occur. For this voltage it was not possible to use the .07 μsec rise-time and the .25 μsec rise-time had to be used. For the smaller electrode ½ inch, 2 inch and 5 inch spheres were used.

The results for the ½ inch and 2 inch spheres show correspondence respectively with the point and ½ inch sphere at 150 kV.

The maximum and minimum speeds with the ½ inch sphere are 2×10^8 and 1.5×10^7 cm/sec respectively, and with the 2 inch sphere 4×10^8 and 1.5×10^7 cm/sec. respectively.

With the ½ inch sphere the corona starts between 100 and 150 kV, while with the 2 inch sphere the start is at 240 kV for the 40 cm gap and at 300 kV for the 80 cm gap. For the 2 inch sphere propagation thus occurs almost under constant voltage conditions.

The critical gap at this voltage for the ½ inch and 2 inch spheres was 60 cm. The corona speed for this gap was 1.5×10^8 cm/sec at the start and 7×10^7 cm/sec at the end for the ½ inch sphere and $2.5 - 2.0 \times 10^8$ cm/sec for the 2 inch sphere.

With the 5 inch sphere corona only occurred for spacings of less than 39 cm, with a speed of 3×10^8 cm/sec for a 32.5 cm gap (also described in 5 - 1 - 1).

Part (b) of the graph shows that for the critical gap of 60 cm the corona reaches the plate with a substantial magnitude of 10 - 20 L. For an 80 cm gap it disappears at 50 cm with the ½ inch sphere but with the 2 inch sphere it can in some cases just reach the plate with a magnitude of 1 L.

Graph G5. At 600 kV the corona was recorded for gaps in the region of the critical gap, which was found to be 110 cm. The fastest speed for the 85 cm gap was 3×10^8 cm/sec and the slowest speed for the 120 cm gap was 4×10^7 cm/sec. For the critical gap

the initial speed was 2 x 10^8 cm/sec at the start and 1 x 10^8 cm/sec at the end. For this gap the corona reaches the plane with an amplitude of about 5 L.

This graph has been included mainly to show the relation between corona and breakdown and will be discussed again later.

Graph G6 (a). In order to determine the length of the corona light volume more accurately than by measurement of the duration of the light pulse and the speed of movement, a series of recordings with different slit widths were made. The measurement was done with a 35 cm gap at 150 kV for .25 μsec risetime with a point and a ½ inch sphere as small electrodes. The scanning position was constant at 10 cm from the small electrode with a slit length of only .2 inch. This was done to reduce the number of streamers recorded. The width of the slit was varied from the normal .01 inch to .25 inch producing a scanning volume at least 25 cm long and 3 cm wide with the height varying from .15 cm to 4.5 cm. If a ball of light, 1 cm diameter, were to pass through the scanning volume in a vertical direction the amplitude recorded would be proportional to the height of the scanning volume, provided the height is a small percentage of the ball diameter. Hence a graph of light amplitude against height of the scanning volume would be a straight line for small heights.

If the height is increased to the diameter of the light ball, the light amplitude will reach the maximum since any further increase in the height will produce the same amplitude and only increase the time length of the light pulse.

By measuring the height at which the increase in amplitude stops, the vertical height of the ball can be determined more accurately, since this measurement is less dependent on the response time of the recording apparatus. The results for this measurement are shown on graph G6(a) where the slope is constant up to 1 cm for the point and 1.2 cm for the ½ inch sphere. After a short level portion, the amplitude

again starts to rise as the height is increased because more than one light volume occurs in the scanning volume at the same time. This measurement indicates that the length of the light volume is approximately 1 cm, which by the pulse length method could only be said to be less than 5 cm. Since this method is cumbersome it was not checked for other conditions but it seems that a length of 1 cm can be taken as the length of the corona ball, especially for gap spacings of the order of the critical gap.

Graph G6 (b). To investigate the occurrence of corona for slowly rising voltages, a 150 kV voltage with a rise-time of 3 μsec (PL 5, No.1 and 2) was applied to a gap with the ½ inch sphere as the small electrode. In most cases a single corona pulse occurred for gaps bigger than 35 cm as shown in PL 5, Nos 3 - 6. These simultaneous recordings of corona light and current show the representative spread in the time of occurrence of the corona. The later the time of occurrence, the larger were the current and light pulses observed.

The peak currents of the corona pulses for different gap lengths plotted against time, are shown in G6 (b). The voltage waveshape is included on the same time scale so that the voltage at which the corona occurred, can be easily determined. The general tendency for all the gap spacings is an increase of current amplitude as the corona occurs later in time, at a higher voltage. Especially at the smaller gap spacings there was a reasonable amount of spread of ± 20% in the readings and the values are indicated as an area instead of an average line.

These results indicate clearly the trigger action of the corona which suddenly occurs at a certain instant and then prevents further pulses even if the voltage is subsequently doubled (Pl 5, Nos. 3, 4 & 6.)

If the voltage rises to more than double of what it was at the start of the corona, it is possible for further pulses to occur (PL 5, No.5). This is the normal condition for the 30 cm gap and representative

oscillograms are shown on PL 5, Nos 7 - 12 for a 29 cm gap.

The secondary current pulses are smaller in amplitude than the first but the proportion of light produced some distance from the ½ inch sphere alters. The light due to the secondary pulses can be more than that due to the first e.g. PL 5, No. 8 and 10. At a distance from the point the light pulses always occur later in time than the current pulses, indicating that the origin of all the pulses is at the electrode.

The most likely explanation is that the first corona pulse forms a space charge, which is able to suppress further ionisation until the voltage has approximately doubled. When the voltage has doubled, a further pulse can occur, which, due to the space charge, is weaker at the start but when it reaches the end of the first corona it occurs at a relatively larger amplitude and extends further e.g. No.11. The first part will be easier to traverse because it can occur along a previously ionised path. More is said about the space charge later.

The speeds and extent of the initial corona were measured but because of the variations due to the different voltages at the instant of occurrence, it is difficult to represent graphically. The speeds were all within the range obtained for the faster rise-times and the gap was only bridged for gaps slightly longer than the critical gap of 27 cm.

For a gap of 20 cm the first corona pulse was strong enough to cross the gap and initiate the breakdown mechanism before a second corona pulse occurred, as shown on PL 14, No.10, and will be discussed in the second part.

Most of the corona pulse amplitudes fall in the range 1 - 2.5 amps for gaps from 20 to 50 cm. Only at the critical gap spacing of 30 cm were larger peak currents up to 6 amps obtained but even for this condition, the amplitude of most of these pulses were less than 2.5 amps.

It appears that the corona starts as soon as there is a free electron available in the volume where the critical gradient is exceeded. As the volume increases the probability of an available electron increases and the corona normally occurs at a voltage less than 130% of the minimum at which corona can occur. The peak current amplitude seems to increase proportionally to the amount of voltage in excess of the minimum corona voltage.

5.1.3. Summary (G1 - G6).

In the range 150 - 600 kV the positive corona propagation seems to be basically the same for rise-times of .07, .25 and 3 μsec. The maximum and minimum speeds were 5×10^8 and 1.5×10^7 cm/sec.

At the critical gap spacing the speeds were approximately 2×10^8 cm/sec when the corona started on the peak of the voltage, decreasing to 5×10^7 for very non-uniform fields when the corona started at 30% of the peak voltage.

The amplitudes of the corona at the plane for the first condition above for a speed of 2×10^8 cm/sec are in the range 15 - 25 L decreasing to 2 - 10 L for the latter condition.

G6 (a) indicated that the length of the light volumes of the corona streamers are about 1 cm and from photographic recordings their width is of the order of 1 mm.

Only for the 3 μsec rise did multiple corona pulses occur, indicating the trigger and suppresion actions and showing that the peak amplitudes are proportional to the amount of overvoltage. From graph G13 a it can be seen that the peak value also depends on the rate of rise of the overvoltage and will be referred to in the explanation of the corona mechanism.

5.2 NEGATIVE CORONA.

5.2.1. Oscillograms (.25 μsec rise-time).

The oscillograms on PL 6 show representative corona pulses when a negative voltage of 300 kV was applied to the gap. The waveshapes are similar to

those obtained for positive corona, but for equal gap spacings the peak amplitude was considerably less. Representative voltage waveshapes are shown in No.1, 2 and 3 for different sweep speeds.

The corona current with a 2 inch sphere for a 30 cm gap is shown in No.4, indicating a capacitive current of about 3 amps at .1 μsec, while the corona current starts at .14 μsec with a peak value of 7 amps decaying to practically zero in .4 μsec at .55 μsec. This is the same rate of decay as obtained for the positive corona. Oscillograms Nos 5 - 10 show the corona light pulses at different points in the gap, indicating the corona growth along the whole length of the gap.

Oscillograms Nos 16 - 19 indicate corona for a 30 cm gap with the ½ inch sphere. The corona pulse starts very early on the voltage wave at about 50 kV and for this condition a second corona pulse occurs at .25 μsec, following the first across the gap. This second pulse occurs when the maximum voltage is reached and seems to move slightly faster than the first but keeps the same relative amplitude. For this condition the Corona disappeared about 10 cm from the ½ inch sphere.

When the gap was reduced to 20 cm, the two corona pulses again occurred at about the same times with slightly more amplitude, but now extending across to the plane (Nos 11 - 15). For the sensitive recordings Nos 14 and 15 at .1 L/div. the corona pulse is slightly obscured by reflected light from the bright corona at the sphere, but can be distinguished at .18 μsec on No. 14 and .22 μsec on No.15. The reflected light is more troublesome for the negative corona because the rate of decay of corona light is much more rapid with distance and also occurs at a fast speed for low illumination, in comparison to the positive corona. However, sensitive enough recordings could still be made.

For the negative voltage the critical gap depended considerably on the size of the small electrode. The critical gap with the 2 inch sphere was found to be 26 cm and with the ½ inch sphere only 18 cm. For

a similar change with the positive polarity the change in critical gap length was not more than 10%.

The oscillograms on PL 7 show the negative corc propagation, with simultaneous current recordings, for the critical gap at 600 kV with the 2 inch sphere as small electrode. Only a single corona pulse occurred and the movement can clearly be seen. The amplitude of the reflected light is considerable for Nos 6 - 11, but the corona can be observed at .2 μsec for No. 7, .3 μsec for Nos 8 and 9, .4 μsec for No.10 and .4 μsec for No.11. No. 12 indicates the reflected light with no corona pulse occurring. The pulses occurring after .5 μsec are those leading to breakdown and will be discussed later.

5.2.2. Graphs (.07 and .25 μsec rise-time).

The results for the negative corona were plotted in the same way as for the positive corona on graphs G7 - 12.

Graph G7. The propagation at 150 kV, for different gap lengths, using a point electrode with .07 μsec rise is shown on graph G7. As with the positive corona the start was on the rising slope of the voltage at about 50 kV. The striking point about these results is that the corona speed is almost independent of the gap length, varying only from 6×10^7 to 1.5×10^8 cm/sec for a change in gap length from 30 to 10 cm with a very divergent field.

Part (b) of the graph shows that the corona intensity decreases very rapidly as it moves along and only reaches the plate for the critical gap spacing of 10 cm. For larger gap spacings the corona only extends about 10 cm into the gap.

Graph G8. When the ½ inch sphere was used as the small electrode at 150 kV the corona started just before the voltage had reached the maximum, at between 125 and 145 kV. In part (a) the propagation of both the start and the peak of the corona are shown. The speeds in both cases are similar and the speed variations are even less than for G7 for different gap lengths. The speeds

increased slightly from 1 x 10^8 cm/sec for a 40 cm gap to 2 x 10^8 cm/sec for a 10 cm gap, which was the critical gap spacing.

The corona amplitude at the start was approximately doubled but the same rapid decrease of amplitude occurred. The corona extended slightly further to between 10 and 15 cm from the point but although the corona reached the plate with more intensity for the 10 cm gap, the critical gap was practically the same at a spacing of 10 cm.

The same condition as for the positive corona seems to apply, where breakdown cannot occur if the corona does not reach the plate but if the corona reaches the plate, even in some instances with reasonable amplitude, it does not mean that breakdown must follow.

Graph G9. At 300 kV the negative corona is plotted for a 2 inch and a 5 inch diameter sphere. The voltage rise-time was .25 μsec and for the 2 inch sphere the propagation was under increasing voltage conditions, while for the 5 inch sphere the voltage had almost reached the maximum. The speeds are in the same range as at 150 kV, the minimum recorded being 1 x 10^8 for the 30 cm gap and the maximum 3.5 x 10^8 cm/sec for the 20 cm gap with the 2 inch sphere and the 25 cm gap with the 5 inch sphere.

The amplitudes decay sharply as before and the corona reaches the plane, at spacings larger than the critical, with recordable amplitude. The critical gap for both the 2 inch and 5 inch sphere was found to be 26 cm, although the corona for the 5 inch sphere was considerably more intense than for the 2 inch sphere for equal gap spacings.

Graph G10. At 600 kV the corona was only recorded for gaps just at and above the critical gap spacing of 55 cm, to show that the mechanism remains the same as at lower voltages.

The small electrode was the 2 inch sphere and the corona started at 250 kV. The maximum speed was 2.5 x 10^8 at the start and 1.2 x 10^8 cm/sec on

reaching the plate. Interesting to note is the fairly rapid change in speed in the vicinity of .25 μsec, coinciding with the time at which the voltage stops increasing, confirming the statement that the field distribution in the gap, neglecting space charge, varies instantaneously with the applied voltage.

Part (b) shows the general sharp decrease of amplitude with distance and corresponding with the previous cases, where the corona started early on the voltage rise, the corona just manages to cross the gap at the critical gap spacing. As in all previous conditions when the corona reached the plane, there is an increase in amplitude over the last few centimetres. For the 60 cm gap the corona does not bridge the gap and disappears at 40 cm from the 2 inch sphere.

Photographic Recordings:

At this point it is advisable to consider a few photographic recordings of the negative corona. On PL 8, corona is shown on Nos. 1, 4, 5, 6, 12 and 14. The other records include ionisation leading to breakdown and are discussed later.

The corona at 150 kV with the ½ inch sphere is shown on Nos 12 and 14 for gaps close to the critical gap spacing. The corona consists of a number of streamers extending radially from the sphere, with one or two extending across to the plane, while the others disappear at some distance from the sphere.

With the ½ inch sphere at 300 kV the steamers also form a hemispherical volume of streamers extending half way across the gap. At gaps just above the critical, some of these streamers manage to cross to the plane as shown in Nos 1 and 2. The same condition occurs with the 2 inch sphere except that the critical gap is larger, as shown in No. 6.

With the 5 inch sphere as small electrode the streamers are less and also occur almost directly towards the plane, in comparison to the previous cases where some streamers can travel in directions almost parallel to the plane. No. 4 shows the corona for a 40 cm gap and No. 5 for a 30 cm gap. The critical gap length was 26 cm. It appears that 4 or 5

streamers are formed in an area of about 1 cm diameter on the sphere. This tends to confirm the theory that the different streamers are started by photon generated electrons (Ch. 5 - 1 - 1), since it seems unlikely that five free electrons will be in the one small area next to the sphere and none in the rest. These photons would mainly produce electrons in the close vicinity of their origin. Due to the space charge of the first avalanche relieving the stress at the sphere, the sideways electron formation due to photons from the secondary streamers does not start new streamers.

5.2.3. Graphs (3 μsec rise-time)

Graph G11: When the slowly rising voltage wave at 150 kV was applied to the gap, using the ½ inch sphere, three corona pulses were obtained for gap spacings close to the critical spacing. The light amplitudes at different distances from the sphere are plotted against the position of occurrence for the different lines at which the pulses occurred and are shown in G11 (a,b,c and d) for gap spacings of 12, 11, 10 and 9 cm. The percentage breakdown and the average times to breakdown are indicated on each graph.

The curves show that the first pulse occurs regularly at .4 μsec, extending 2 cm into the gap for the 12 cm gap and increasing to 3 cm for the 9 cm gap.

The second pulse occurs regularly at 1.5 μsec for a, b and c and between 1 and 1.3 μsec for d, extending roughly the same distance for the different gap lengths. The amplitudes are also about the same for all four conditions and this second pulse never reaches the plane.

The third pulse occurs at 4 - 6 μsex for the 12 cm gap and normally does not reach the plane. For the 11 cm gap it occurs at 4 μsec and reaches the plane with an amplitude of 1 L, giving 60% breakdown. For the 10 cm gap the pulse occurs at 3 - 4 μsec reaching the plane with considerable amplitude and giving 100% breakdown. For the 9 cm gap the third pulse occurs still earlier at 2.5 - 3 μsec and with a larger amplitude.

The picture represented by this set of graphs show three corona pulses occurring consecutively in

time, while the applied voltage is rising slowly. The first pulse grows 2 cm into the gap, the second about 7 or 8 cm and the third about 10 cm, reaching the plane for spacings equal or shorter than the critical gap of 10 cm.

Graph G12. This graph shows the corona for the slowly rising 300 kV voltage, using the 2 inch sphere, the point and the ½ inch sphere as electrodes. The general picture for the ½ inch and 2 inch spheres is the same as for 150 kV except that the pulses occur slightly later and each pulse extends further into the gap, with the critical gap occurring at 24 cm for both electrodes.

This is a very important point because the critical gap with the .25 μsec rise-time was 18 cm for the ½ inch sphere and 26 cm for the 2 inch sphere, indicating that the corona is extremely important in determing whether breakdown is going to occur or not.

Graph G12 a and c are both for a 20 cm gap which is less than the critical gap and shows that the third corona pulse reaches the plate with considerable magnitude.

When the point was used, another important effect emerged. Breakdown only occurred at a 17.5 cm gap length and then not quickly but normally after more than 40 μsecs. The corona again occurred in bursts but started at a much lower voltage and with no measurable regularity. The overall effect was that the corona grew to the volume shown by graph G12 (b) in about 4 μsec, extending to within 5 cm of the plane.

When the gap was decreased to 16 cm, the corona bridged the gap and breakdown occurred within 8 μsec. For the 17.5 cm gap the corona prevented further ionisation for at least 40 μsec before breakdown occurred. It must be kept in mind that after 40 μsec the voltage has already decayed to about 220 kV (PL 6, No.3), which means that the space charge due to the corona must have undergone an appreciable change to allow breakdown to occur. This may be of importance since this time is about the average of the time taken between steps in the leader of the lightning discharge. This change could be due to recombination or a substantial movement of the space charge volume.

Oscillograms for this condition are shown on PL 10, Nos 6 & 7.

Oscillograms and Photographs:

The simultaneous oscillograms and photographs obtained for a 25 cm gap when a 3 μsec rise 300 kV voltage was applied are shown on PL 9. The voltage waveshapes are shown on Nos 1 and 7. Nos 2 - 6 show the recordings for scanning levels consecutively further away from the ½ inch sphere. The actual scanning level of the oscillogram recording the light is shown by the upper white horizontal line on the photograph. The lower white line indicates the position of the plane.

On set No. 2, where the scanning level was adjacent to the sphere, the current and light pulses are similar in time of occurrence and relative amplitude, except for the oscillatory capacitive current occurring during the initial .5 μsec. As the scanning level moves away from the point, the initial light pulses remain at approximately the same amplitude, indicating that the first pulses do not extend so far as the later pulses, as shown by graphs G11 and G12.

The photographs indicate very concentrated streamers growing in stages from the ½ inch sphere. Between the different stages, best seen on set No. 2, there are dark spaces of about 2 cm. The first stage seems 1 or 2 cm long while the second and third are about 5 cm long. If the ionisation occurred only along the steamers shown photographically, the stress at the end of each should be high enough to continue its growth. However, from the photomultiplier recordings it seems that the corona extends further than shown photographically, e.g. No.5. It also appears that the photomultiplier indicates four stages of growth, while photographically there only appears to be three. If it is assumed that there is a spherical volume of faint corona streamers ahead of the stems photographically visible, it offers a possible explanation since this volume would form a space charge that could prevent further corona until the voltage had risen a further appreciable amount. The bright stems recorded photographically would thus be channels connecting the

invisible ball back to the sphere through volumes which had been ionised before the stems became visible.

It could also be that the corona just occurs around and a bit further than the concentrated streamer and not as a separate stage. However, the additional stage seems a better explanation, also indicated by set No. 4, where the first light pulse at 1.7 μsec would represent the first light recorded at the scanning plane from the second corona stage, which would be invisible photographically. The second pulse at 3.7 μsec would represent the stem feeding the invisible third stage and the pulse at 5 μsec, the stem brightening to feed the invisible fourth stage.

The evidence of a ball or brush discharge appears to be just visible photographically in the set of No.6, for which the photomultiplier recorded a pulse in excess of 16 L.

The occurrence of these photographically invisible volumes of light and the consecutive growth of the ionisation in stages, as the voltage rises slowly, will probably explain most of the uncertainties found in previous photographic investigations[3].

The simultaneous recordings on PL 10 indicate representative recordings for conditions similar to those for which G12 a and c was plotted. Nos 1 - 3 indicate conditions with the voltage chopped before breakdown occurred. Here again three stages are observed by the photomultiplier while only two are seen, photographically shown in No.1. No. 2 (b) indicates light of 1.5 L peak at 2 μsec while on the photograph the light has disappeared about 5 cm before.

Nos.4 and 5 indicate conditions where the voltage was chopped after the corona had bridged the gap and shows that once this has happened, the breakdown occurs in the same way and in approximately the same time as with a faster rise of voltage.

Similar to the positive corona, the negative corona is able to suppress further pulses until the applied voltage has approximately doubled.. This is shown by the times of occurrence of the corona pulses for 150 kV, from G11, of .4, 1.5 and 4 μsec. This

means that the voltages were 40, 100 and 150 kV respectively. The reason why multiple corona bursts occur much more readily than with a small positive electrode is due to the fact that although the corona starts at approximately the same voltage when the electrodes, the gap spacings and the rise-times are the same, the distance of growth is much less for a small negative electrode. This also results in a much smaller critical gap spacing for the negative polarity.

Since the corona was investigated in the region of the critical gap spacing, the spacings used with the negative sphere were approximately half of those with a positive sphere. If the spacing with the negative sphere is equal to the positive critical gap spacing, the same number of corona pulses will occur for both polarities, but with the positive corona extending much further. If the spacing were equal to the negative critical gap spacing, the positive corona would start at the same voltage but extend across the gap and initiate ionisation leading to breakdown before the voltage had risen to a point where a second corona pulse would be produced.

5.3. CORONA CURRENTS:

Graphs showing the peak corona currents plotted against gap spacings are shown on G13 for the different conditions of the variables.

The general tendency is an increase of peak current as the gap spacing is reduced. This tendency is more marked with the fast rise-times than with the slow rise-times. The effect of the rise-time is to increase the peak current as the rise-time is decreased. As the diameter of the small electrode is increased, the peak current amplitude also increases.

The two important conditions determining the starting magnitude are: (1) the rate of rise of over-voltage, determining the stress in excess of the minimum required for the production of ionisation (24 kV/cm), at the instant when the corona is triggered off, This is determined by the rate of rise of voltage. (2) The divergence of the field. When the field is very

non-uniform the amplitude is less than with a more uniform field.

For the negative polarity the peak magnitude is less than with the positive polarity for the same conditions, although the starting instants are about equal.

5.4. EXPLANATION OF THE CORONA MECHANISM.

A summary of the observed corona speeds is given in table 3. This shows the wide range of speeds for positive corona from 1.5×10^7 cm/sec to 5×10^8 cm/sec.

At the critical gap spacings the corona speeds fall in the range 4×10^7 to 2.5×10^8 cm/sec for positive corona and $1 - 2.5 \times 10^8$ cm/sec for the negative corona. The slower speeds were obtained when the corona started on the rising slope of the voltage wave. Except for very non-uniform fields, the propagation speeds with a rise-time of less than .3 μsec are similar for positive and negative corona, for the critical gap spacing, and are in the range $1 - 2.5 \times 10^8$ cm/sec.

Although the speeds of propagation at critical spacing are similar, the extent is much less for the negative corona, resulting in a much shorter critical spacing, since it has been found that no breakdown can occur unless the corona bridges the gap. This shows that there must be a localised charge effect determining the motion of the corona because the field distribution is the same for both polarities when space charge is neglected.

The corona propagation appears to be due to a combination of photo-ionisation and the electron avalanche mechanism, described by Loeb and Meek[9], taking the space charge effect of the avalanche into account.

5.4.1 The Electron Avalanche and Streamer Theory of the Spark:

The theory which has been developed for spark development by Loeb, Meek, Raether and others[9] p. 252 is called the streamer theory of the spark. It is based on considerations of individual electron avalanches,

TABLE 3

	POSITIVE CORONA:			NEGATIVE CORONA:		
	150 kV	300 kV	600 kV	150 kV	300 kV	600 kV
Maximum Speed cm/sec.	5×10^8	4×10^8	3×10^8	2×10^8	3.5×10^8	2.5×10^8
Minimum Speed cm/sec.	1.5×10^7	1.5×10^7		6×10^7	1×10^8	1.2×10^8
Speed at Critical Gap Spacing cm/sec.	4×10^7 - 1.6×10^8	7×10^7 - 2.5×10^8	1×10^8 - 2×10^8	1.5×10^8 - 2×10^8	2×10^8 - 3.5×10^8	1.2×10^8 - 2.5×10^8
Critical Gap Length cm.	30	60	110	10	25	55

TABLE 3

	POSITIVE CORONA:			NEGATIVE CORONA:		
	150 kV	300 kV	600 kV	150 kV	300 kV	600 kV
Maximum Speed cm/sec.	5×10^8	4×10^8	3×10^8	2×10^8	3.5×10^8	2.5×10^8
Minimum Speed cm/sec.	1.5×10^7	1.5×10^7		6×10^7	1×10^8	1.2×10^8
Speed at Critical Gap Spacing cm/sec.	4×10^7 $- 1.6 \times 10^8$	7×10^7 $- 2.5 \times 10^8$	1×10^8 $- 2 \times 10^8$	1.5×10^8 -2×10^8	2×10^8 $- 3.5 \times 10^8$	1.2×10^8 $- 2.5 \times 10^8$
Critical Gap Length cm.	30	60	110	10	25	55

the transition from an avalanche into a streamer and the mechanism of advance of the streamers. It involves ionisation processes due to electron collisions, photo-ionisation and space-charge field effects caused by the avalanches and streamers.

In the avalanche process, an electron with sufficient energy produces one or more free electrons on collision and these in turn, when they collide, produce more electrons. In a uniform field this cumulative process will continue across the length of the gap, leaving behind it an increasing density of positive ions.

In a non-uniform field this process may not continue across the gap because the avalanche moves into a weaker field and a condition may be reached where the collision energy is not enough to produce a multiplication of electrons and the avalanche thus disappears.

This avalanche process occurs in air that has not previously been ionised and for its start depends on the availability of a free electron. The corona observed show exactly these characteristics. The only difficulty lies in the speed of propagation. For a single electron avalanche the speed of propagation of the tip is that of the drift velocity of the electrons. In a field of the magnitude required to cause breakdown, the electrons travel at a speed of the order of 2×10^7 cm/sec, while the positive ions move at 2×10^5 cm/sec[9] p. 253. Schonland's estimate[7] of the drift velocity in a field with the critical gradient is 4×10^7 cm/sec with a mean free path of about 4×10^{-5} cm, while Park and Cones obtained a drift velocity of 2×10^7 cm/sec in a field of 100 kV/cm.

These speeds are just equal to the minimum observed for the positive corona but are considerably less than the corona speeds for breakdown conditions, which are $1 - 2.5 \times 10^8$ cm/sec.

Schonland calculated that the field strength required for an avalanche speed of 2×10^8 cm/sec is 8,000 kV/cm, which seems unlikely to be produced by any space charge effect.

It is also important to note that for a velocity of 4×10^7 cm/sec and a mean free path of 5×10^{-5} cm the average energy before collisions is

2.5 EV, while the ionisation energy required is 14 EV[7].

The final velocity for an energy of 14 EV is given by

$$v = 5.93 \times 10^7 \sqrt{EV}. \text{ cm/sec (ref:10, p.26)}$$
$$= 2.2 \times 10^8 \text{ cm/sec.}$$

which gives an average velocity in the range observed for the corona. Thus the indication is that the distance between ionising collisions is more than generally estimated or that the space charge field strength is extremely high at the tip of the avalanche.

The only other means by which such a high speed of propagation can be obtained is by photoionisation in the volume ahead of the avalanche tip from photons produced by the avalanche. Photoionisation can definitely occur in sparks as indicated by light shielding of the gaps of an impulse generator, which produces very irregular triggering, as opposed to the regular triggering when the gaps are in sight of each other. However, very little is known about the amplitude and extent of the photoionisation. The only information available is that of the absorbtion of light by gases[9] p. 12.

The following first ionisation potentials for the gases of air have been obtained (Ref: 9, p. 10).

H_2	15.6 EV
H	13.5
N_2	15.6
N	14.5
O_2	12.5
O	13.6

The wavelengths for these ionisations are in the range 800 - 1,000 angstroms.

Apparently no cumulative photon effect can occur and the photon cannot release part of its energy. Thus for photoionisation to occur, excitation at an energy in excess of the minimum ionisation potential must occur, producing a photon with enough energy to produce ionisation when the photon is completely absorbed.[10] p.395 425.

In a mixture of gases such as air, this can happen quite easily since an excited state of the one gas can have a higher energy than the ionisation potential of

another gas[9] p.19. Thus excitation of an atom in the head of the avalanche may produce a photon, travelling at the speed of light, which will be absorbed in the volume ahead of the avalanche to produce an electron which can start a new avalanche in the increased field intensity produced by the space charge of the original avalanche.

Due to the movement of the photon at the speed of light, speeds higher than the drift velocity can be obtained. The propagation speed is limited by the average distance that the photons travel, and the time taken for the photon-produced electron, to be accelerated, to produce a collision providing another photon, with enough energy for photoionisation.

It thus seems that the corona is an avalanche effect moving into the gap with the speed of movement enhanced by photo-ionisation. The action of an avalanche takes place in the tip where new electrons are produced and light is given off by excitation collisions. In the region behind the tip the stresses are lower and no excitation or ionisation is produced in it. Thus an avalanche will appear to be a ball of excitation moving across the gap.

The start of the corona depends on a free electron being available in the volume where the critical gradient is exceeded. Once an avalanche has started it grows in concentrated fashion into the gap. To explain this movement it is necessary to consider the influence of polarity and the formation of the space charge.

5.4.2. Negative Corona.

With a negative small electrode the electrons of the avalanche move in the same direction as the head of the avalanche. When an ionising collision occurs the electron and the positive ion produced are still in close vicinity of each other, and considered with respect to the field distribution, does not produce any change. However, due to the forces of the field, the electron is forced away from the small electrode while the positive ion is pulled towards it. Due

to the much slower mobility of the positive ion, it can be considered stationary in relation to the electron. After a short time the electron has moved so far away from its positive ion that it acts as a unit charge and produces a field around it which is superimposed on the existing field distribution. The head of the avalanche is made up of a large number of these electrons which are forced away from the small negative electrode. These electrodes are in the form of a negative cloud producing a higher stress ahead of itself. In addition, the electrons repel each other and do not stay in a concentrated volume but tend to move into positions where they reduce high gradients.

If photoionisation is produced ahead of the avalanche, the increased field due to the space charge will enable the electrons to start new avalanches. However, for the negative corona it does not seem essential for photoionisation to occur to produce the high speeds of propagation, if an avalanche tip field strength of 8,000 kV/cm is assumed, or if the electron mean free path is taken to be longer than generally assumed.

From the corona observations it is seen that the intensity of the corona decreases rapidly as it moves away from the small electrode. With a negative avalanche positive ions are left behind. The intensity of the positive ions depends on the intensity of ionisation in the head of the avalanche when it passed the point considered. Thus if all the electrons are considered to be carried away in the head of the avalanche, a positive space charge distribution will be left behind, which will be intense at the small electrode, decreasing with distance from the electrode. Although the negative space charge in the avalanche tip will reduce the field behind it, the positive space charge will tend to increase the field at the small electrode and lead to further ionisation.

If the movement is by electron movement only. the speed of movement of the charge will not alter rapidly when ionisation stops and practically all the electrons will be found in the tip. Thus it seems that if all the electrons are assumed to be in the tip, the positive charge left behind must produce further

ionisation. This is, however, opposite to the observed mechanism where the corona is able to suppress further ionisation even for a substantial increase in applied voltage.

This can only be explained if the electrons are considered to move slower than the head of the corona. If photoionisation occurs it is not necessary for the electrons to move at the speed of the head of the corona. If the electron movement is taken to be substantially slower, itis seen that the field distribution will be the same as before the avalanche,because each electron will be cancelled by its positive ion. If relative movement of the electrons are taken into account, considering the decrease in intensity with distance from the electrode, it can be seen that there is a slight excess of electrons in all positions, producing a negative space charge. At any position, after a short time, the electrons will be those produced in a volume slightly closer to the small electrode where the intensity was a bit more. The only position where a high field may be generated is at the small electrode where there may be no electrons to cancel the effect of the positive ions, but it is quite likely that secondary electrons produced by the positive ions bombarding the electrode, will keep the gradient below the critical.

It seems that the most likely explanation of the negative corona is that of a volume of ionisation moving into the gap at a speed substantially higher than that of a free electron. The high speed is obtained by photoionisation and a localised increase in field intensity due to the separation of the electrons and positive ions in the head of the corona. In the volume behind the corona ball, electrons and positive ions are left behind, with an excess of electrons in all positions. These electrons form an overall space charge, because there are a number of corona streamers extending approximately radially from the small electrode, which is able to suppress further ionisation for at least 30 μsec and for almost a doubling of supply voltage after the initiation of the corona.

When the corona does not reach the plate it is

able to suppress further ionisation as described above, but when it reaches the plate the corona ball is reflected back along the same path and by moving up and down consecutively, produce enough ionisation to make the air fully conducting as described in the breakdown process.

5.4.3. Positive Corona:

With a positive small electrode the movement is also away from the electrode, but since it is at a speed of the same order as for the negative corona, it can definitely not be due to the actual movement of positive ions at that speed. If there were a large number of free electrons available the propagation could be explained by an avalanche growing towards the small electrode from a short distance away. The start of this avalanche would produce a space charge that can initiate an avalanche from slightly further away, growing into the first. By continuation of this process the ionisation can grow across the gap. However, the free electron density required for this does not exist and the only mechanism which can account for the high speeds of 1.5×10^7 to 5×10^8 cm/sec observed is photo-ionisation.

For the first ionisation a free electron is required. Once this ionisation has occurred electrons are produced further away from the small electrode by photo-ionisation. These electrons are accelerated to produce ionisation, and photo-ionisation still further ahead. The electrons move towards the small electrode while the positive ions tend to move away. For photo-ionisation in the volume ahead of the corona ball, the electrons produced will move towards the ball and leave behind the positive ions, which due to their smaller mobilities, will form a concentrated space charge. The field concentration will be higher than with a cloud of electrons of the same charge, because the movement due to the repelling action of the positive ions will be less. This explains the easier growth of the positive corona which due to the higher concentration of the space charge, can grow into weaker existing fields, although the amount of photo-ionisation is the same.

The speed of the positive corona ball depends on the average distance, from the origin of the photon, at which photo-ionisation is produced and the time taken for the electrons to produce excitations, in the high field strength region ahead of the ball, which can produce further photo-ionisation.

As with the negative corona there is a decrease in corona intensity with movement from the small electrode, except at very short spacings. In the volume left behind the corona ball, there is an excess of positive ions in all positions due to the movement of the electrons into a region of higher positive ion concentration. This excess of positive ions produces a space charge that makes the field distribution more uniform and can prohibit further ionisation for a subsequent doubling of voltage and for at least 40 μsec.

The decrease of corona amplitude thus indicates the formation of a space charge because the speed of movement without photo-ionisation is slow, and if an electron is not produced by photo-ionisation to cancel the positive ions in the corona ball, they remain in that position as a positive charge.

The corona starting amplitude depends on the amount by which the critical gradient is exceeded before the corona starts. The higher this excess of voltage, the larger the amplitude because the ionisation and excitation due to the first avalanche is more intense. The rate and extent of growth depends on the divergence of the field and the starting magnitude. Basically this depends on the field ahead of the corona ball and the amount of photo-ionisation. The divergence of the field determines the field strength at a certain position ahead of the ball and the intensity of the ball determines the amount of photo-ionisation and the stress to be added due to the space charge effect.

Thus each corona streamer moves as a concentrated ball into the gap and leaves behind an overall space charge effect, which prevents further ionisation in the region behind the corona balls. If the stress ahead of the ball falls below the critical value for the existing photo-ionisation, the fast ball propagation stops, the light production disappears and a slowly

moving space charge is left. The separate corona streamers and the overall ball of space charge effect can be seen on PL 8 Nos. 1, 2, 6, 12 and 14 for the negative corona, and are indicated by the graphical corona results for gap spacings larger than the critical.

5.4.4. Corona with a slowly rising voltage:

With a slow rise of voltage the critical gradient can successively be exceeded because the corona starts close to the minimum voltage at which corona can occur and the propagation stops before the voltage has risen appreciably, because it cannot extend very far. After a time the voltage reaches double the starting amplitude and then the critical gradient is again exceeded, producing another corona pulse extending further into the gap, also occurring under practically constant voltage conditions.

For the condition of a start on the rise of the voltage with a faster rise-time of .3 μsec, the voltage normally reaches the peak before the corona growth has stopped and only one corona pulse occurs.

5.4.5. Formation of Negative Ions:

The decay of the corona current pulse also provides valuable information. For all the conditions observed the corona current pulse had a rapid rise of less than 20 nsec and a complete decay time of .4 μsec. Corona was investigated by Meek and Saxe[5] for the different gases of air and corona pulses were observed in all the gases. The important point is that for oxygen a pulse of very short duration was observed while the decay in the other gases were of the order of 20 μsec or more. This indicates the attachment of electrons to oxygen molecules to form negative ions. Once an electron has been captured to form a negative ion, the mobility is equal to that of a positive ion, and it cannot produce ionisation as before. Thus it loses the property of producing ionisation but retains the property of a space charge. In gases where no oxygen is present the electrons drift into the electrodes producing the slow decay of current. In air, where oxygen

is present the electrons are attached to the oxygen in a time of .4 μsec. During this time the electrons can take part in producing ionisation but after their capture they only maintain the space charge distribution. Due to the slower mobilities the space charge changes much more slowly than would be the case if the electrons remained free. This is probably the reason why the corona can prevent further ionisation for times as long as 40 μsec. (Ref: 1 p. 219 and 5 p. 7 - 9).

5.4.6. Return Ionisation:

When the voltage is switched off for the chopped wave testing, it is possible for return ionisation to occur, because the space charge will produce a potential between itself and the small electrode, which is now at earth potential. Because this path has been ionised by the corona, it is easier for propagation to occur. This can produce streamers on photographic recordings which can be misleading since they are not part of the normal ionisation mechanism. This return ionisation can be seen on the photo-multiplier as a light pulse occurring at the instant of chopping when the photo-multiplier scans the volume between the spare charge and the small electrode. One exception is shown by the recordings on PL 10 Nos 1 - 3, where the light pulses are due to scattered light from the shunt gap. The return pulses can be seen on PL 15 and 16 as a very sharp light pulse at the instant of chopping. It was also observed for recordings of the negative corona but the recordings are not reproduced here as it does not influence the results of this investigation. Normally the return ionisation can be neglected but it is important to keep in mind for photographic interpretation of ionisation.

C H A P T E R V I.

BREAKDOWN

6.1. TRANSITION TO BREAKDOWN:

From the corona observations it was seen that the corona had to bridge the gap before breakdown occurred. However, if the corona bridged the gap, breakdown did not necessarily occur and from breakdown recordings it was found that the factor determining whether breakdown was to occur or not, was the return of the ball of ionisation to the small electrode. When the corona ball reaches the plate it is reflected back and if it manages to return to the small electrode it starts further ionisation which continues until breakdown is complete. If the ionisation ball does not return to the small electrode, breakdown does not occur. The propagation of the return ionisation also depends on the polarity but because it travels along a path that has previously been ionised, the growth is easier than for corona which moves into air that is free from existing ionisation.

The reason why reflections occur is not obvious. It seems to be due to the increase in intensity at the plate, as shown by the increase in intensity of corona in all cases where it reached the plate. This would form a space charge point at the plane which would be able to initiate ionisation movement backwards along the corona path. The increase in intensity may be caused by the reflection of photons by the plate or may be due to a higher stress generated over the last few centimetres by advancing corona space charge.

The stress will depend on the relative increase of capacity because the corona is an isolated charge and the voltage of the corona ball is determined by $V = Q/C$. As the corona approaches the plate, C is increased and hence the voltage will decrease because the charge Q is approximately constant. At the same time the stress will be increased if the voltage remains constant because of the shortening gap spacing. If the stress distribution increases faster than the

increase of capacity, the actual stress will increase and produce increasing ionisation.

The return ionisation never seems to start before the plane is reached because two light pulses are observed even when scanning only one centimetre from the plane and it seems as though there may be a short delay period (approximately 50 nsec.) before the return starts.

Schonland[7(b)] has shown that much higher speeds of ionisation propagation can occur along a length which has previously been ionised.

The velocity of propagation is given by

$$V = n \tfrac{1}{3} \times v \times d$$

where n = original electron density.
v = mean electron drift velocity.
d = length of ionised path.

From this it can be shown that speeds of 1×10^9 cm/sec is possible with a density of 10^3 electrons/c.c. and a length of 6 cm.

6.2. POSITIVE BREAKDOWN:

From the corona observations it was seen that the positive corona grew much further and into weaker fields than negative corona. Thus with a positive small electrode the corona reaches the plate relatively easily but the return ionisation is similar to the growth of negative corona and would not have been able to return if the previously ionised path did not exist. But even with this ionised path it is still possible for the ionisation to disappear on the return journey. For the negative breakdown it will be seen that the return is much easier because it is similar to positive corona and in addition, occurs along a previously ionised path.

The conditions determing the transition to positive breakdown is best shown by G5 and PL 4. The critical gap spacing giving 90% breakdown was found to be 110 cm. From G5 (a) it is seen that for

an 85 cm gap the corona reaches the plate at .5 μsec and immediately the return ionisation starts moving back at a slightly faster speed than the corona, at 5×10^8 cm/sec to reach the small electrode at .65 μsec.

The oscillograms for this condition are shown on PL 4 Nos 12 - 17. The current oscillograms show a second current pulse occurring at .65 - .7 μsec, corresponding to the time of return of the ionisation balls. The light oscillograms show the light pulses occurring closer together, and in time between the two current pulses, as the scanning level is moved towards the plane. G5 (b) shows that for the 85 cm gap the intensity starts at 80 L and decreases to 30 L in the centre of the gap to reach the plate at 120 L. The return ionisation exhibit almost the same intensities.

For the 110 cm gap the corona crosses the gap to the plate at a slower speed to reach it at 1.05 μsec. The balls are again reflected at a higher speed of about 3×10^8 cm/sec to reach the small electrode at 1.5 μsec. This corresponds to the time of occurrence of the second current pulse as shown on PL 4 Nos 1 - 5.

The light oscillograms show the propagation of the corona pulse and the return pulse for Nos 4 and 5. On Nos 2 and 3 the return pulse is not seen because a fast sweep speed was used to show the shape of the corona pulse. G5 (b) shows that the corona starts at 75L and decreases rapidly to reach the plate with an amplitude of about 5L. It is reflected back at an almost constant amplitude to reach the small electrode with an intensity of 10 L.

With the 120 cm gap, where breakdown did not occur, the corona reached the plate with an amplitude almost equal to that for the 110 cm gap, but on the return path the ionisation disappeared at about 35 cm from the small electrode, as shown by G5 (b). The speeds of propagation are much slower and as shown by G5 (a) the speed of the return ionisation is about

4×10^7 cm/sec when it disappears. The representative oscillograms for this condition are on PL 4 Nos 6 - 11, showing that the return pulse has almost disappeared on No. 9 at 3.0 μsec when it was 47.5 from the small electrode. No. 6 shows that there is no secondary current pulse and that no further ionisation occurs.

Thus the requirement for the transition to breakdown appears to be the return of at least one ionisation ball to the small electrode. The return ionisation is also in the shape of an elongated ball as for the corona because the light pulse shapes are the same as obtained for the corona. This return of ionisation was observed for all transitions to breakdown. The correspondence of the light and current pulses, when scanning next to the small electrode, and the occurrence of two light pulses, in time between the first and second current pulses, when scanning close to the plane, are shown by PL 12 Nos 8 and 11; PL 13 No. 7 and 8 and PL 14 Nos 10 and 11.

When the return ionisation reached the small electrode, it started new balls of ionisation moving towards the plane. This up and down movement continued until breakdown was complete. Due to the number of corona balls and the fact that they do not all cross the gap in the same time because of the difference in speeds and length of travel, the up and down movement cannot be distinguished for very long because the ionisation balls are fairly independent of each other, especially after the corona has bridged the gap and some can be moving towards the plane while others are returning. In some cases the overall up and down movement can be distinguished up to three pulses as in PL 12 Nos 8 - 12 but usually the spread becomes so great that only a large number of small pulses are observed, each pulse representing a ball of ionisation either moving up or down. This random nature makes it almost impossible to sort out a single pulse to obtain the speed of movement after the ionisation has been going on for some time. The large number of small pulses, gradually increasing in magnitude, can be seen on all oscillograms of positive

breakdown. Pl 11 - 16. The best examples are given by PL 12 Nos 8 - 14. In No 12 (b) the light pulses occurring during the first two microseconds are shown while No. 13 indicate the pulses for the next two microseconds and No 14 represent the pulses in the time range from 5 - 7 μsec. In all three cases the pulses appear to be almost random with about the same rise and fall time for each separate pulse, while the overall amplitude increases with time.

Once the ionisation has returned to the small electrode a secondary mechanism occurs. This is the formation of the positive leader, which is a volume of intense ionisation growing across the gap at a speed slower than that of the corona. The positive leader is seen on the light oscillograms as a pulse, occurring in time between the corona pulse and the instant of breakdown. It is best shown by the oscillograms on PL 12 and 13 Nos 1 - 6. On PL 13 the leader pulse occurs at 2 μsec for No.1; 3 μsec for No.2; 4.5 μsec for No.3; 10 μsec for No. 4; 10 μsec for No. 5 and 11 μsec for No. 6. This shows the movement of the leader volume across the gap, with a rapid increase in speed and intensity when it comes close to the plane.

The propagation of the positive leader has been extensively studied by Saxe and Meek[5]. The results obtained for this investigation confirm those obtained by Saxe and Meek and provides some additional information. The positive leader has also been studied photographically[1,2], and the relation between the recording methods are given by PL 15 and 16, where simultaneous recordings of current, light recorded by the photomultiplier and the photograph of the ionisation are reproduced. The scanning level of the photomultiplier is indicated on the photograph by the upper white line.

PL 15 shows the growth of the positive leader at 300 kV with a ½" sphere and .25 μsec rise-time for a gap length of 57 cm. No.1 and 2 show results with a time before chopping of 4.5 μsec. The return of the ionisation to the sphere can be seen

at 1.3 μsec on No.1 and at 1.2 μsec for No. 2, and also on the subsequent oscillograms. After this sudden rise, the current increases gradually with only small fluctuations occurring. The slight drop in current between 1 and 1.5 μsec before the chopping instant is due to the spark-over of gap G2 (fig. 6) causing a slight drop in voltage. The 1.5 μsec is the delay in the breakdown of gap G1, after G2 has broken down. (Ch. 2-1-3).

The light oscillogram of No.1 shows the leader pulse occurring at 3 μsec at an amplitude of 20 L, with the light production stopping at the chopping instant of 4.3 μsec. The photograph of the ionisation does not show any corona streamers, due to lack of sensitivity, but shows the positive leader growing from the sphere and branching in two shortly afterwards. The one branch had just crossed the scanning plane while the other was stopped just before it. The longest branch produced the leader pulse on the light oscillogram.

On No.2 the leader was stopped before reaching the scanning plane and no leader pulse was observed. Only small light pulses due to the up and down ball movement were recorded.

Nos 3 - 7 show recordings when the voltage was chopped after 8 μsec. The photographs show that a large difference in the length of leader growth occurs for different sparks and that extensive branching can take place. When branches occur at the scanning plane, multiple leader pulses are observed. If a branch is weaker and slower than the main branch it will reach the scanning plane later than the first and produce a pulse occurring later in time than the first main pulse. If the branches are equal in rate of growth and intensity at the scanning plane, they can produce a single pulse as shown by Nos 4 and 5. For conditions where the growth of the leaders differ extensively as shown by the photographs of Nos 6 and 7, a number of separate leader pulses are observed on the corresponding light oscillograms. The main leader pulse always occurs first and with the largest amplitude.

The corona was photographed, but no recordable traces were obtained as shown by No. 8, except right next to the small electrode. At the scanning plane the photomultiplier recorded a peak amplitude of 12 L_0 but nothing was visible photographically. It is also important to realise the proportions of light intensities between the corona and the leaders. The leaders appear much brighter photographically because the light is concentrated in a few channels while the corona is made up of a number of streamers which occur so close together in time at a scanning plane, that their intensities are added by the photomultiplier, while on the photographs they are recorded as separate volumes of light. Therefore, as shown by PL 15 No.1, although the light oscillogram indicates equal amplitudes for the corona and the leader, only the leader is recorded photographically.

PL 16 indicates the leader growth for conditions similar to those for PL 15 except that the small electrode was the 2 inch sphere. The same mechanisms are indicated but due to the higher intensities the corona can be seen photographically on No.1. The recordings for the leaders are similar to those for the ¼ inch sphere except that the branching was less and with a smaller spread in the times of arrival of the leader pulses.

On this set of recordings another very important effect of the ionisation ahead of the leader can clearly be seen. As the leader moves across the gap the up and down movement of balls of ionisation continuously takes place in the remaining gap volume, with increasing intensity and number of balls of ionisation.

This is clearly shown by the photograms and the light oscillograms Nos 2 - 6. On No. 2 a number of streamers, similar to the corona streamers but more in number, can be seen crossing from the tip of the leader to the plane. On Nos 3 - 6 where the leader has grown further they can be seen to be more intense and much larger in number. These streamers, visible photographically, are indicated

by the continuous pulses on the light oscillograms. No. 6 shows this particularly well, indicating light pulses up to a peak of about 35 L, even before the leader reached the plane.

The leader pulse is seen to consist of a number of sharp pulses similar to the up and down ionisation pulses but just larger in amplitude. It is definitely not a single smooth pulse for every branch, as shown by PL 11 Nos 10 and 11; PL 12 Nos 9 and 10. Thus the leader head seems to be a volume where the up or downward ionisation balls attain an increased intensity in comparison to the rest of the gap. The relation of light intensities before and after the passage of the leader head, for different positions in the gap, are shown by graph G18 a and b. These results are obtained by the superimposition of representative light oscillograms for different scanning levels. Part (a), for a gap 5 cm less than the critical gap, shows that the intensity increases almost equally with time for all positions in the gap when the leader intensity is neglected. Thus the leader head is a volume of strong intensity moving across the gap with an intensity superimposed on the average intensity.

Part (b) shows the same condition except that there is more scatter in the results, because the gap only gave 40% breakdown and consequently there were considerable variations in the initial ionisation. The leader is not a line of light intensity as may be deduced from photographic recordings, but is a reasonably short volume. If the time duration of the pulse at S3 from G18 (a), being from 2.7 to 2.3 μsec, is transferred to G14 (a), it gives a length of about 1 cm; for S5 the length is about 3 cm and for S10 about 4 cm.

This shows that the length of the leader ionisation is in the range 1 - 5 cm with a cross section of less than 1 cm diameter from photographic recordings. The head of the leader is not a volume of ionisation growing into unionised air but is due to the ionising action of the balls of ionisation moving up and down in the gap.

Graphs:

The growth of the positive leader across the gap and the intensity as it moves along for the different conditions of the variables are plotted on graphs G 14 - 17. In agreement with the results of Saxe and Meek[5] it shows that the growth into the remaining portion of the gap, once the ionisation has started, is practically independent of the all variables except the applied voltage.

In contrast to the results of Saxe and Meek the times and distances are not plotted as percentages but are plotted as actual distances vs time before the instant of breakdown. By plotting the results in this manner the consistency of the leader is brought out even more.

Graph G 14 shows that the points for gap lengths from 31.5 to 20 cm all lie on practically the same curve with a relatively small amount of scattering. Even the amplitudes for the different conditions are very close to the average curve. This shows that once the leader has started, its growth is independent of the corona ionisation and only depends on the remaining gap length and the voltage. The leader head acts as an extension of the small electrode and takes the potential of the small electrode with it. This is shown by the fact that when the leader was, for example, 20 cm from the plane, the time to breakdown was 2 μsec whether the gap was 31 or 21 cm. If any noticeable potential drop occurred along the leader channel, this effect would not have been observed.

The leader movement was also recorded when the slowly rising voltage was applied, using the ½ inch sphere or a point as small electrode. The results are shown on G 15 and it can be seen that after 2 cm of leader movement from the start, the propagation fall on the average curve, which coincides with that on G 14. The amplitudes are also close to the average curve, showing that the leader propagation is almost independent of electrode shape and rate of rise of voltage.

Graph G 16 represents leader condition at 300 kV, for different small electrodes of ½ inch, 2 inch and 5 inch spheres, where the same propagation consist-

ency can be observed. For the amplitudes some change in amplitude occurred, but the change was never more than 2 : 1.

The propagation at 600 kV is shown by G 17. It is important to note the change in speed as the voltage is increased. The speed appears to increase by 1.8 for a doubling of the applied voltage. In the following table, the distances covered for equal times of the different voltages are given.

	Voltage (kV)		
Time (μsec)	150	300	600
1	15 cm	27 cm	45 cm
2	20	35	62
3	22.5	42	75
4	25	47	82

Average ratio 1 : 1.8

Representative oscillograms showing the type of recordings from which the readings for graphs G 14-17 were taken are included on plates PL 11 - 14. In the cases where branching occurred, as in PL 11 No.3, the first leader pulse was always taken for the readings because this represents the main leader which will lead to breakdown.

The current oscillograms show the corona pulse and sometimes a small current pulse indicating the return of ionisation and the start of the leader. After this the current increases slowly at first and rapidly later as the leader moves further across the gap. During this increase of current the oscillograms do not show a smooth line but indicate small pulses which are due to the discreet balls of ionisation combining to produce the overall current flow. This is best shown by current oscillograms on PL 12 Nos 1 - 5 and 8 - 12, and PL 14 Nos 6 - 11.

Oscillogram No. 10 on PL 13 shows the increase of current to a peak value of 400 amps at the instant of breakdown and then an exponential decay as the condensors of the impulse generator discharge through the series resistances and the test gap. The peak current

is limited by the series resistance R_S which for this condition was 1125 Ω. The voltage at the instant of breakdown had decayed to 450 kV thus giving an estimated peak current of 400 A.

The variation in the time to breakdown for a positive small electrode thus seems to be due almost entirely to the difference in the time taken by the corona to bridge the gap and for the ionisation to return to the small electrode, where it initiates the leader. In the above it has been shown that once the leader has started, the time to breakdown is very consistent.

The oscillograms on PL 14 have been included to show the start of the leader with a slowly rising voltage. They indicate that the corona intensities are much lower and that it may take up to 2.5 μsec before the ionisation returns to start the leader e.g. No.1. No. 10 shows the corona and the return pulse which initiates the leader. From graph G 15 it has been shown that the propagation after the leader has been established is almost identical for different sparks.

Explanation of the Positive Breakdown:

It has been shown that the requirement for the transition to breakdown is the return of at least one of the balls of ionisation to the small electrode. Once the gap has been traversed in this way there are ionised paths existing and due to the reflection of the ionisation balls at the electrodes, this up and down movement continues with increasing intensity. The leader, which starts as soon as the first ionisation returns to the small electrode, is probably due to the high intensity of the return ionisation, in the high field region next to the small electrode, which produces enough ionisation to provide a fully conducting path over a short distance. This probably occurs when more electrons are produced than can be absorbed by the oxygen to form negative ions. Every time a ball of ionisation reaches the small electrode it will add a short conducting length to the existing conducting path. Since there will be a copious supply of electrons in this length it will transmit a pulse with very low resistance and thus

act as an extension of the electrode. Due to the fact that the ionisation balls moving away from the small electrode will travel along the fully conducting path as far as it extends and then move along the previously ionised paths, the return ionisation will very likely return along the same path. In this way a single fully conducting channel will be formed. When two ionisation balls return simultaneously along different paths they would form two conducting spikes,which can lead to branching.

The largest amount of ionisation will be produced in the region just ahead of the fully conducting path because this is the region of highest stress caused by the action of the fully conducting length. In the conducting paths a small amount of ionisation will be required to transmit the balls of ionisation and in the region towards the plate the ionisation intensity is less due to the weaker field strengths. Thus the leader head volume is the volume of intense ionisation where the ionisation balls form short conducting lengths. By the addition of a short distance to the conducting length every time, the leader grows across the gap. Because the leader is an extension of the point the field strengths increase as the leader grows and the speeds and amplitudes of the ionisation balls and the length of conduction added by each ball is increased. This produces the rapid increase of conduction as the leader approaches the plane.

Because the channel is an extension of the small electrode it determines the field distribution ahead of itself and thus makes the leader propagation independent of electrode size and shape once it has started.

As the voltage is increased the field intensities ahead of the conducting channel is increased and each ball of ionisation will thus add a longer conducting length which explains the almost proportional increase of speed with voltage.

When the leader has bridged the gap the air can conduct the full flow of current. The current is then determined by the series resistance and the voltage.

6.3. NEGATIVE BREAKDOWN:

In contrast to the positive breakdown where the corona crosses the gap relatively easily, with a more difficult return of ionisation, the negative corona finds it difficult to cross the gap while the return is relatively easy. For transition to breakdown the return of ionisation is also required, but because the return is almost certain in most cases, once the corona has reached the plane, the crossing of the corona can almost be taken as the criterion determining whether breakdown will follow. (G10).

Once the ionisation has returned to the small electrode, the up and down movement continues and builds up to full conduction of current. With the negative breakdown the up and downward moving balls of ionisation keep much more in step than with the positive breakdown, so that the up and down movement can be observed until breakdown occurs, from the current and light oscillograms.

Plate 17: 300 kV.

Plate 17 shows simultaneous light and current recordings for a 26 cm gap with a 2 inch sphere as small electrode and .25 μsec risetime, indicating the ionisation leading to breakdown.

Oscillograms Nos 1 and 2 indicate light recordings at the small electrode and shows the correspondence, in time of occurrence and relative amplitude, with the ionisation current recordings. The only difference in the shape of the pulses is the slightly longer decay time of the current pulses. This decay is due to the drift of electrons, which are not captured by the oxygen (Ch. 5-4-5), into the electrode. The decay time is similar to that for the corona. The peak of the current pulse indicates the time of arrival of the ionisation balls at the small electrode. Time measurements are taken with reference to the light oscillogram scale (Ch. 4-3).

Before the up and down movement is indicated it is advisable to consider the general shape of the light and the current pulses. The first pulse is due to the corona traversing the gap. The pulses following

the corona (normally 4 or 5 in number) and having amplitudes of the same order, are due to the subsequent ionisation movement. The rapid build-up to full conduction normally occurs at 1.4 to 1.8 μsec. The reason for this delay of about 1 μsec before the rapid build-up start , will be discussed later.

On Nos 1 and 2 it can be seen that the light pulses lie vertically below the corresponding current pulses, while on Nos 11 and 12 the light and current pulses occur at different times. For the latter recordings the photomultiplier was scanning 1 cm from the plane, so that a difference in time between current and light pulses indicates movement between the small electrode and the plane.

The sequence of events on No. 11 are as follows. The corona starts at .12 μsec at the small electrode, indicated by the first current pulse, and reaches the plane at .19 μsec to be reflected back, almost immediately, at .23 μsec. The return arrives at the small electrode at .36 μsec to be reflected again to reach the plane at .52 μsec. The return starts at .6 μsec and reaches the sphere at .7 μsec to be returned to the plane at .88 μsec. The next movement starts at .95 μsec reaching the sphere at 1.0 μsec and the plane at 1.04 μsec. It starts returning at 1.12 μsec and reaches the sphere at 1.18 μsec when a large increase of current occurs. This causes a light increase at 1.2 μsec with a further increase at 1.4 μsec.

On No. 12, the same sequence of events are indicated by a start at .12 μsec, a plane reflection at .22 μsec, a sphere reflection at .56 μsec, a plane arrival at .7 μsec with the return at .76 μsec, a sphere reflection at .86 μsec, a plane reflection at 1.05 μsec, a sphere reflection at 1.26 μsec, a plane reflection at 1.46 μsec, with the large current increase at 1.56 μsec and the light increase at 1.6 μsec.

It is also important to consider a representative light oscillogram when the scanning plane was approximately in the centre of the gap, e.g. No. 7. In this case the light pulses do not occur

as single or two closely spaced pulses, about halfway in time between the two current pulses, but always occur as two pulses with a longer time between them. This confirms the up and down movement of the ionisation because the times between the light pulses are those for moving to the electrode and being reflected back until it reaches the scanning plane again. The corona passes the slit at 1.9 μsec, and the return ionisation at .32 μsec. Reflection occurs at the sphere at .42 μsec, to pass the slit at .46 μsec and to return at .56 μsec. Another sphere reflection occurs at .66 μsec with the ionisation passing the slit at .74 μsec and returning at .8 μsec. In this way the up and down motion continues until the rapid increase, with each step, starts at about 1.3 μsec.

This up and down movement is observed for every spark but with considerable variation in the amplitudes of the pulses occurring between the corona and the rapid increase of ionisation. The speeds at which this ionisation moves and the time delays before reflection occurs are not consistent enough to allow worthwhile graphical representation of the movement.

The speeds for both the up and down movement were in the same range with a minimum of 1.5×10^8 cm/sec and a maximum of 5×10^8 cm/sec, with the peak amplitudes rarely exceeding that of the corona, except when the rapid build-up of current occurred. The amplitudes of the ionisation pulses were normally in the range 10% - 100% of the peak corona amplitude.

The oscillograms on Plates 18 and 19 show the ionisation leading to breakdown at 600 kV. The results and the mechanisms indicated are the same as at 300 kV. In general it appeared that fewer pulses occurred between the corona and the increase to breakdown, and the stepped increase leading to breakdown can be seen more clearly.

PL 18 shows that there was a reasonable consistency in the current waveshape with the corona pulse at .1 μsec, a second current pulse of about double the corona amplitude at .42 μsec, a

third current increase, with another doubling in amplitude, at 1.2 μsec leading to breakdown at 1.6 μsec.

Due to the large difference in amplitudes between the ionisation approaching the plane and the reflection, it is not always easy to observe the up and down movement of ionisation. For scanning positions close to the small electrode the correspondence between the current and light pulses can again be seen (PL 18 Nos 3 - 6).

The up and down movement is best shown by PL 19 Nos 3 - 6 and Nos 9 - 12. Nos 3 - 6 is for a scanning plane 10 cm from the plate. The corona reaches the scanning plane at .31 μsec and the return passes at .4 μsec to reach the sphere at .44 μsec with the reflected ionisation passing the slit at .52 and .56 μsec and the return at .62 μsec to reach the sphere at .68 μsec. This movement continues until full conduction is attained at about 1.6 μsec. Nos 3, 5 and 6 indicate similar movements.

Nos 9 - 12 indicate the light recordings when the scanning plane was 2 cm from the plate. No 11 shows the corona reaching the plane at .32 μsec, and the return at the same time. The sphere is reached at .41 μsec returning to the plane at .45 μsec. The up and down movement continues until the rise to full conduction occurs at 1.6 μsec. With the different light sensitivities for Nos 7 - 12, the different portions of the ionisation mechanism can be seen. Nos 7 and 8 indicate the step-like increase to breakdown, while Nos 9 - 12 indicate the up and down movement during the initial ionisation. The other oscillograms for scanning positions in the centre of the gap shows that the movement of the ionisation is at an approximately constant speed as it moves across the gap.

Oscillogram No. 1 on PL 18 shows the similarity of equal waveshape reproduction on the two oscilloscopes when the same waveshape was reproduced on both, using the same horizontal and vertical sensitivities.

No. 2 indicates the increase of current

up to breakdown at 1.6 μsec, with a current of 530 amps, decaying slowly as the condensers discharge.

The oscillograms on PL 20 indicate ionisation with a ½ inch sphere as small electrode at 600 kV. The results are basically the same as for the 2 inch sphere but the corona amplitude is less, being only about 8 L on reaching the plate. The return of the ionisation is here clearly indicated by oscillograms Nos 8 - 11. On No. 9 the corona is 10 cm from the plane at .51 μsec and the return occurs at .65 μsec to reach the sphere at .77 μsec as indicated by the current oscillogram. Due to the lower sensitivity, No. 8 does not show the corona pulse, but only the return ionisation at .53 μsec, the current pulse at .63 μsec and the ionisation reaching the scanning plane again at .66 μsec. Nos 10 and 11 show only one pulse as the corona reaches the plane and the return is started to reach the sphere at .6 μsec on No. 10 and .58 μsec on No.11.

It is now necessary to consider the photographic results to see how this up and down movement produces breakdown of the gap. On plate 8 representative photographs of the ionisation leading to negative breakdown are shown.

Oscillograms Nos 11 and 13 indicate ionisation at 150 kV. It can be seen that the corona streamers have bridged the gap and that in one or two of these paths, return ionisation has occurred. It is important to note that the paths are followed for the first portion but that afterwards branching to another streamer or a brush formation may occur.

This brush formation is shown more clearly by the photographs for 300 kV on PL 8, Nos 2, 3 and 7 - 10. The brush discharges are best shown by Nos 7 and 8, which is for a gap just less than the critical gap, so that only one or two of the corona streamers manage to cross the gap. The reason for the brush discharge is due to the fact that there are many streamers which do not manage to cross the gap but peter out a few centimetres from the plane, where they form a space charge. When the return ionisation starts it has only the one ionised path to move along, but after a few centimetres it reaches the volume

where the charges have stopped and due to the higher stresses produced by the return ionisation, it grows to the nearby charge volumes and thus forms the brushlike ionisation. The ionisation does not stop there but continues along the different smaller streamer paths up to the sphere where it is re lected back along more or less the same paths, as these paths have been previously ionised and because there are no more space charges left along the path. The up and down movement continues along these paths, forming fully conducting channels for short distances at the plane and at the sphere as indicated by the bright filaments on Nos 7 and 8. These bright channels are similar to the positive leader for the positive breakdown. Thus the two leaders grow, apparently simultaneously, as a short length is added to each leader alternatively by the up and down movement of the ionisation.

For a shorter gap spacing at 300 kV, more corona streamers bridge the gap and less streamers disappear to leave a space charge, so that the return ionisation tends to be more along the corona paths with no brush formation occurring as shown by Nos 9 and 10. Branching does occur in some cases due to the few charges which are in the volume when the ionisation returns. This effect is also shown by Nos 2 and 3 which is for a ½ inch sphere at 300 kV. Another interesting effect which is observed for these recordings is the formation of light spots along the ionisation paths at irregular intervals. The most likely explanation for these is the presence of free electrons, producing more intense ionisation in the locality of its position. It was also noticed that the short visible branches normally occurred at these brighter spots.

Photographic recordings with simultaneous light and current recordings are given on PL 21 and 22, for different scanning positions. The oscillograms indicate the step-like increase in amplitudes, with chopping occurring just before full conduction is reached. The corona and initial return ionisation cannot be seen on the light oscillograms because a low sensitivity was used to show the light amplitude at the chopping instant.

The photographs show the same pattern as at 300 kV, with the plate stems a few centimetres long, then a brush formation with numerous threads extending to the small sphere, where it converges to form the conducting negative leader growing from the small electrode. In cases where the ionisation is not very bright, the oscillograms indicate smaller amplitudes (PL 21 No. 6), and the leaders do not extend very far from the electrodes. On PL 22 No. 2 the two leaders have almost met and the oscillograms show very high amplitudes.

Thus negative breakdown is obtained by the growth of two conducting leaders, one from each electrode, growing until they meet o form a full conducting path. Both leaders grow by cirtue of a small conducting length being added to each in turn, as the balls of ionisation move up and down in the gap with increasing amplitude.

On the oscillograms at 150 kV an effect is observed which is not as pronounced at higher voltages. This is shown by No. 15 on PL 8. These oscillograms are representative of normal oscillograms at 150 kV and it appears as though there is only the corona pulse and then the rise to breakdown. If it is studied closely it will be seen that the initial pulse consists of more than one part. Three different peaks occur and the times between the pulses indicate a speed of 2×10^8 cm/sec, if return ionisation is accepted.

The question is, why does the ionisation diminish and then suddenly start to rise at about 1.4 µsec. The most likely explanation seems to be that if ionisation with a positive front, grows into a region where a strong concentration of electron exists, it may happen that the positive space charge is cancelled by the increasing number of electrons, which neutralizes the action of the positive ions, and thus decreases the ionisation intensity. If the electrons are attached to oxygen to form negative ions they apparently do not have this effect to the same extent, probably due to the different mobility. Because the electrons are attached in less than .4 µsec, it seems that if the return ionisation returns very quickly, it is damped out by the cloud of electron whereas when it returns

later (> .4 μsec), the negative ions do not absorb it and the up and down movement continues. This would explain why there are fewer pulses than at 300 or 600 kV. In some cases a number of pulses occurred at 150 kV as indicated by No. 16, which are very similar in waveshape to that at the higher voltages.

The waiting period, before breakdown occurs, seems to be the time taken for a secondary action to come into operation. This action is most likely that of positive and negative ions requiring that time to move far enough to be able to cause ionising collisions, or the time that it takes to saturate oxygen with electrons.

At the higher voltages, where the times to return are so long that full attachment takes place before the return arrives, this delay is not so easily noticed although the time taken before increasing reflections occur is probably due to the same effect.

It is also important to note that the time taken for breakdown at different voltages from 150 kV to 600 kV, for the critical gap, is a constant of about 1.5 μsec.

C H A P T E R V I I.

CONCLUSIONS

(1) CORONA:

When an impulse voltage was applied to a non-uniform air gap, ionisation was observed, starting at the small electrode and growing towards the plane, as soon as the critical stress at the small electrode was exceeded. This ionisation, moving into air that has not previously been ionised, is called Corona. The corona occurs as a number of elongated balls of ionisation, each about 1 cm long, starting almost simultaneously.

The speeds of growth recorded, depend on the polarity of the gap and the stress existing just ahead of the corona balls. The minimum speed, observed for a positive small electrode was 1.5×10^7 cm/sec, and seems to be the minimum at which positive corona propagation can occur. The maximum speed observed was 5×10^8 cm/sec and it seems that the maximum is only limited by the overvoltage, obtainable with a fast voltage rise-time, before the corona starts. The speeds varied with the intensity of the corona, higher intensities being associated with higher speeds and with corona extinction occurring at the minimum speed.

With a negative small electrode the speeds were more constant for variations of the variables and a minimum of 6×10^7 cm/sec and a maximum of 3.5×10^8 cm/sec were recorded. The speeds for most conditions fell in the range $1 - 3 \times 10^8$ cm/sec. The extent of corona growth was observed to be much less with negative than with positive corona.

The growth of the corona depends on the stress at the starting instant and the divergence of the field. More basically, it can be stated that it depends on the amount of photo-ionisation and the stress, produced by the applied voltage and the space charge of the corona ball, in the volume just ahead of the corona ball.

A larger small electrode and a shorter gap length

produce higher stresses with a fast rise-time and consequently higher speeds. A faster rise-time produces a higher overvoltage before the corona starts and thus higher stresses and a bigger ionisation intensity also resulting in higher speeds. The applied voltage does not change the speeds or intensities appreciably for the critical gap length. The difference in speed with polarity is due to the different mobilities of the electrons and the positive ions.

Positive ions and electrons are left behind in the path travelled by the corona, but due to the space charge formed when the intensity is decreasing with movement, they do not cause further ionisation. The electrons attach themselves to oxygen atoms within .4 μsec to form an immobile space charge which can prevent ionisation for more than 30 μsec.

Each corona ball moves due to photo-ionisation occurring ahead of the ball, which produces higher speeds than that of the electron movement. If the corona streamers do not bridge the gap they produce an overall effect of a ball of charge, made up of the number of simultaneous corona balls, which is able to suppress further ionisation for at least 30 μsec.

If the voltage rises slowly to more than double the corona starting magnitude, another set of corona balls are initiated, growing from the first. This process continues until the gap has been crossed or until the voltage has stopped increasing.

(2) TRANSITION TO BREAKDOWN:

When the corona has reached the plane, the ionisation is reflected back, to travel along the same path. Breakdown only occurs when the ionisation balls return to the small electrode, indicating that a possible path has been established. The up and down motion can now occur with step-like increase in intensity until full conduction has been obtained.

With the positive corona, the return is similar to negative corona growth, but because the path has previously been ionised it is possible for the ionisation to return. However, in a certain range the

corona can bridge the gap while the ionisation disappears on the return journey.

With the negative corona the first crossing is the more difficult while the return is easy, being similar to positive corona and occurring along a previously ionised path. For this condition the crossing of the corona can be considered as the criterion determining whether breakdown will occur. The return may be partly diverted to form brush or branch-like ionisation.

(3) BREAKDOWN:

(a) Positive Breakdown.

As the up and down ionisation ball movement continues with increasing intensity, a secondary mechanism occurs by which a short, fully conducting channel is added to the existing conducting channel every time a ball of ionisation approaches it. The channel is started when the first return ionisation reaches the small electrode. This is the growth of the positive leader, which is a volume of intense ionisation. The leader grows slowly at first with a minimum speed of 1.5×10^6 cm/sec, increasing to at least 5×10^8 cm/sec just before it reaches the plate. When the leader reaches the plate, breakdown is complete and the main current flow occurs. The growth of the leader acts as an extension of the electrode with no volt drop along the established path. This causes the growth to be practically independent of the electrodes or the rise-times once the growth has started.

An increase in voltage produces an almost proportional increase in the speed of the leader.

(b) Negative Breakdown.

For the negative breakdown the up and down movement also continues, after the return of the first ionisation, to form a fully conducting path. The pulses keep more in step and it is possible to observe the up and down movement until breakdown is complete. The leader does not only grow from the small electrode, but also from a conducting plate stem, which really changes the gap to a point-point discharge. The two leaders grow simultaneously from each electrode to meet approximately midway.

The results show that the photomultiplier is extremely useful for the investigation of fast moving volumes of ionisation and that by means of simultaneous recordings with the photomultiplier and of the ionisation current it was possible to observe the up and down ionisation movement leading to break-down.

REFERENCES:

(1) J.H. Park and H.N. Cones. "Surge Voltage Breakdown of Air in a Non-uniform Field". Journal of Research of the National Bureau of Standards, Vol.56, No.4, April 1956 p 201.

(2) H. Norinder and O. Salka. "Mechanism of Positive Spark Discharges with Long Gaps in Air at Atmospheric Pressure". Arkiv für Fysik. 3 1951, p 347.

(3) H. Norinder and O. Salka. "Mechanism of Long-Gap Negative Spark Discharges in Air at Atmospheric Pressure". ibid, 5, 1952 p. 493

(4) H. Norinder and O. Salka. "Screens in Long Discharge Gaps". ibid. 6, 1953 p 151.

(5) R.F. Saxe and J.M. Meek. "The Initiation Mechanism of Long Sparks in Point-Plane Gaps. Inst. of E.E. London, Monograph No. 124 M, April 1955.

(6) I.A.D. Lewis and F.H. Wells. "Millimicrosecond Pulse Techniques". Second (Revised) Ed. Pergamon Press 1959.

(7) B.F.J. Scholand. "Progressive Lightning". Proc. of Royal Society. A.

(a) 1934, 143, p 654
(b) 1935, 152, p 595
(c) 1938, 164, p 132

(8) B.F.J. Schonland. "The Pilot Streamer in Lightning and the Long Spark". ibid, 1953, 220 p 25.

(9) J.M. Meek and J.D. Craggs. "Electrical Breakdown of Gases". (Oxford University Press 1953).

(10) W.G. Dow. "Fundamentals of Engineering Electronics". (Wiley 1952). Second Edition.

REFERENCES:

(1) J.H. Park and H.N. Cones. "Surge Voltage Breakdown of Air in a Non-uniform Field". Journal of Research of the National Bureau of Standards, Vol.56, No.4, April 1956 p 201.

(2) H. Norinder and O. Salka. "Mechanism of Positive Spark Discharges with Long Gaps in Air at Atmospheric Pressure". Arkiv für Fysik. 3 1951, p 347.

(3) H. Norinder and O. Salka. "Mechanism of Long-Gap Negative Spark Discharges in Air at Atmospheric Pressure". ibid, 5, 1952 p. 493

(4) H. Norinder and O. Salka. "Screens in Long Discharge Gaps". ibid. 6, 1953 p 151.

(5) R.F. Saxe and J.M. Meek. "The Initiation Mechanism of Long Sparks in Point-Plane Gaps. Inst. of E.E. London, Monograph No. 124 M, April 1955.

(6) I.A.D. Lewis and F.H. Wells. "Millimicrosecond Pulse Techniques". Second (Revised) Ed. Pergamon Press 1959.

(7) B.F.J. Scholand. "Progressive Lightning". Proc. of Royal Society. A.

(a) 1934, 143, p 654
(b) 1935, 152, p 595
(c) 1938, 164, p 132

(8) B.F.J. Schonland. "The Pilot Streamer in Lightning and the Long Spark". ibid, 1953, 220 p 25.

(9) J.M. Meek and J.D. Craggs. "Electrical Breakdown of Gases". (Oxford University Press 1953).

(10) W.G. Dow. "Fundamentals of Engineering Electronics". (Wiley 1952). Second Edition.

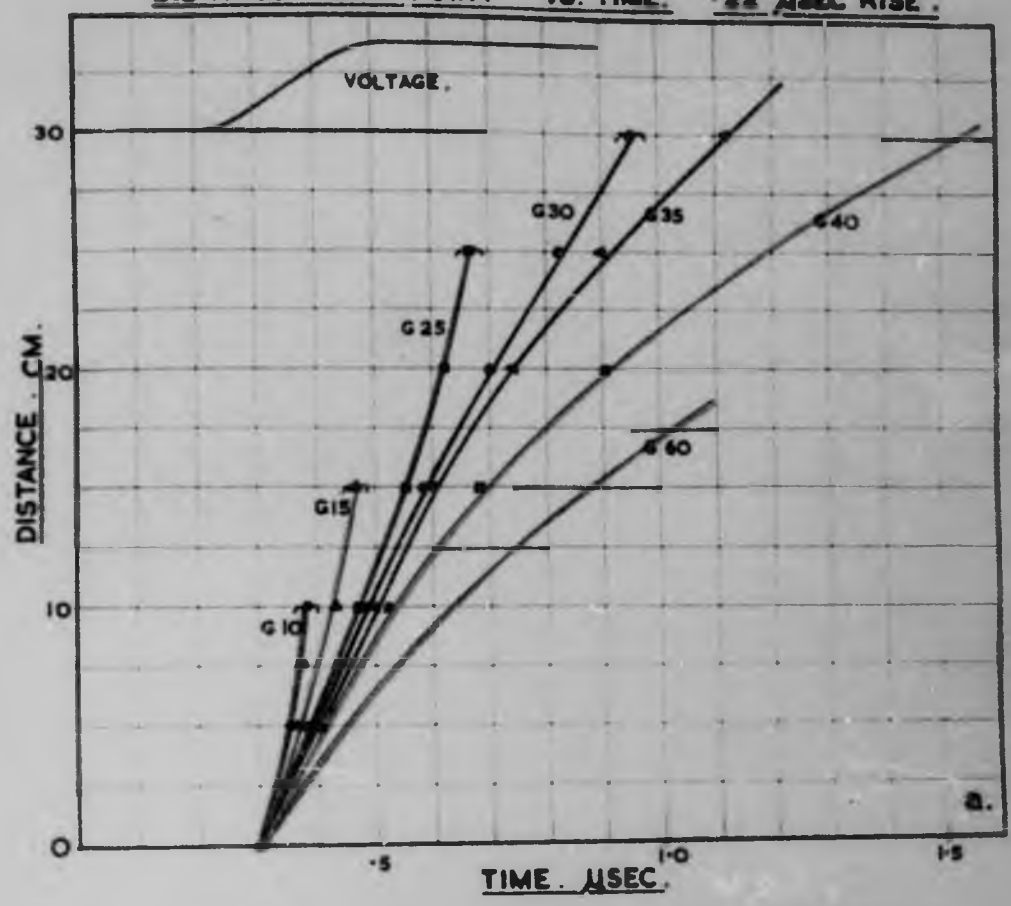
CORONA.

+ 150 KV. G 1.

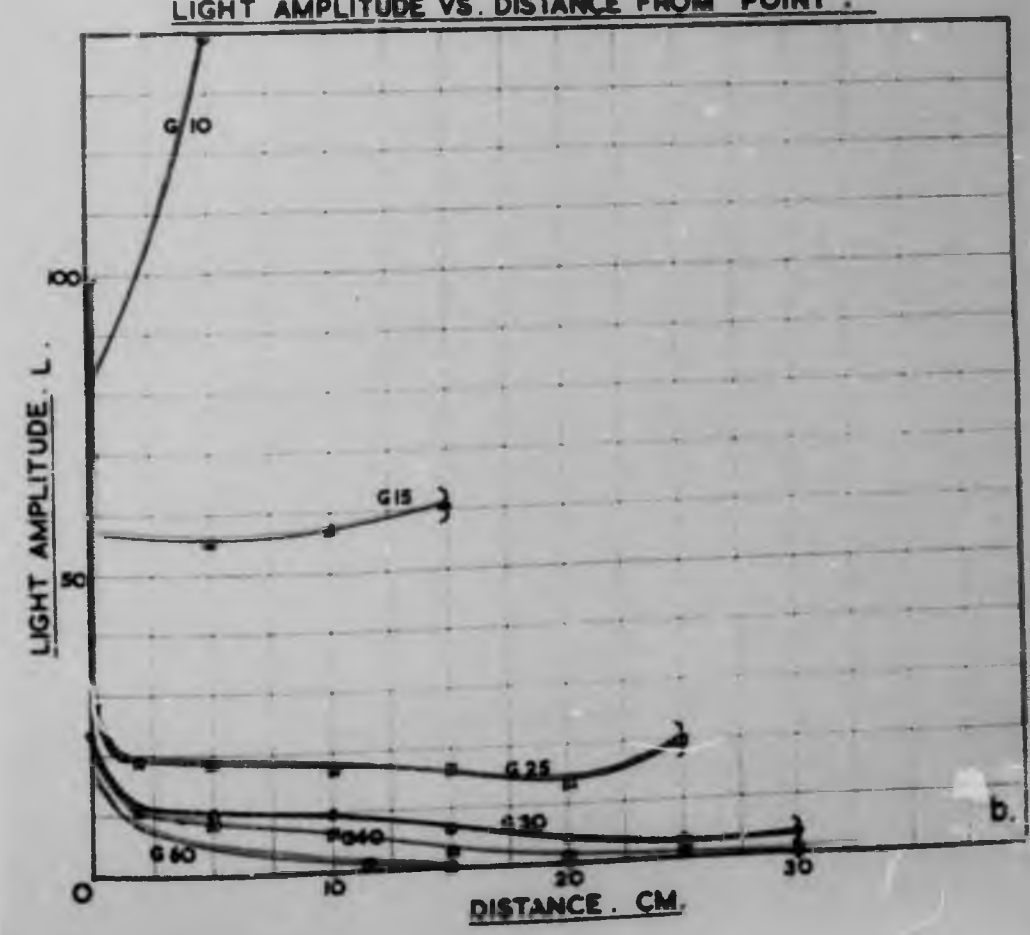
POINT — PLANE.

·22 μSEC RISE.

DISTANCE FROM POINT VS. TIME.



LIGHT AMPLITUDE VS. DISTANCE FROM POINT.



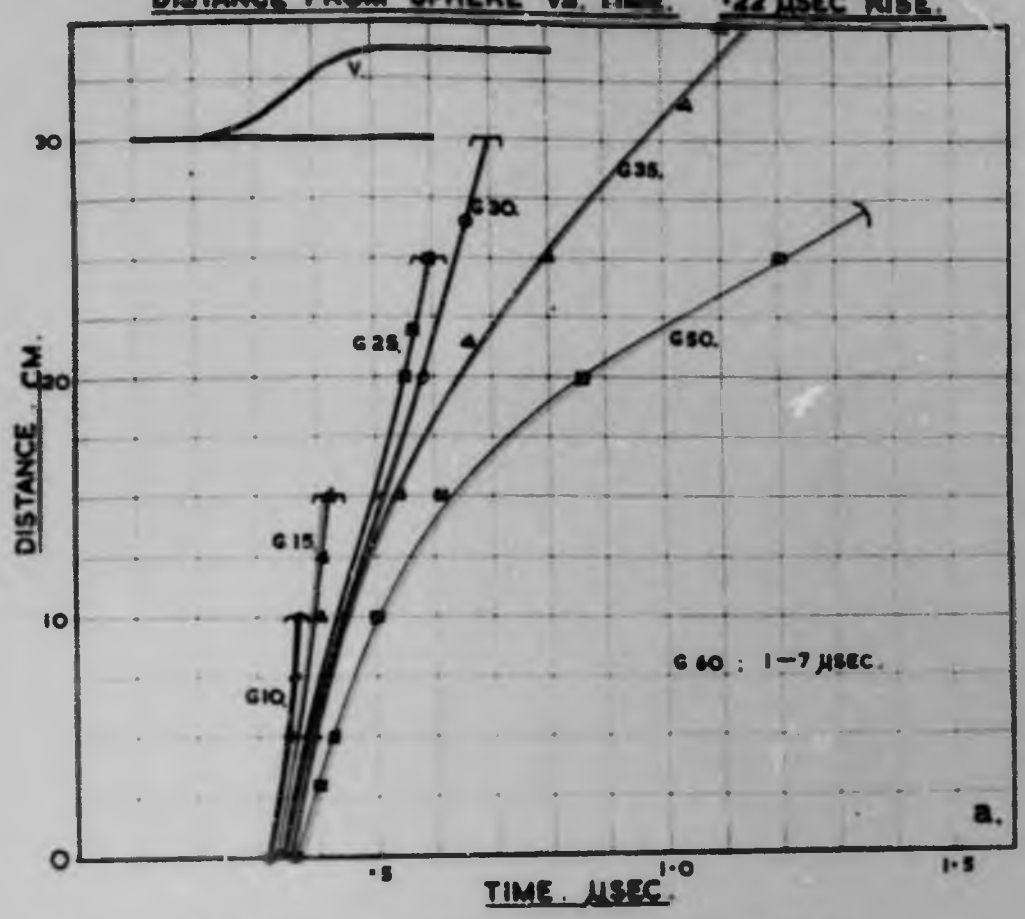
CORONA.

+ 130 KV. G 2.

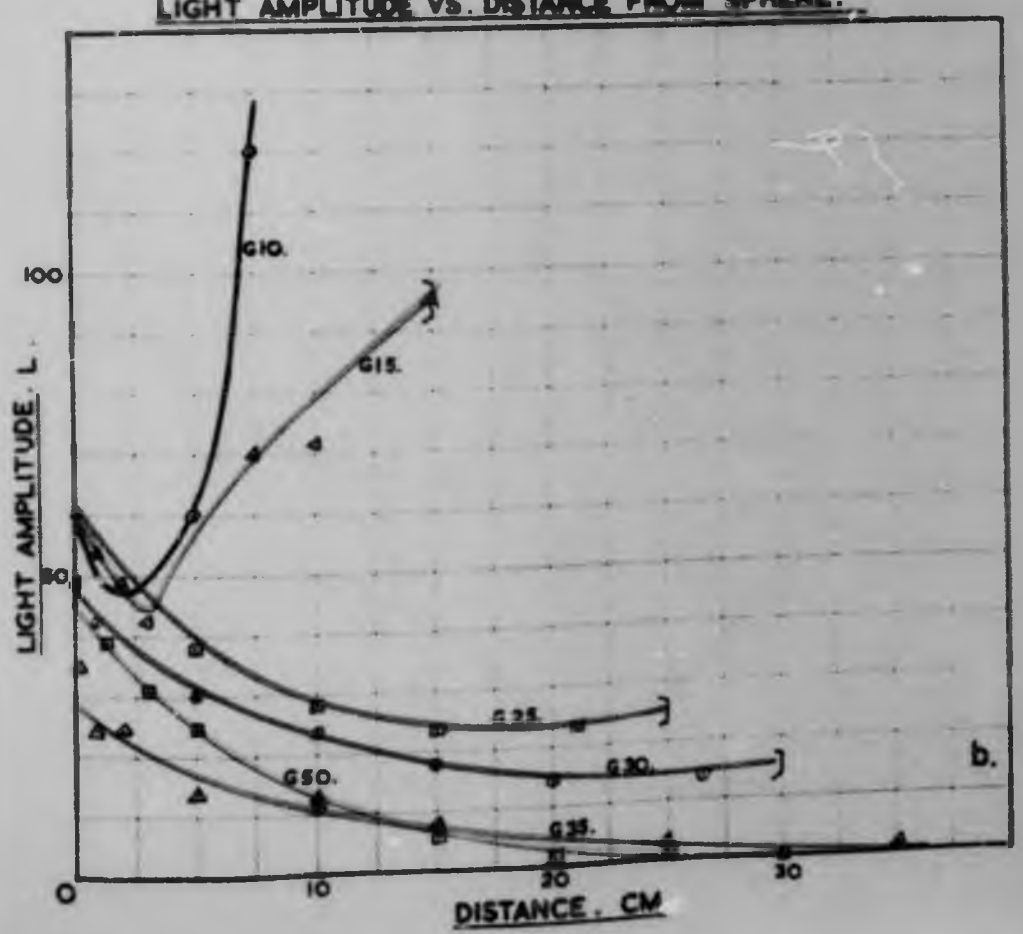
½" SPHERE — PLANE.

·22 μSEC RISE.

DISTANCE FROM SPHERE VS. TIME.



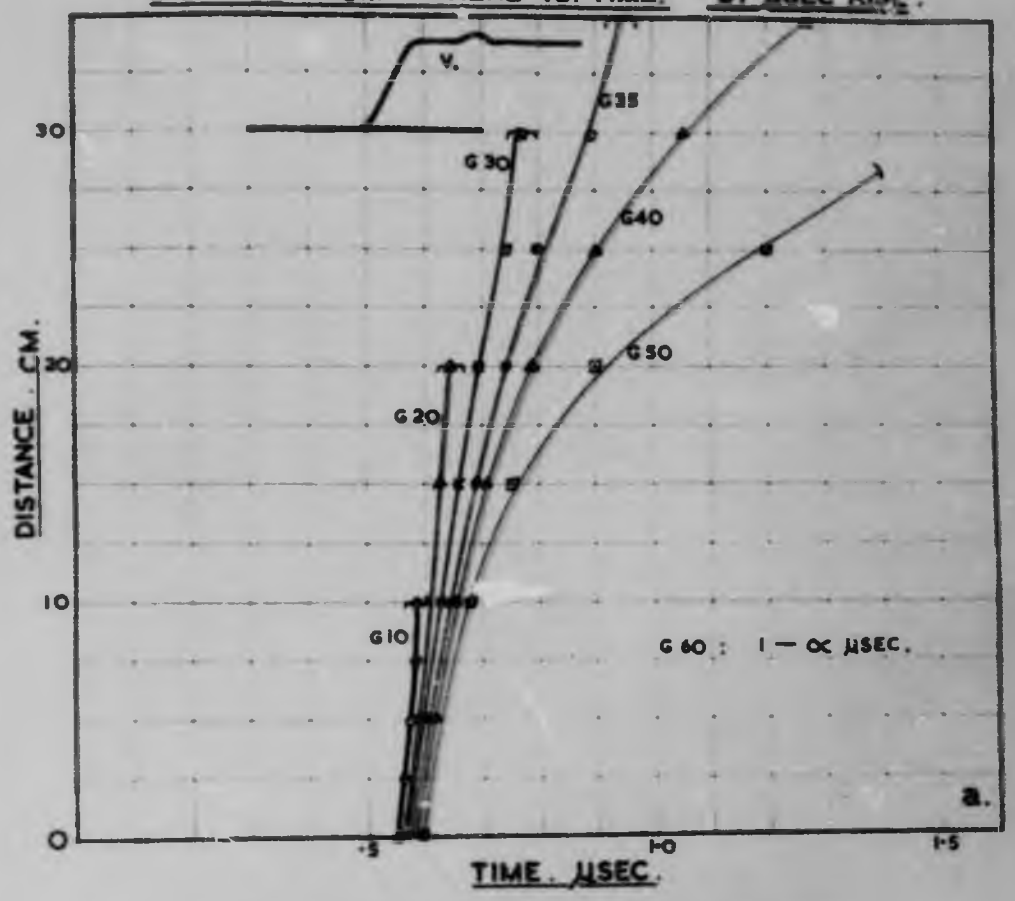
LIGHT AMPLITUDE VS. DISTANCE FROM SPHERE.



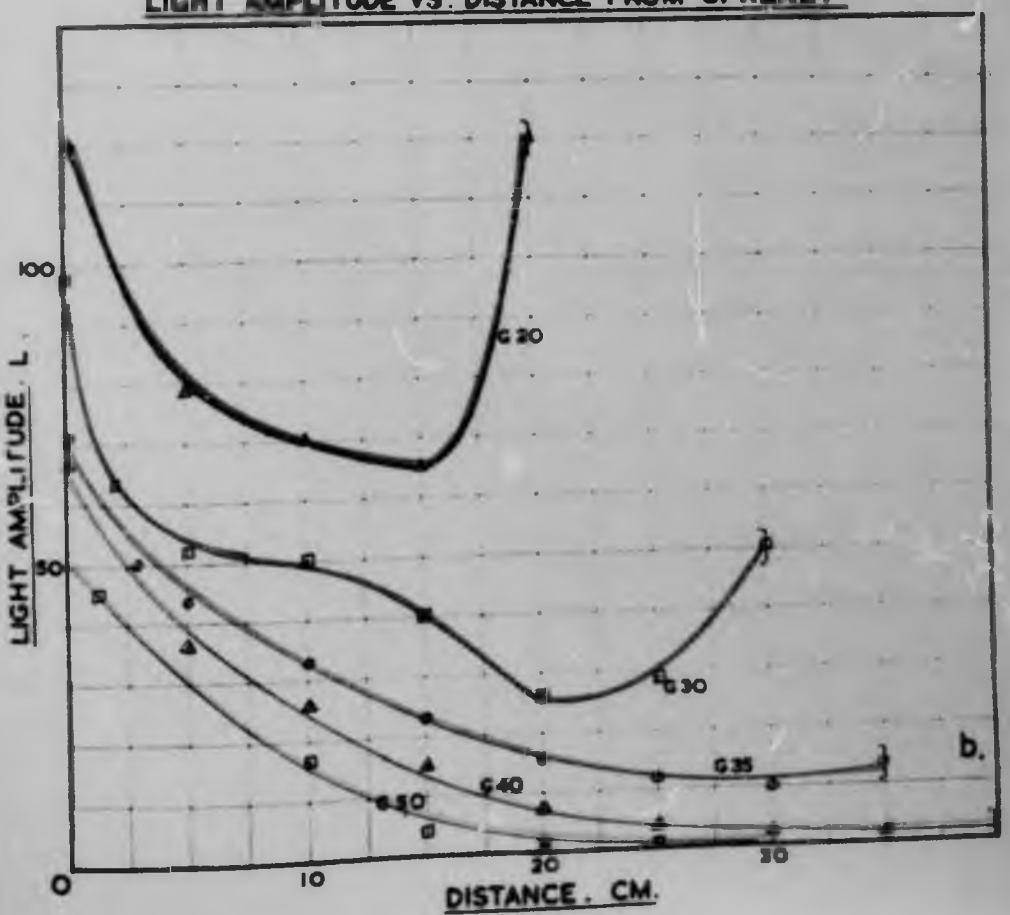
CORONA.

+150 KV. G3.
½" SPHERE—FLANE.
·07 μSEC RISE.

DISTANCE FROM SPHERE VS. TIME.



LIGHT AMPLITUDE VS. DISTANCE FROM SPHERE.

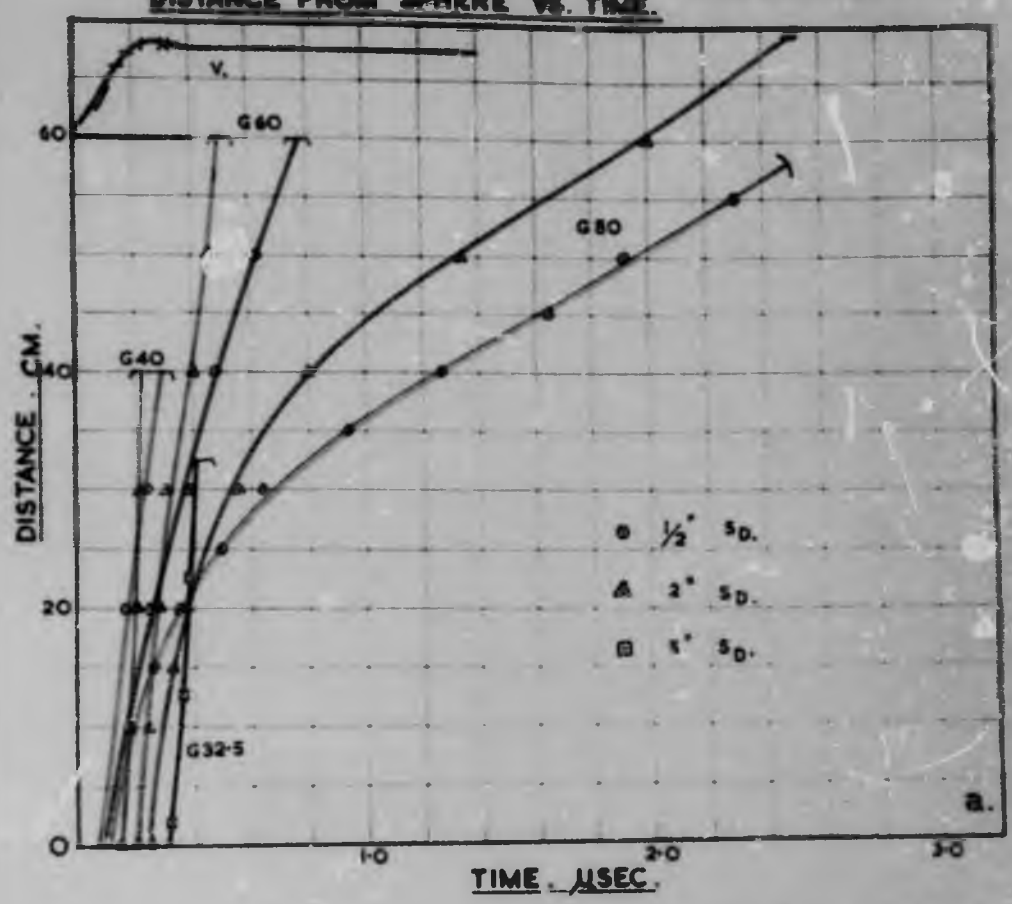


CORONA.

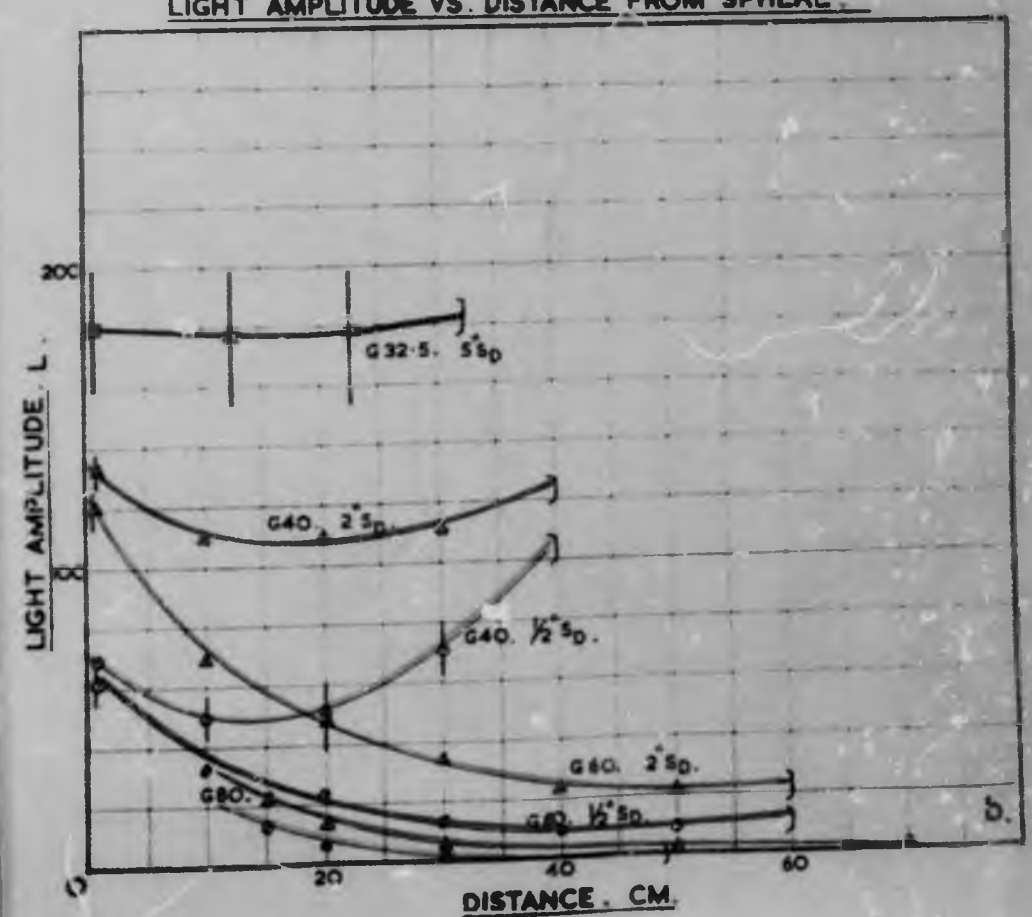
+30[illegible] V. G4.

·25 μSEC RISE.

DISTANCE FROM SPHERE VS. TIME.



LIGHT AMPLITUDE VS. DISTANCE FROM SPHERE.



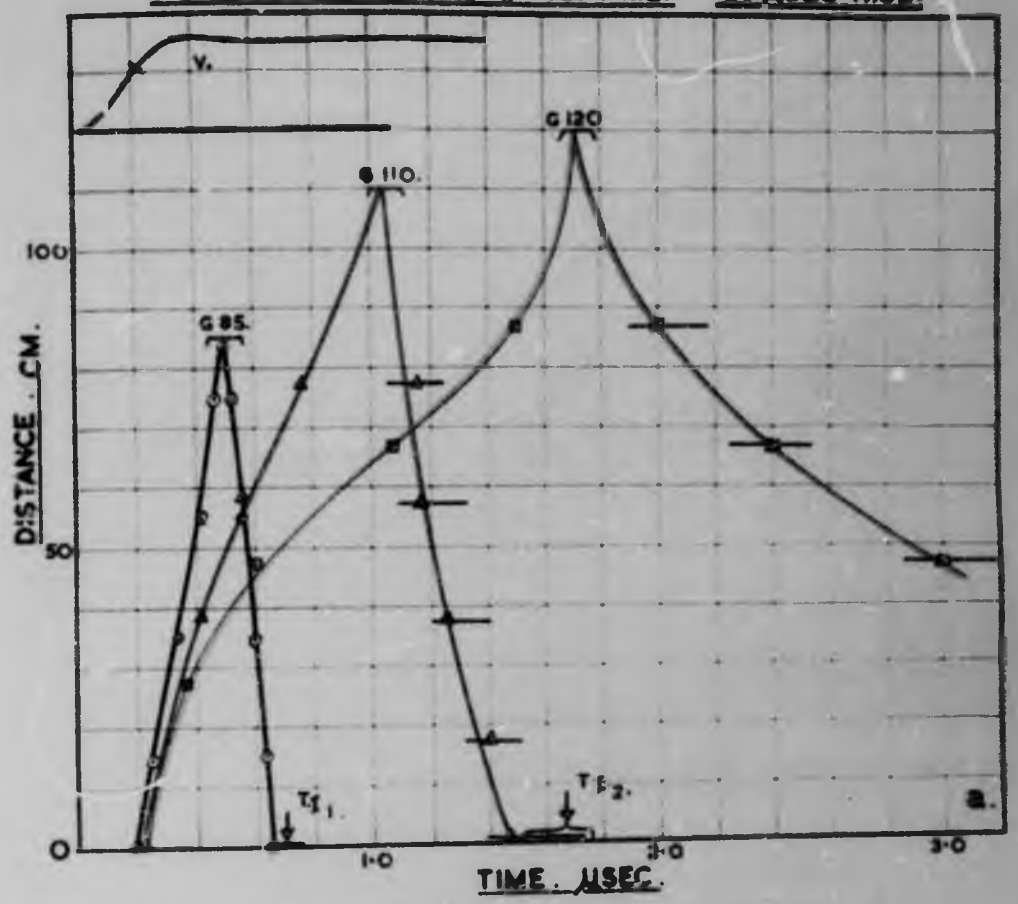
CORONA.

+600 KV. G5.

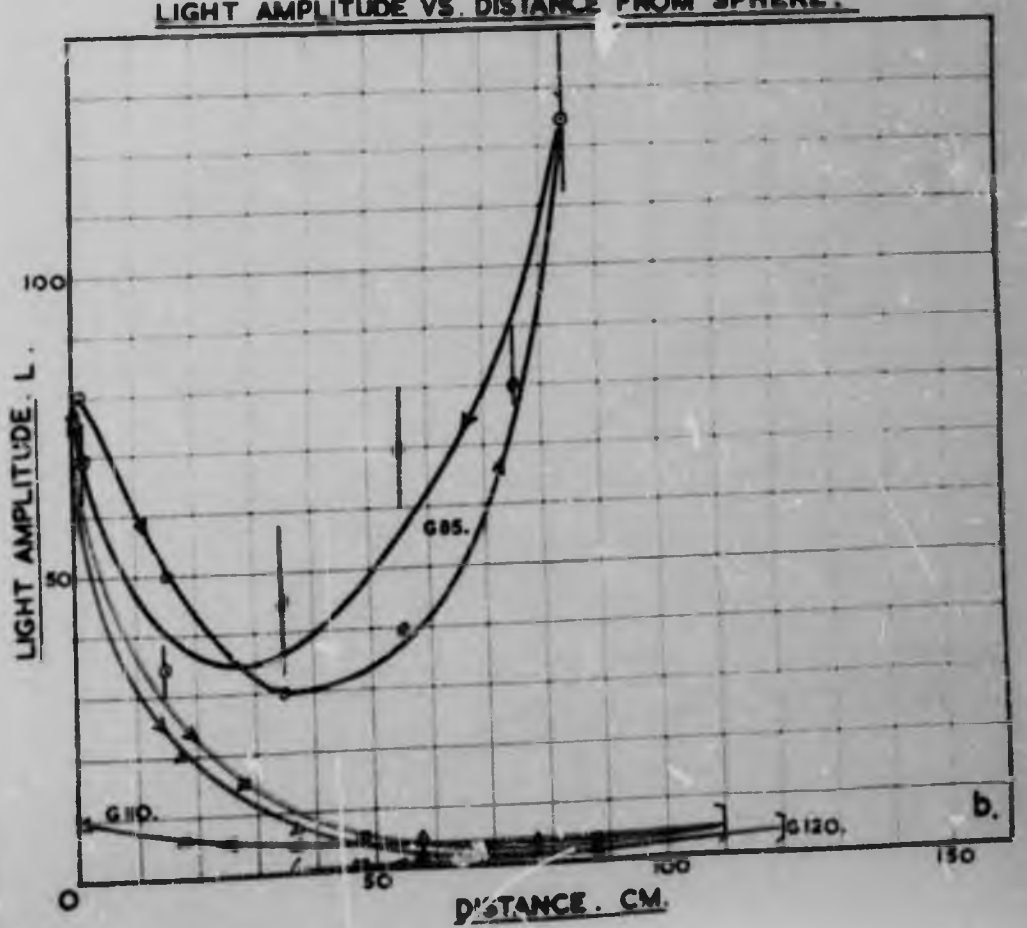
2" SPHERE — PLANE.

·25 μSEC RISE.

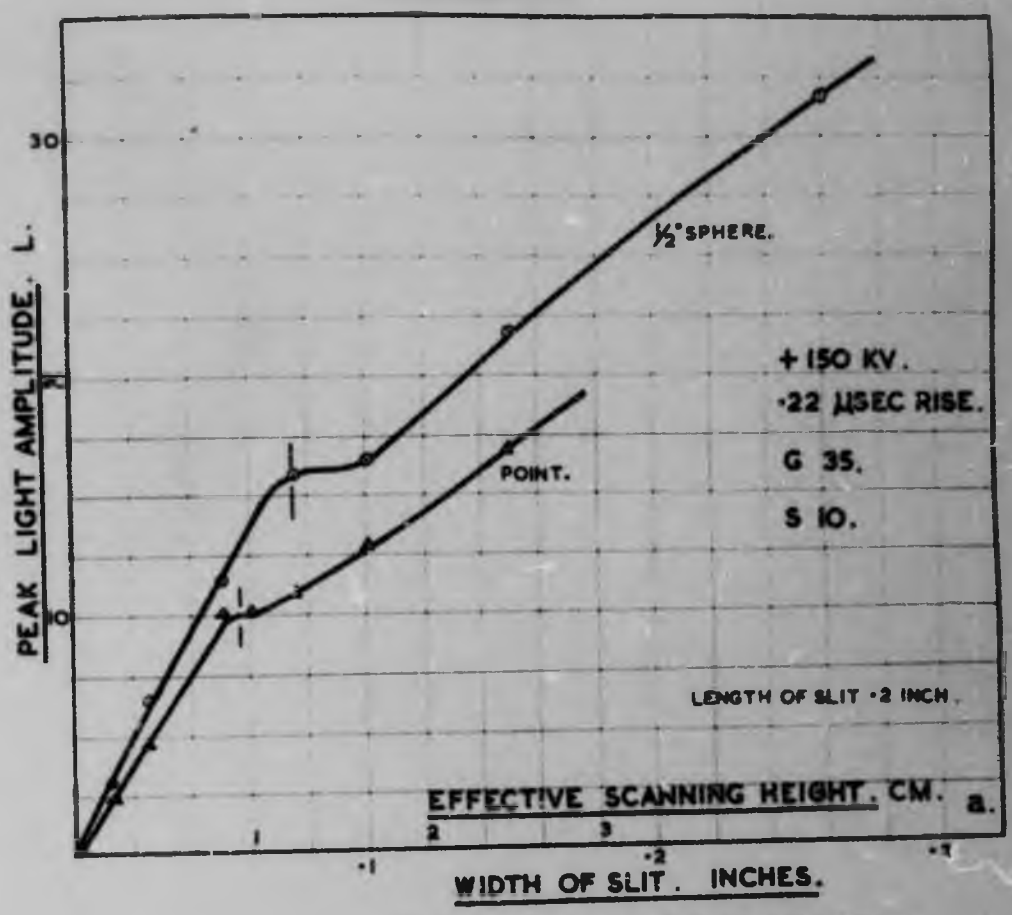
DISTANCE FROM SPHERE VS. TIME.



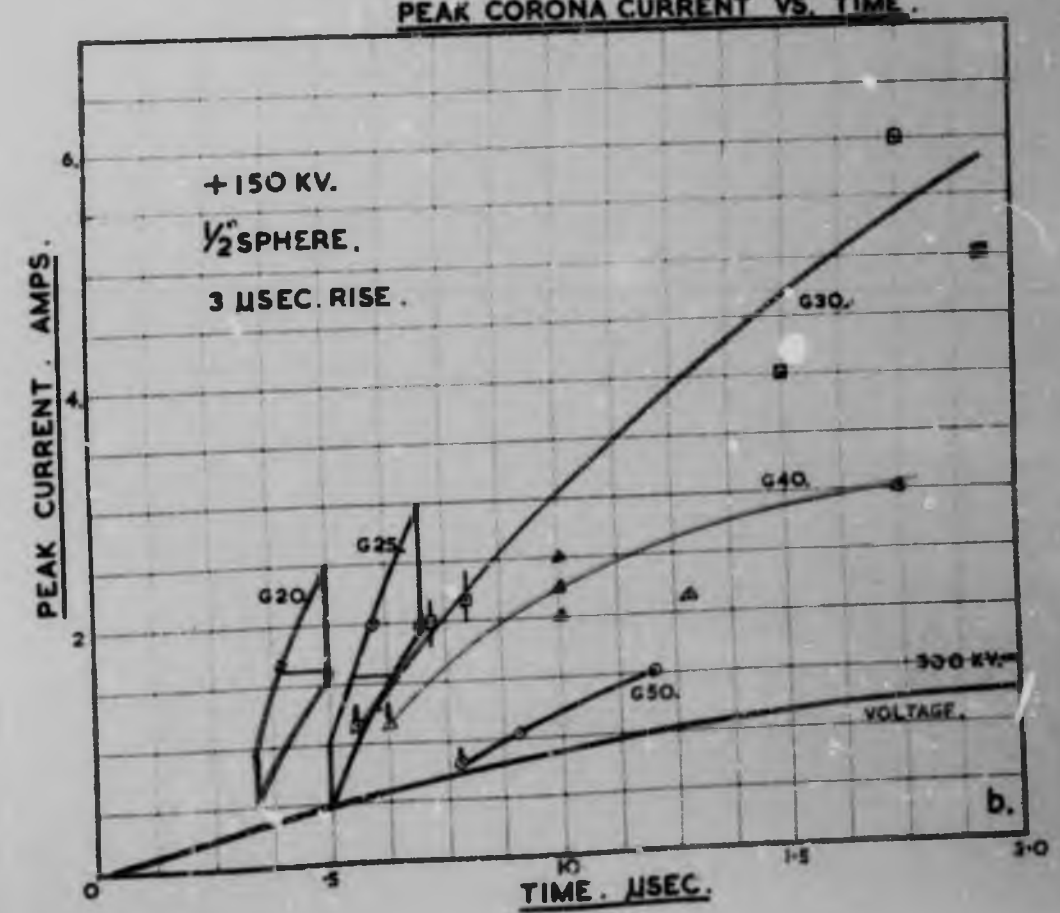
LIGHT AMPLITUDE VS. DISTANCE FROM SPHERE.



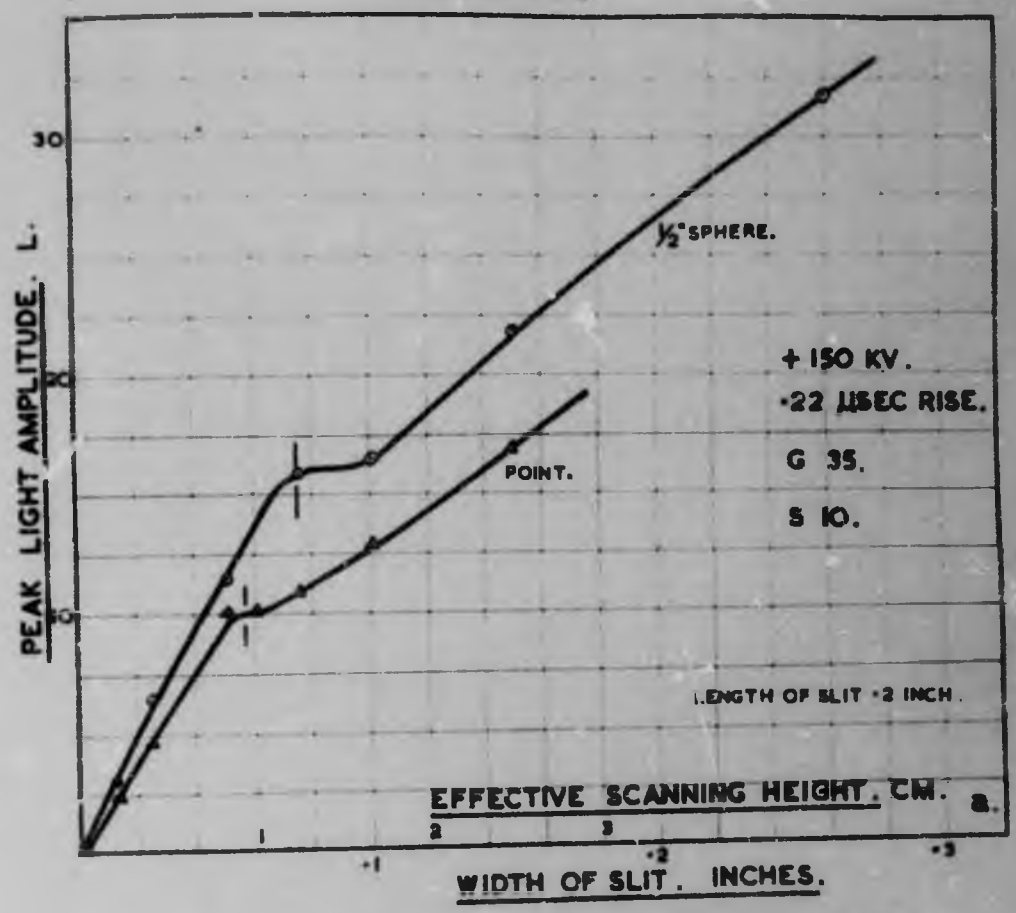
CORONA SIZE.



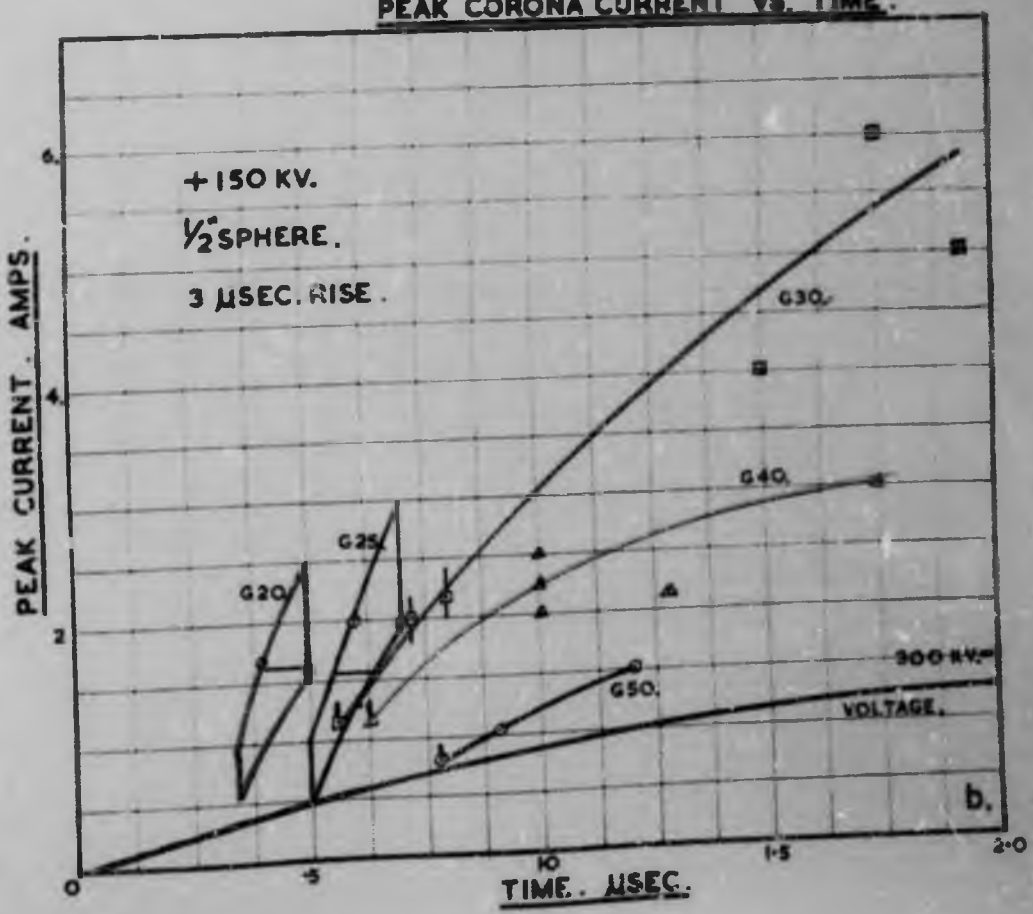
PEAK CORONA CURRENT VS. TIME.



CORONA SIZE.



PEAK CORONA CURRENT VS. TIME.



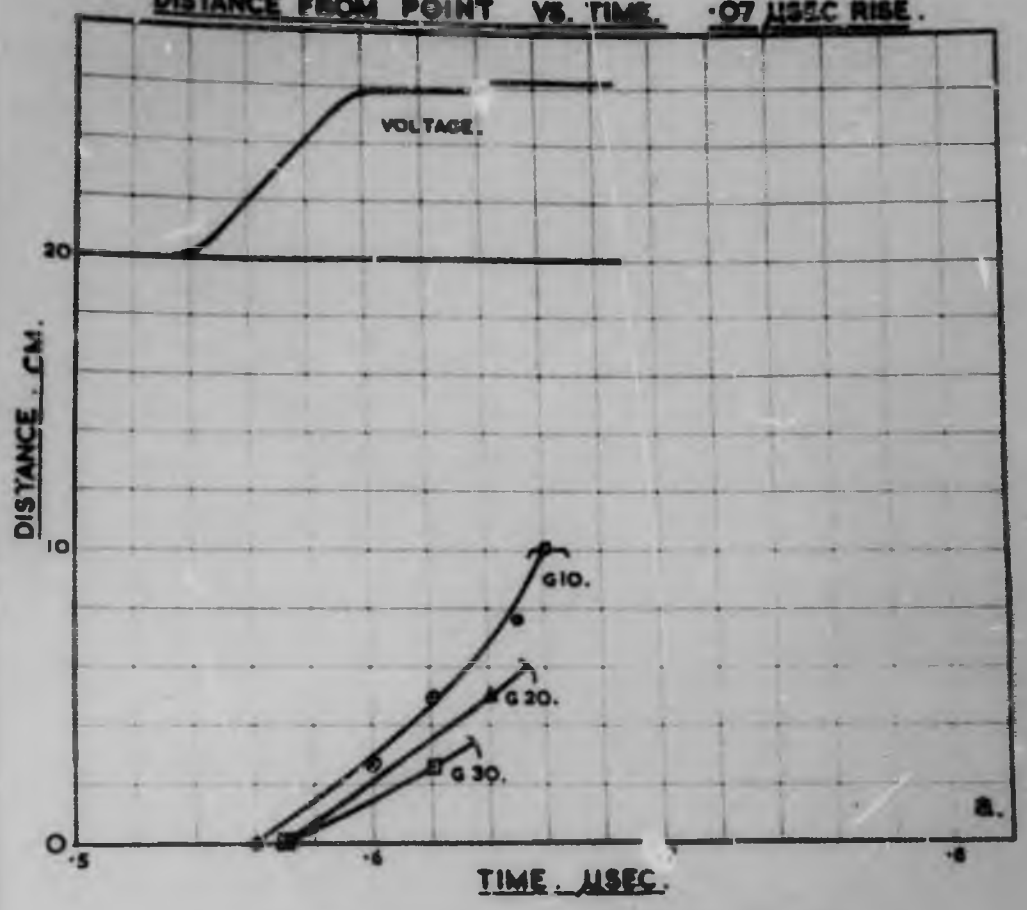
CORONA.

−150 KV. G 7.

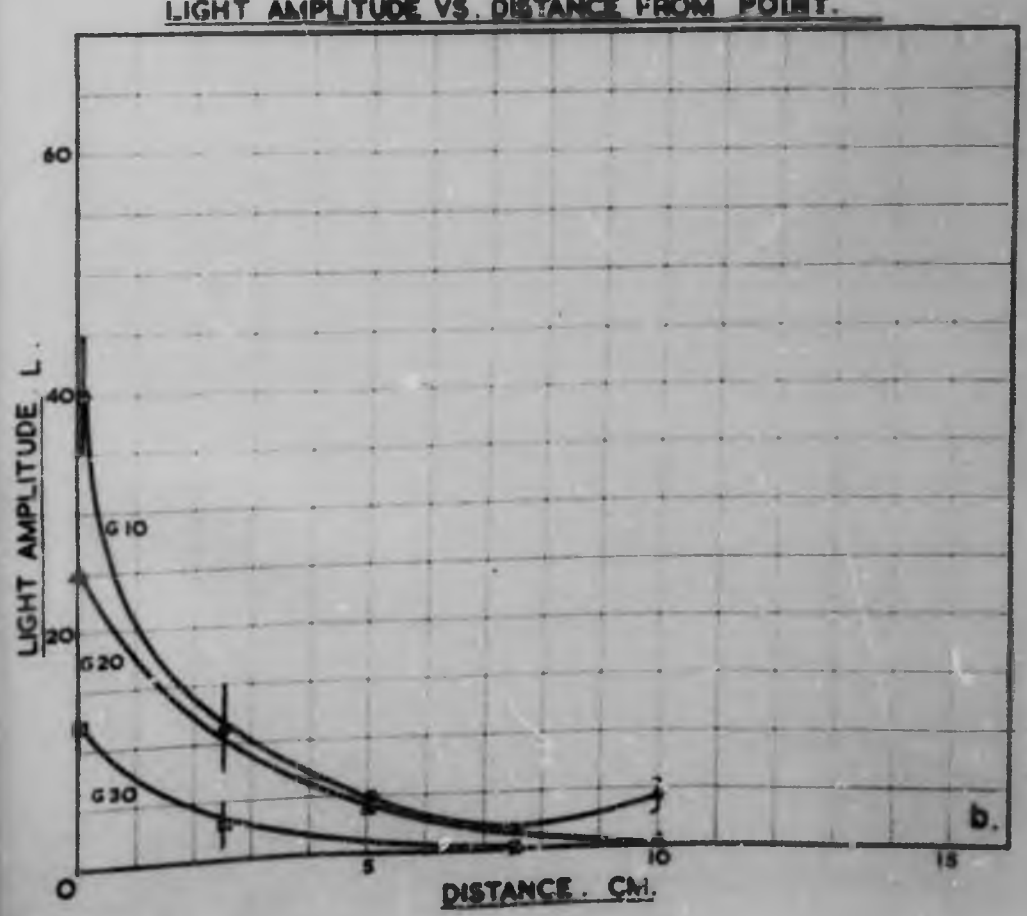
POINT — PLANE.

·07 μSEC RISE.

DISTANCE FROM POINT VS. TIME.



LIGHT AMPLITUDE VS. DISTANCE FROM POINT.



CORONA.

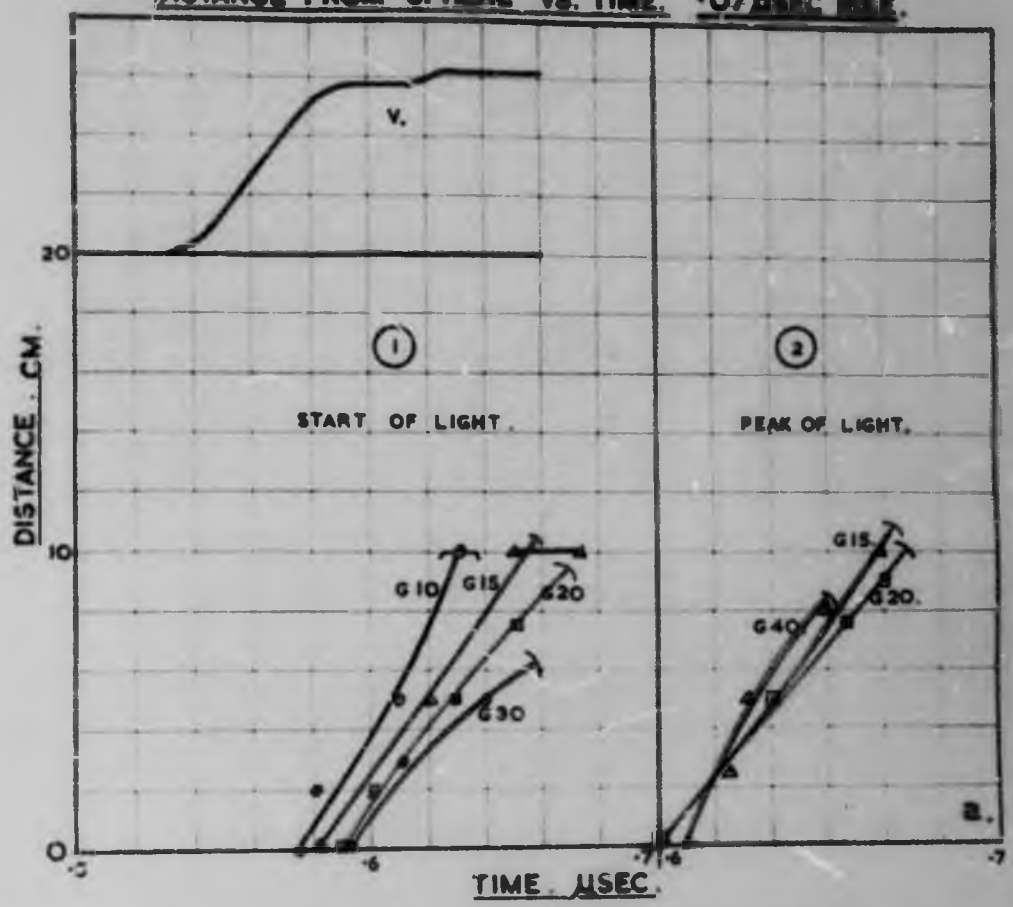
G 8.

−150 KV.

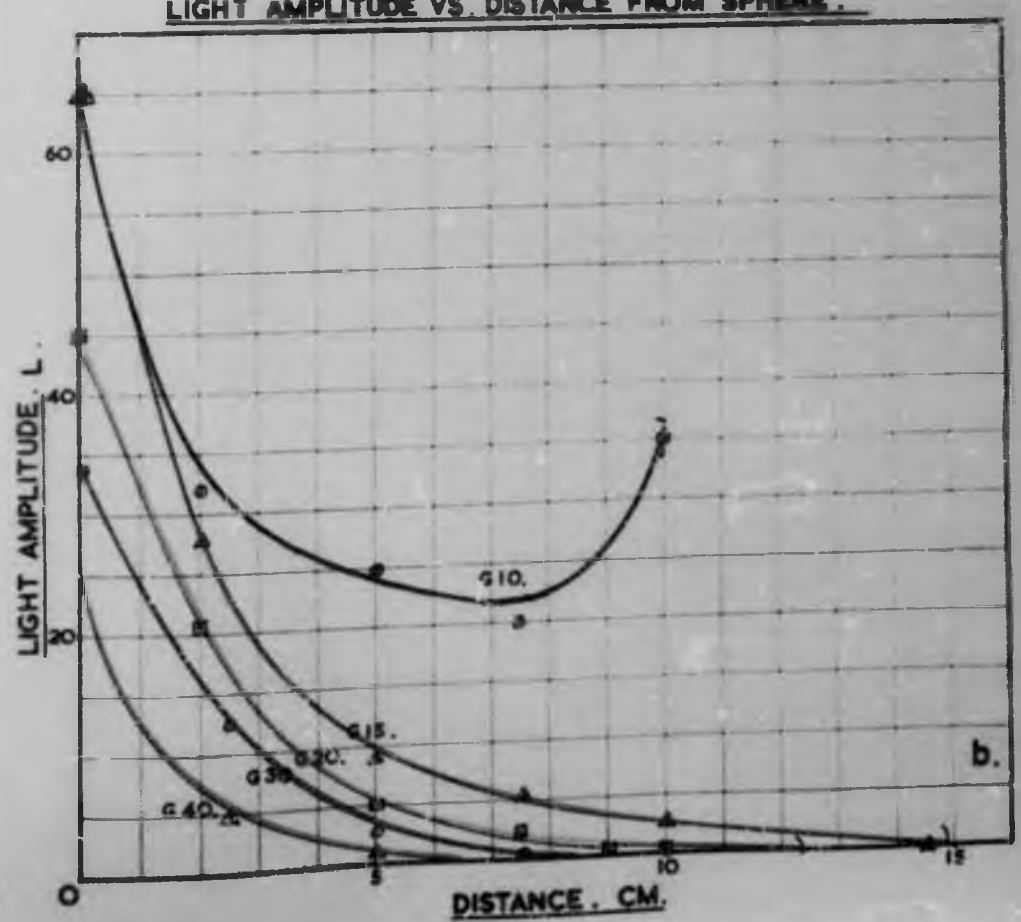
½" SPHERE — PLANE.

·07 μSEC RISE.

DISTANCE FROM SPHERE VS. TIME.

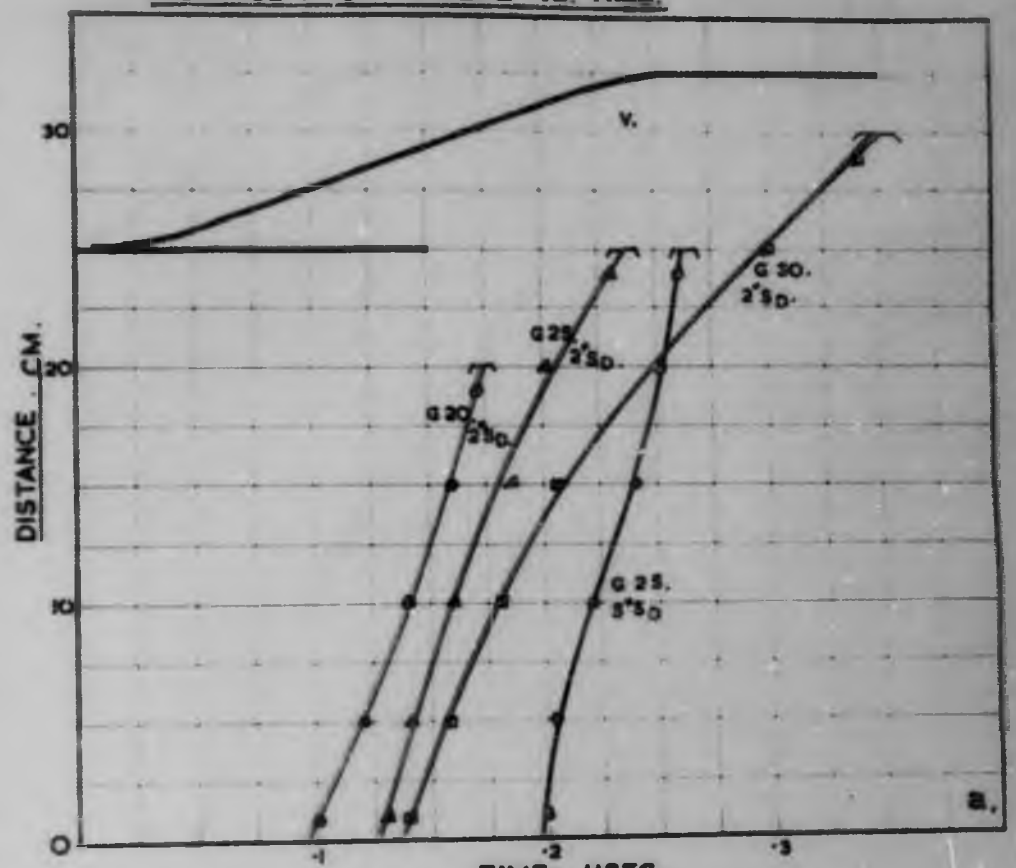


LIGHT AMPLITUDE VS. DISTANCE FROM SPHERE.

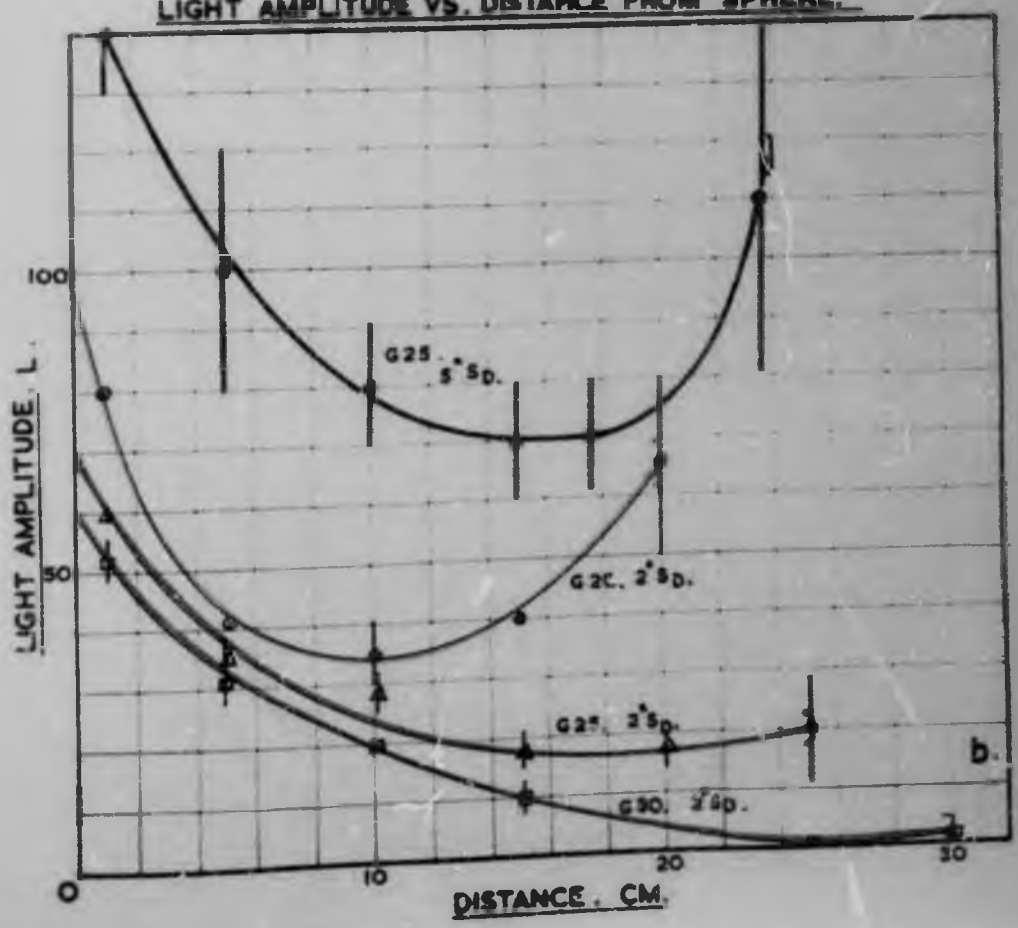


CORONA. — 300 KV. ·25 μSEC RISE. G 9.

DISTANCE FROM SPHERE VS. TIME.



LIGHT AMPLITUDE VS. DISTANCE FROM SPHERE.

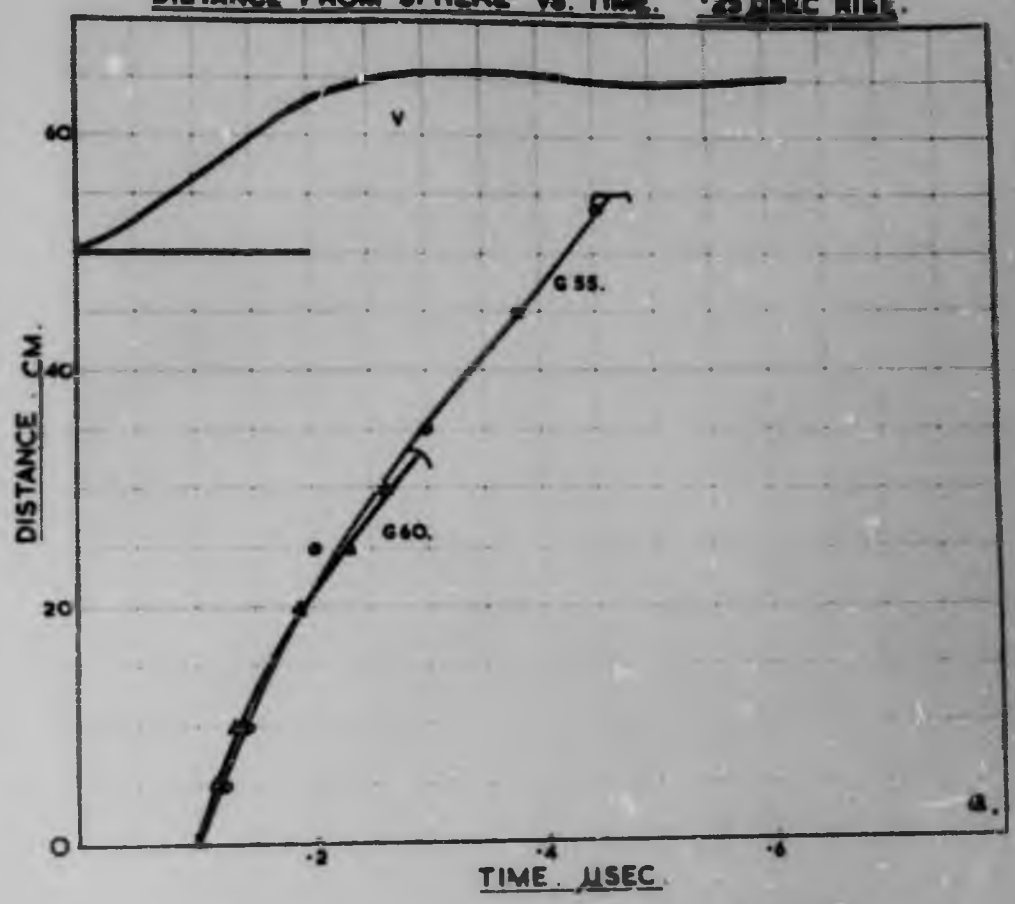


CORONA.

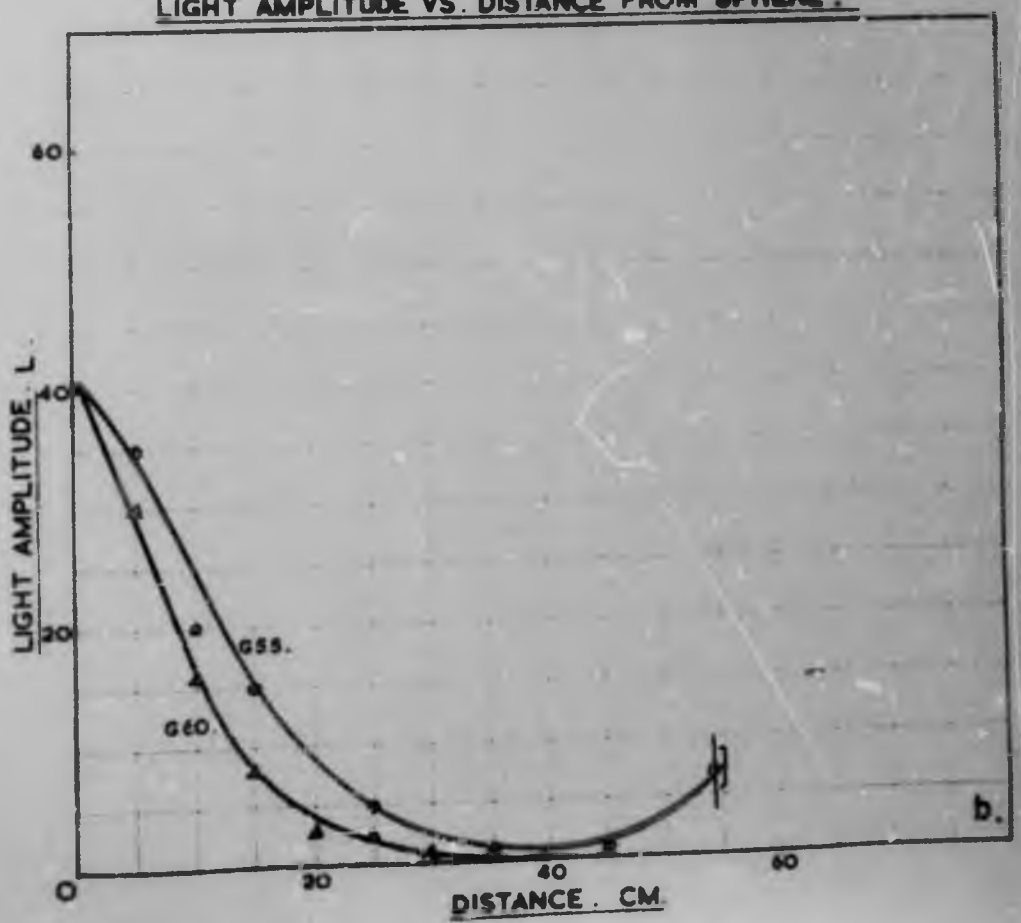
−600 KV.
2" SPHERE.
·25 μSEC RISE.

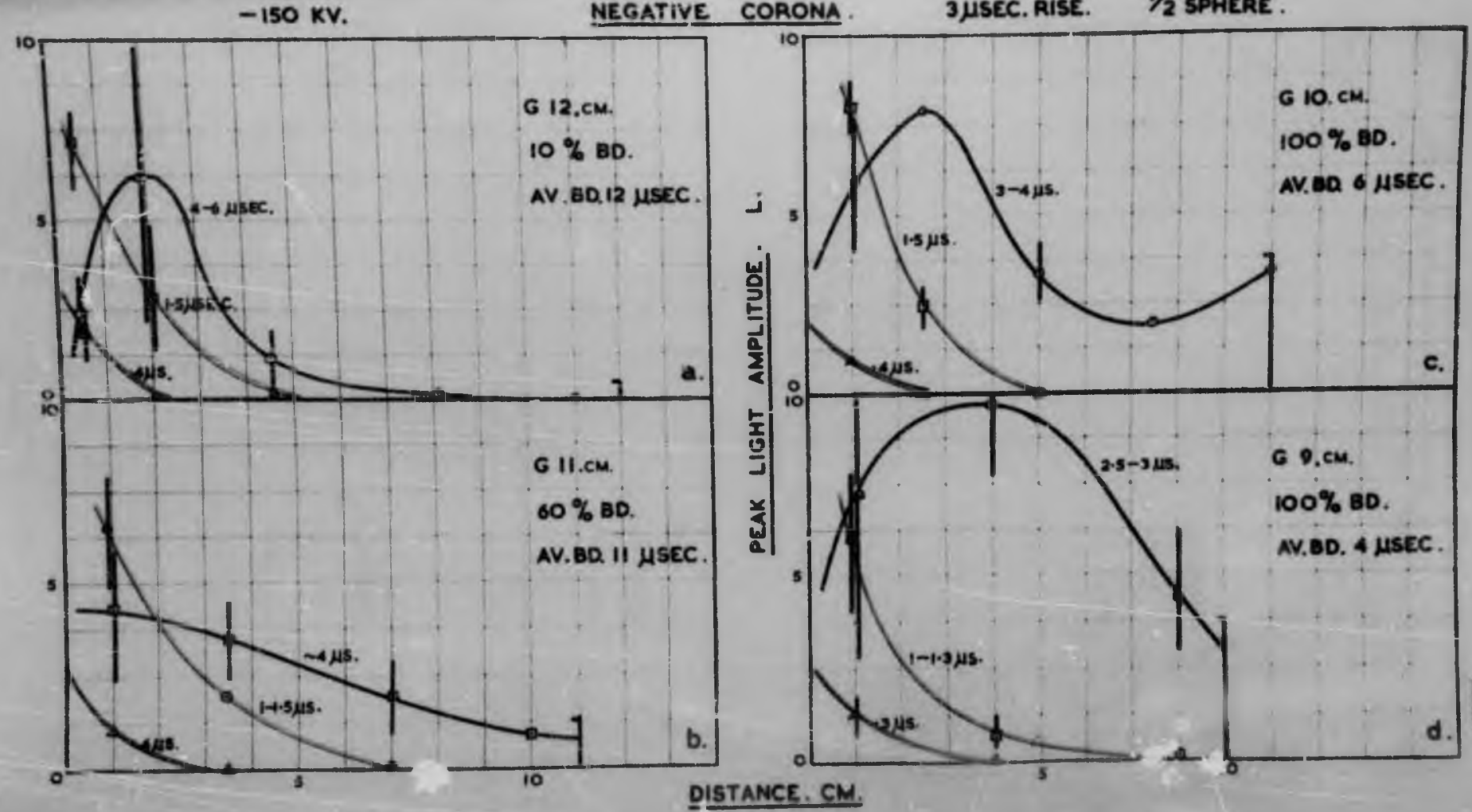
G 10.

DISTANCE FROM SPHERE VS. TIME.



LIGHT AMPLITUDE VS. DISTANCE FROM SPHERE.

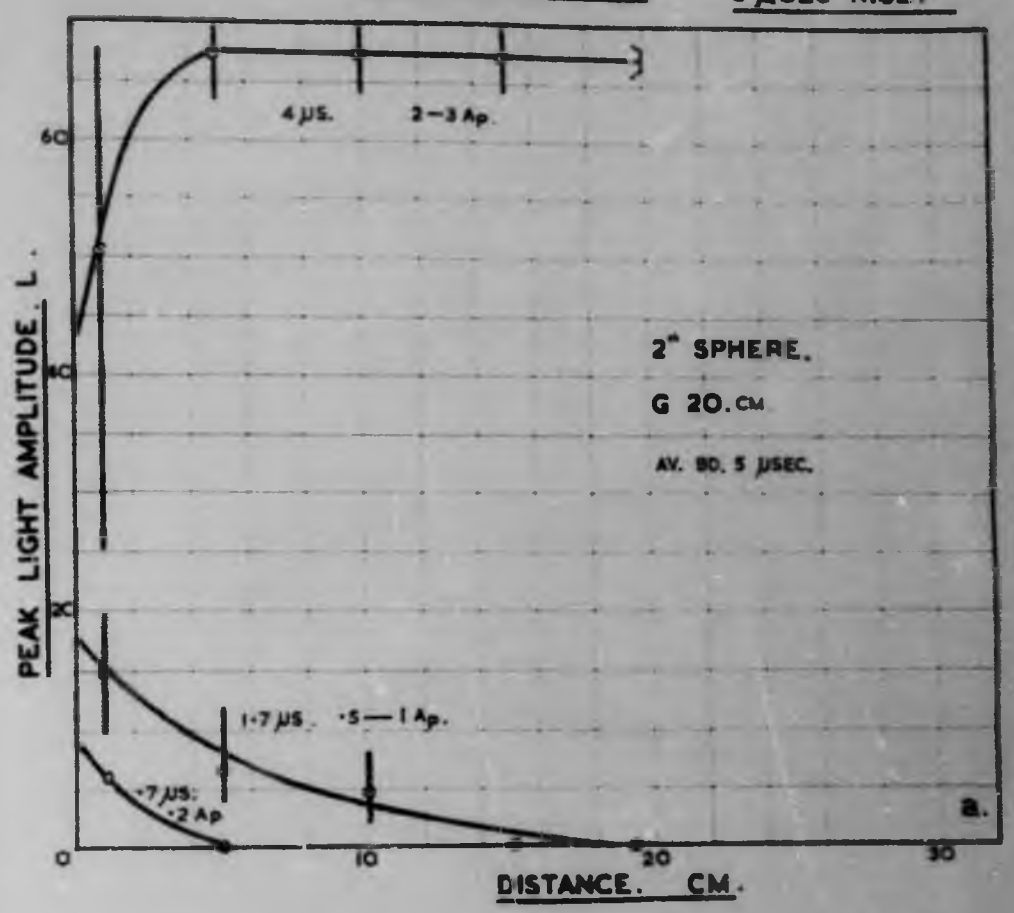


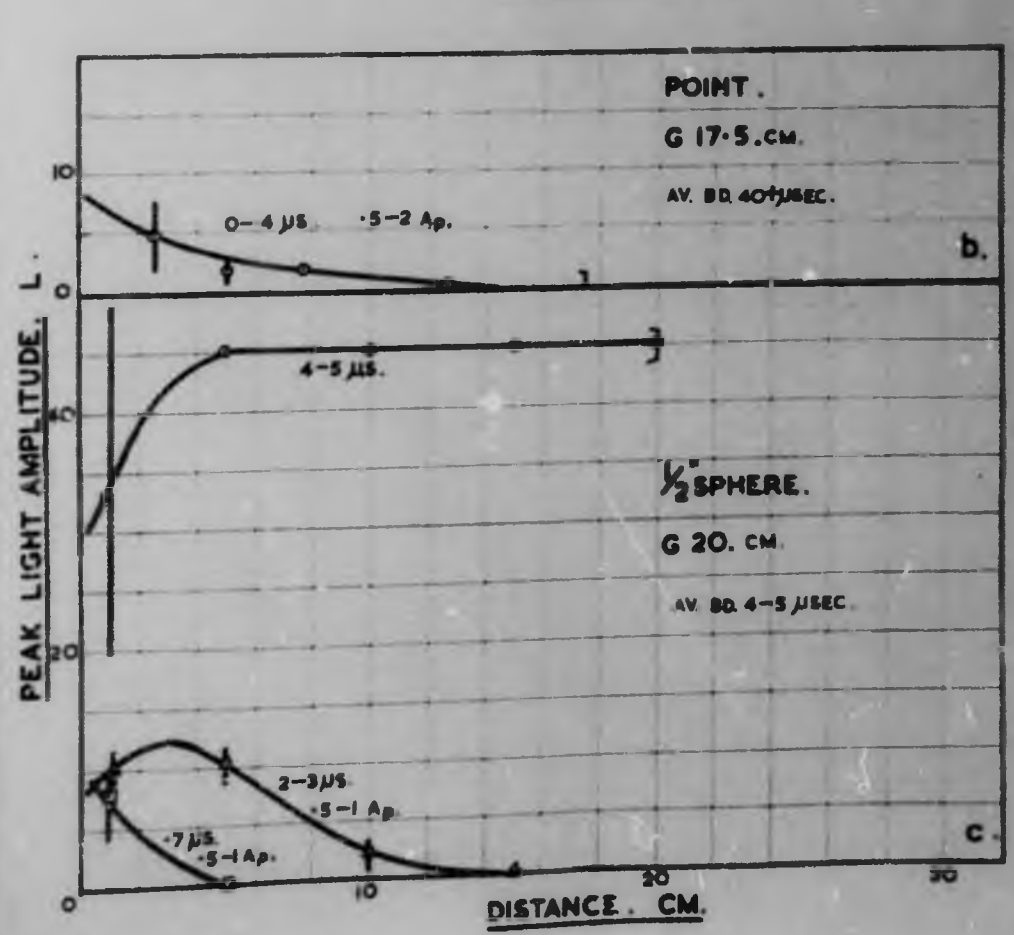

−150 KV.
NEGATIVE CORONA.
3 μSEC. RISE.
½" SPHERE.
G 12. CM.
10 % BD.
AV. BD. 12 μSEC.
4-6 μSEC.
1-5 μSEC.
4 μS.
a.
G 10. CM.
100 % BD.
AV. BD. 6 μSEC.
3-4 μS.
1-5 μS.
4 μS.
c.
G 11. CM.
60 % BD.
AV. BD. 11 μSEC.
~4 μS.
1-1.5 μS.
4 μS.
b.
G 9. CM.
100% BD.
AV. BD. 4 μSEC.
2.5-3 μS.
1-1.3 μS.
3 μS.
d.
PEAK LIGHT AMPLITUDE. L.
DISTANCE. CM.
0
5
10

G11.

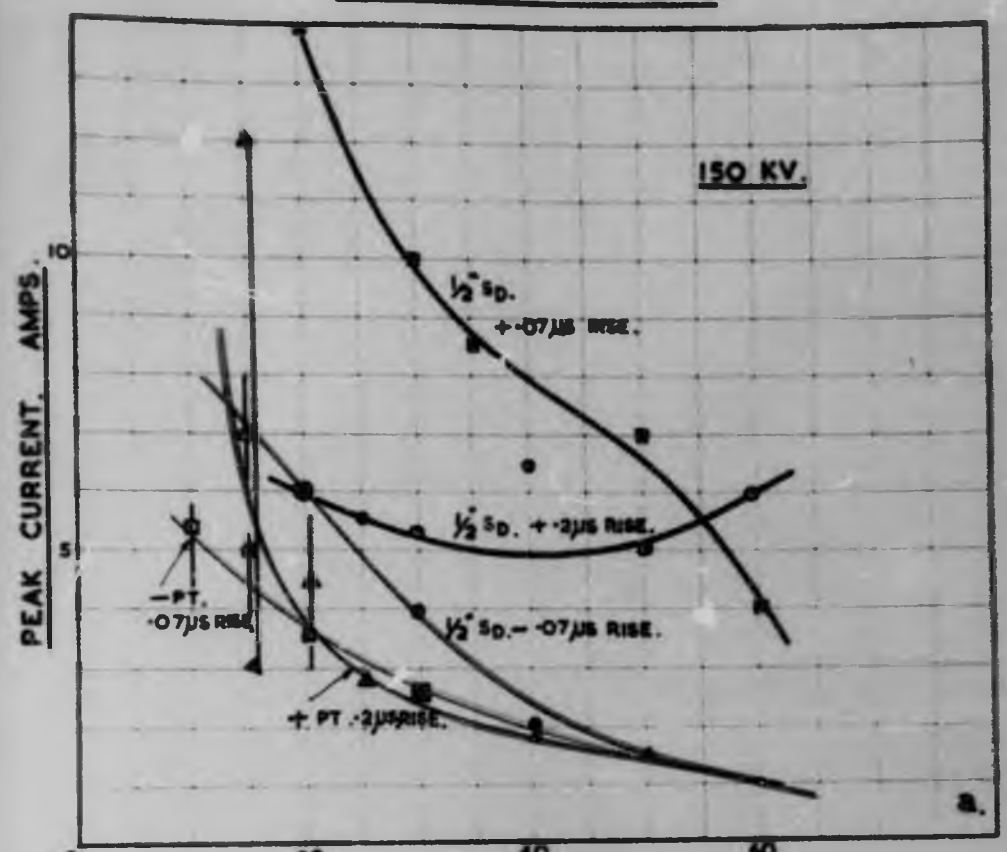
G 12.

NEGATIVE CORONA. — 300 KV. 3 μSEC RISE.

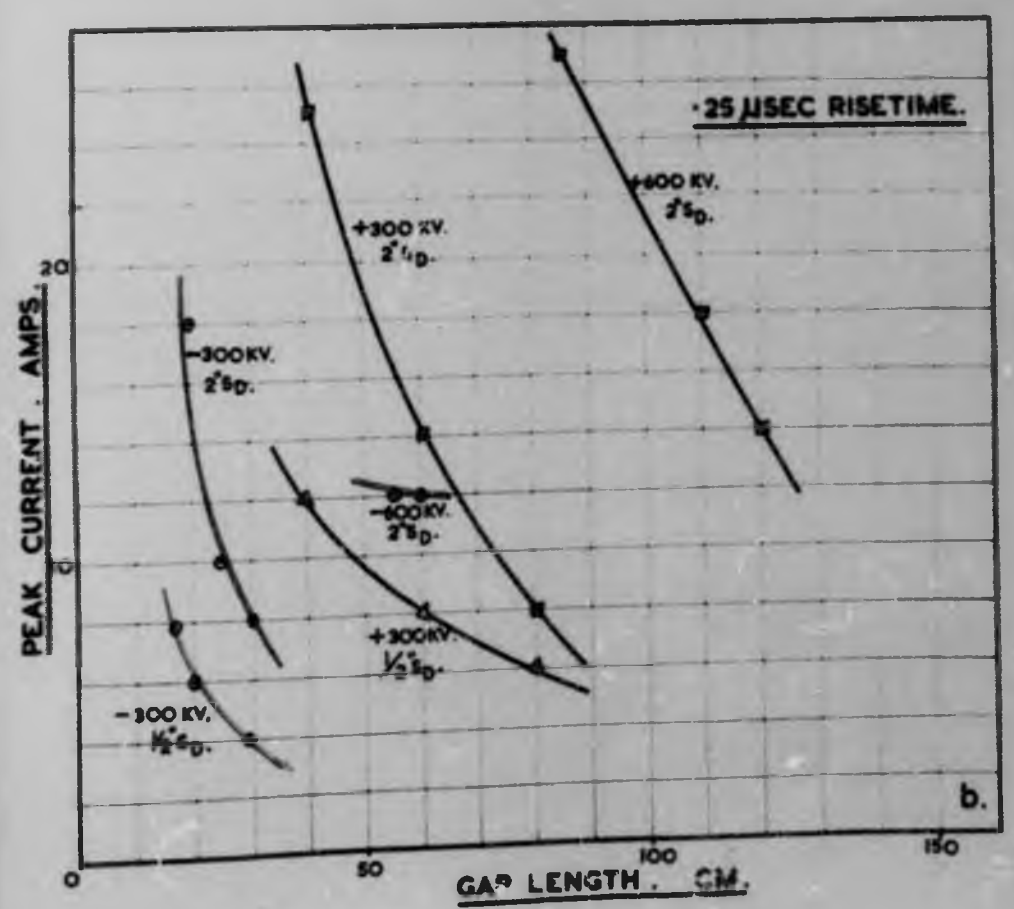




PEAK CORONA CURRENTS.



GAP LENGTH. CM.



GAP LENGTH. CM.

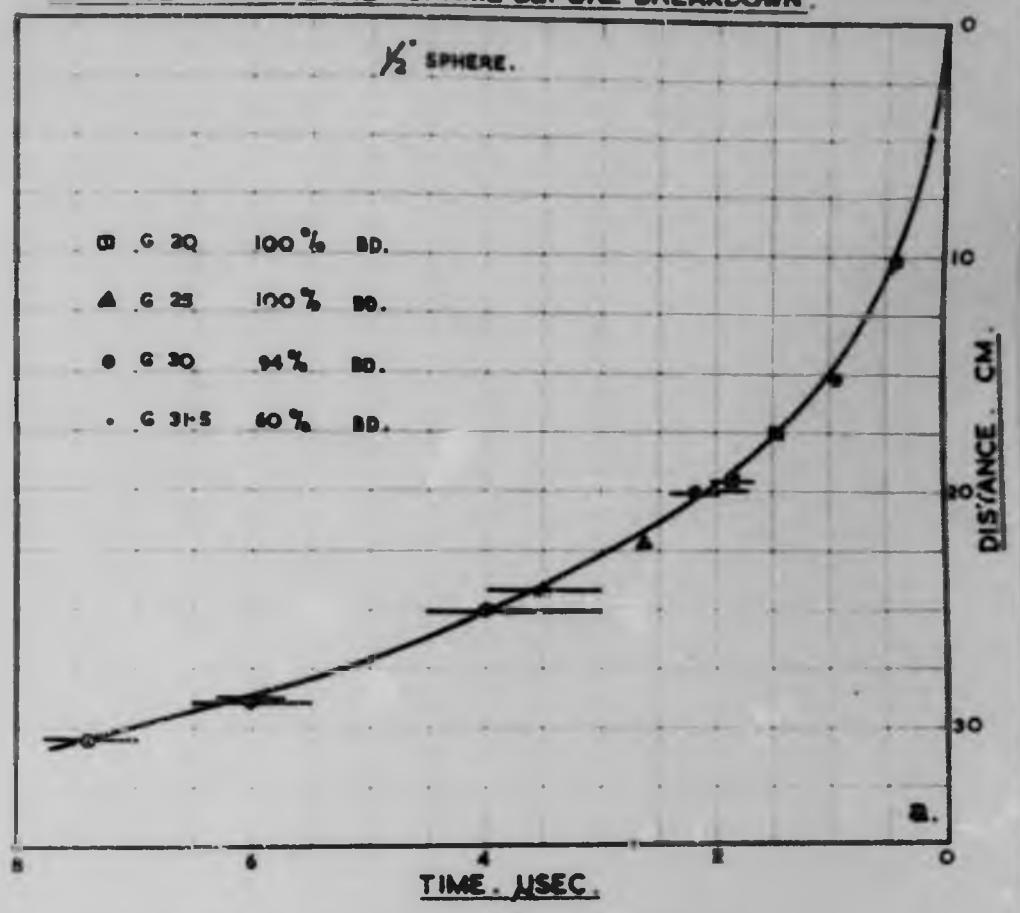
POSITIVE LEADER.

G 14.

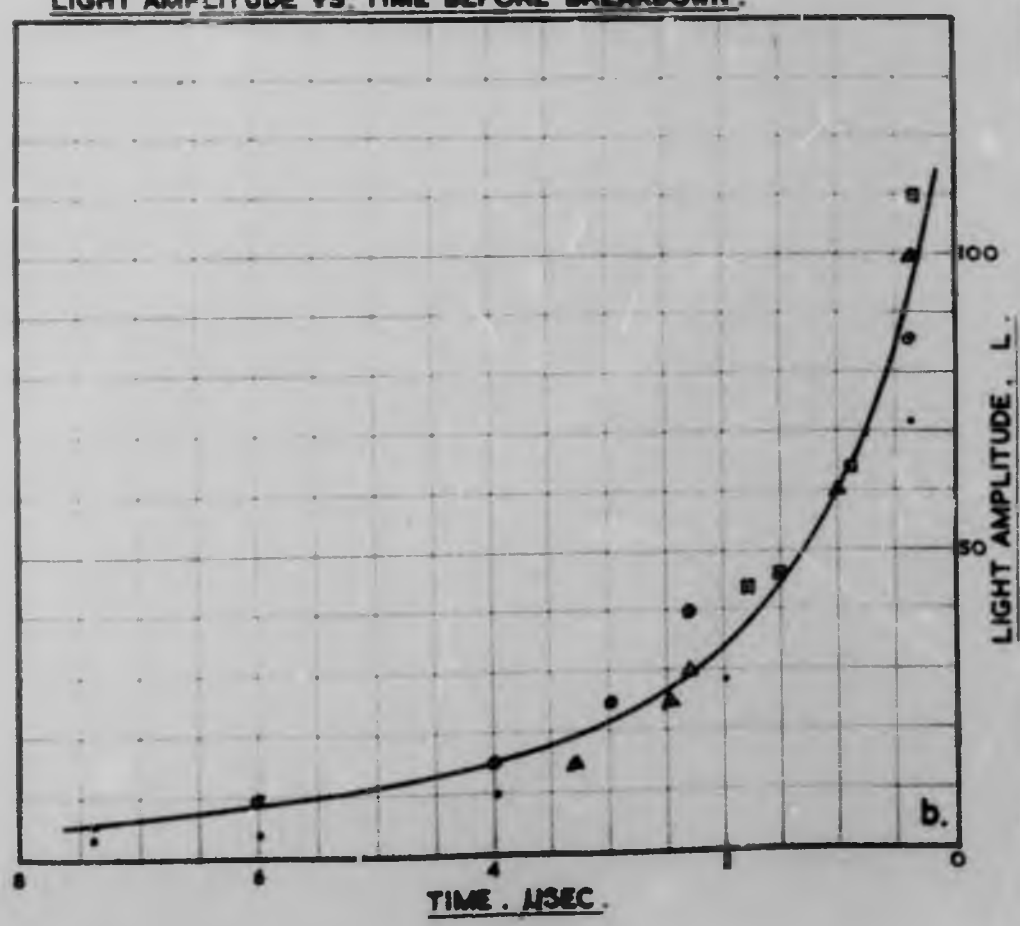
150 KV.

·22 μSEC RISE.

DISTANCE FROM PLANE VS. TIME BEFORE BREAKDOWN.



LIGHT AMPLITUDE VS. TIME BEFORE BREAKDOWN.

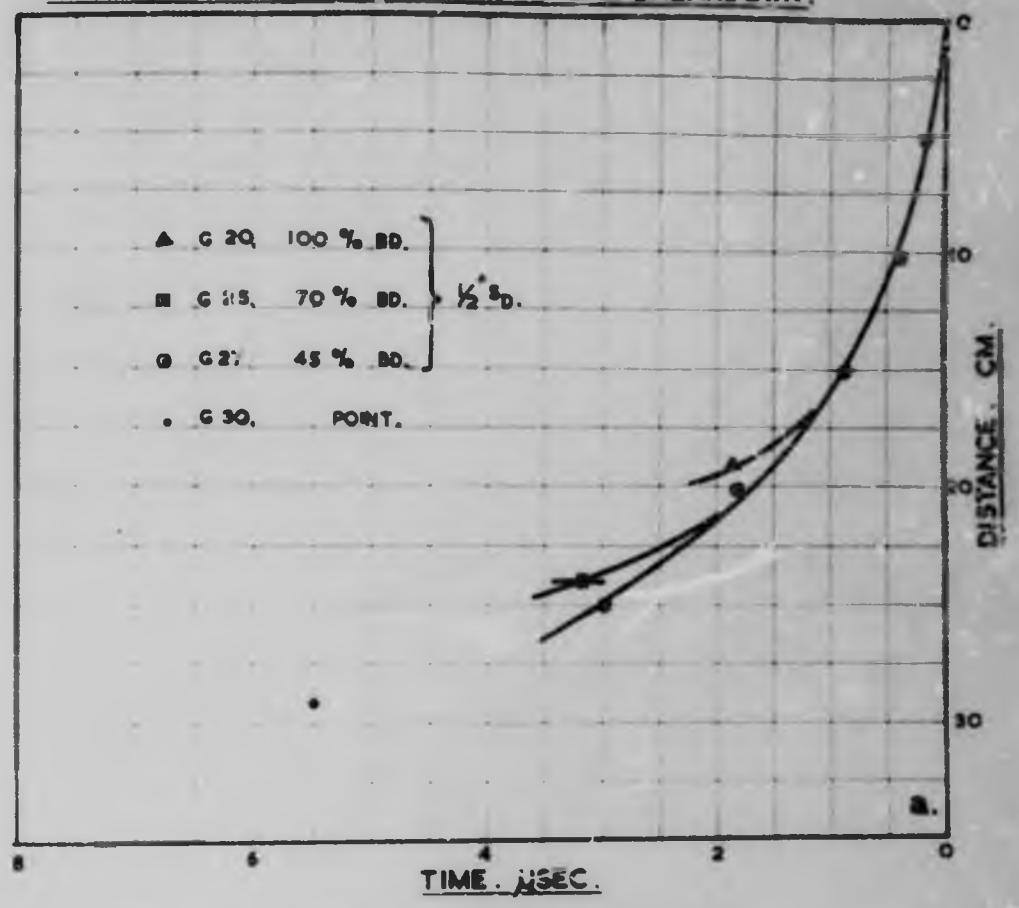


G 15.

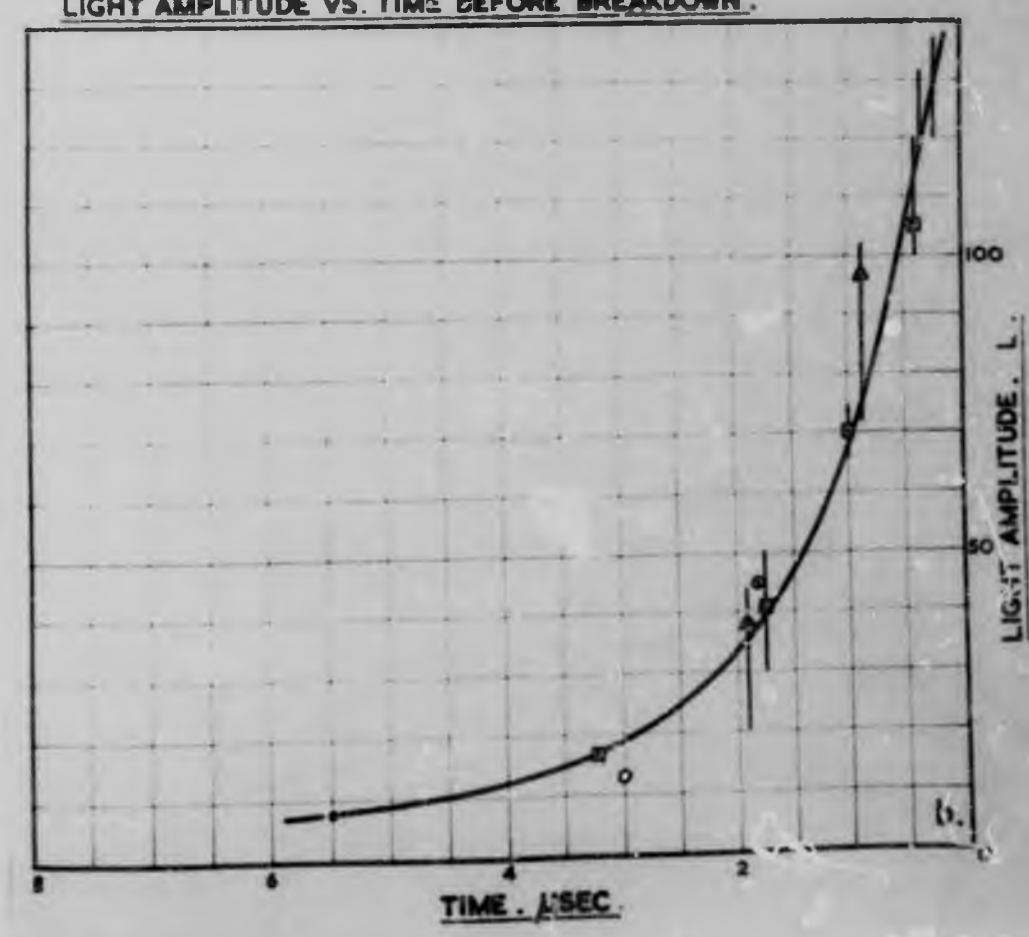
POSITIVE LEADER.

150 KV.
3 μSEC. RISE.

DISTANCE FROM PLANE VS. TIME BEFORE BREAKDOWN.



LIGHT AMPLITUDE VS. TIME BEFORE BREAKDOWN.

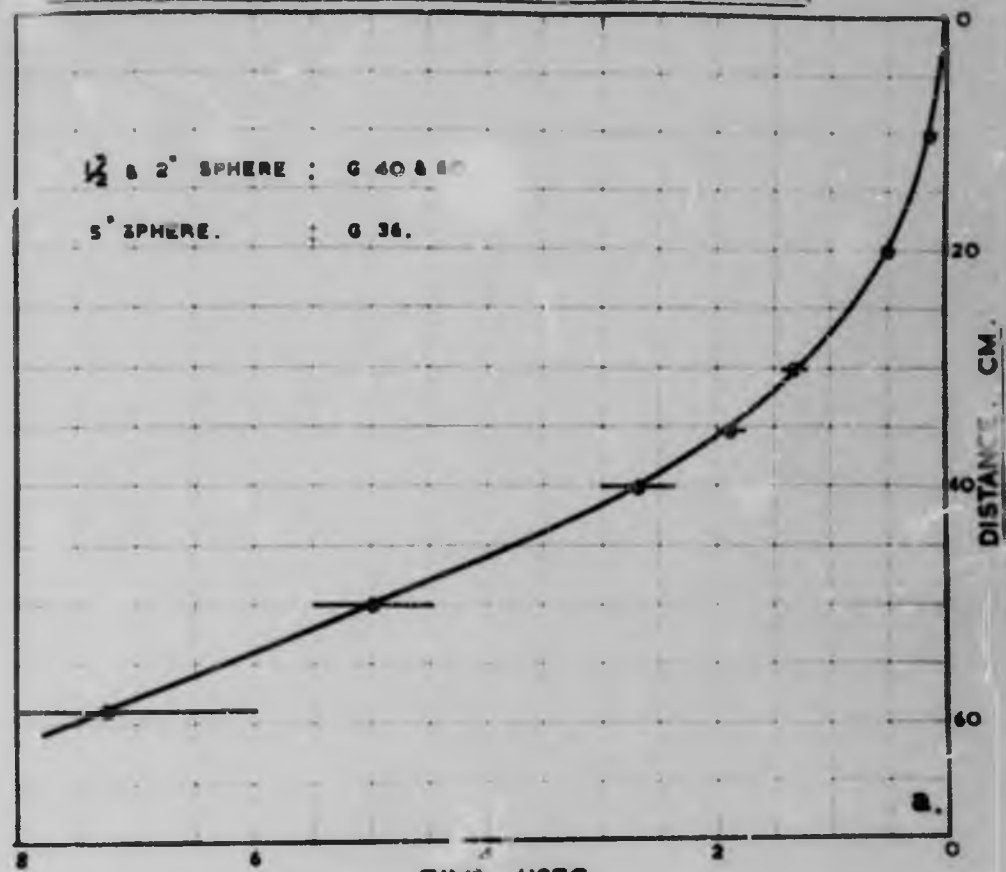


G 16

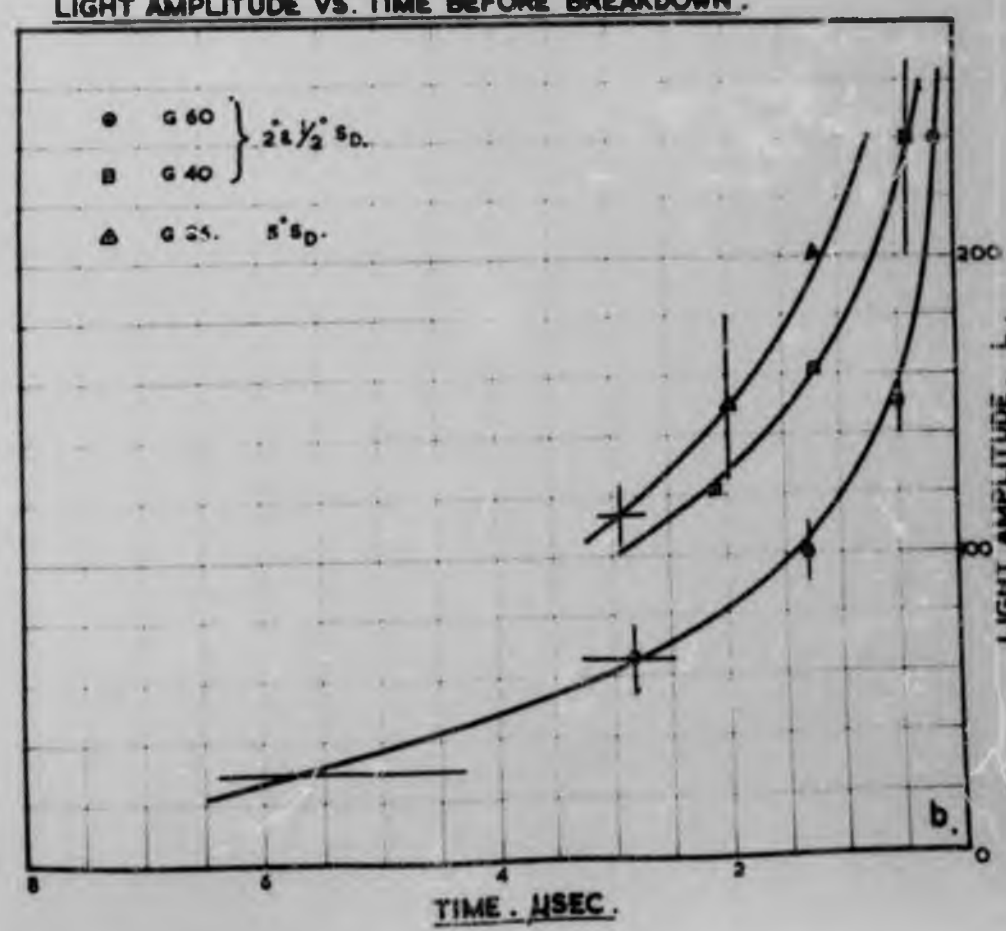
POSITIVE LEADER.

300 KV.
·25 μSEC RISE.

DISTANCE FROM PLANE VS. TIME BEFORE BREAKDOWN.



LIGHT AMPLITUDE VS. TIME BEFORE BREAKDOWN.

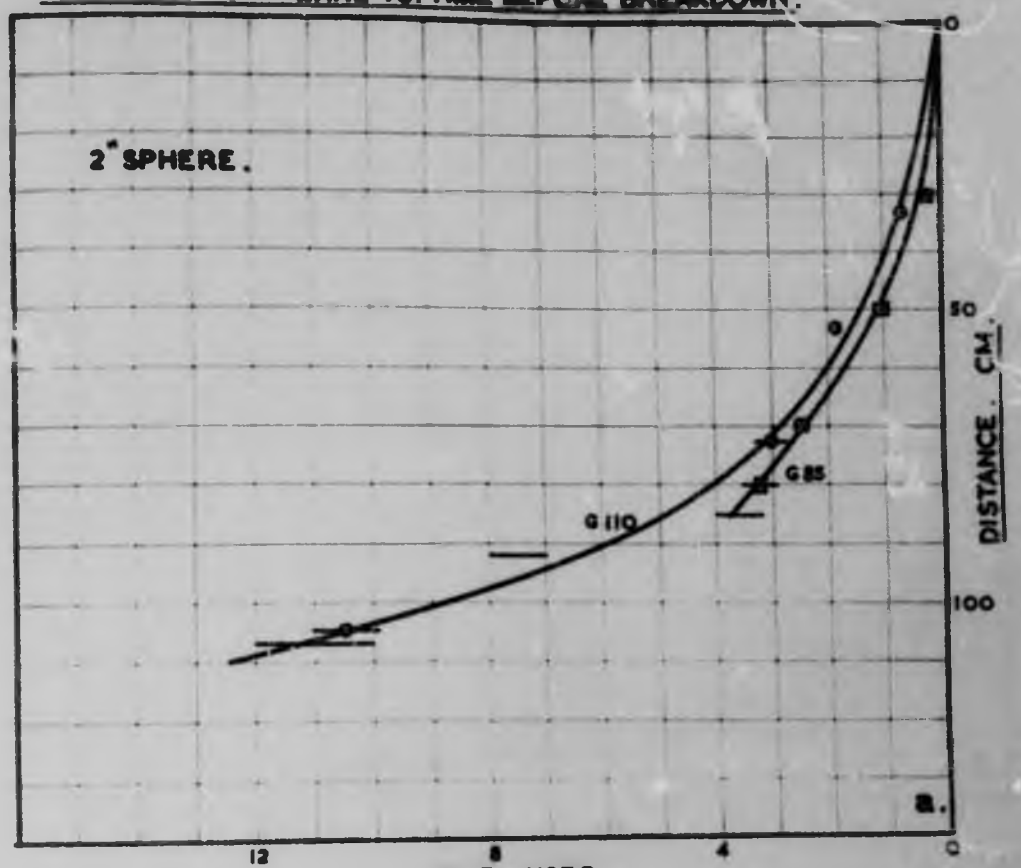


G.17.

POSITIVE LEADER.

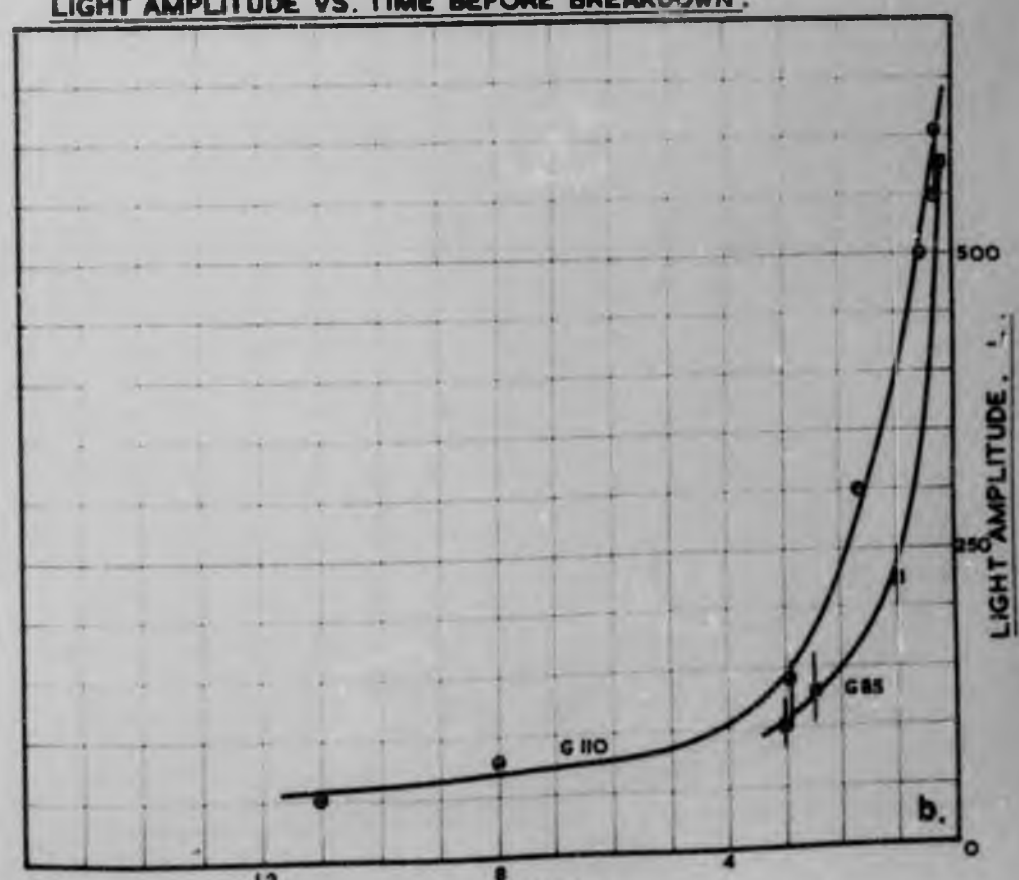
600 KV.
·25 μSEC. RISE.

DISTANCE FROM PLANE VS. TIME BEFORE BREAKDOWN.



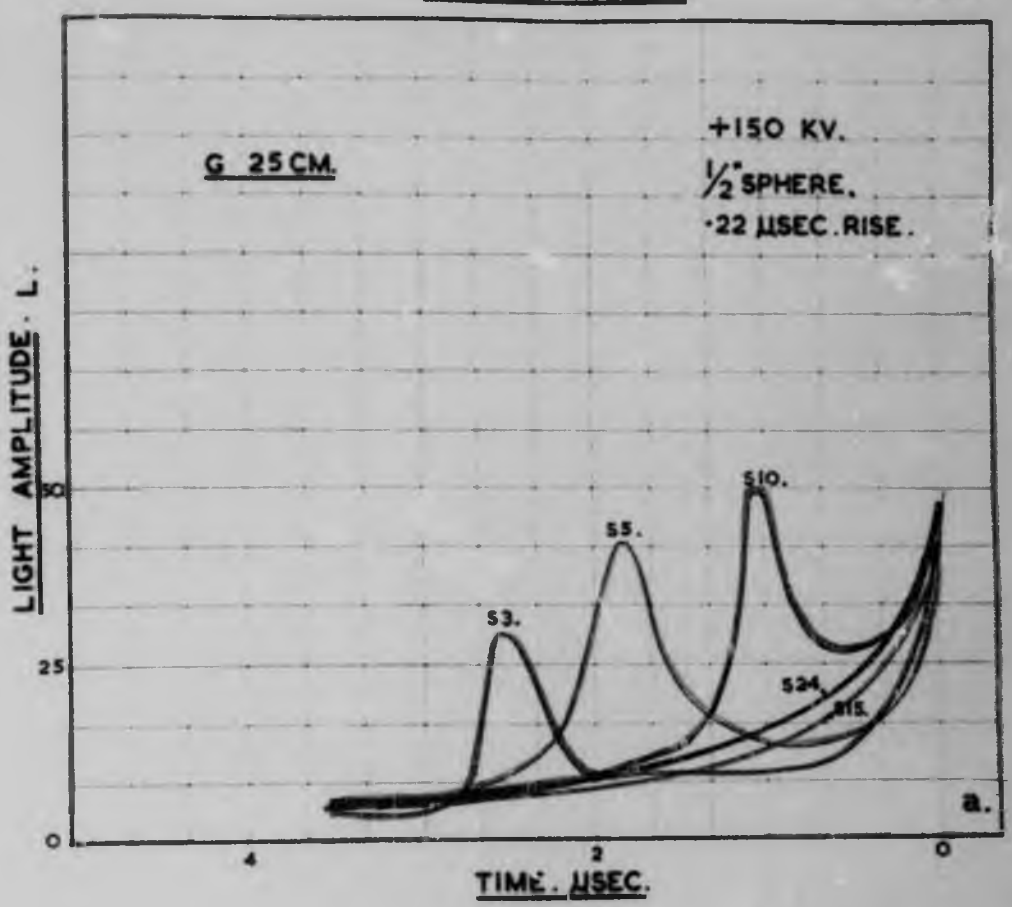
TIME. μSEC.

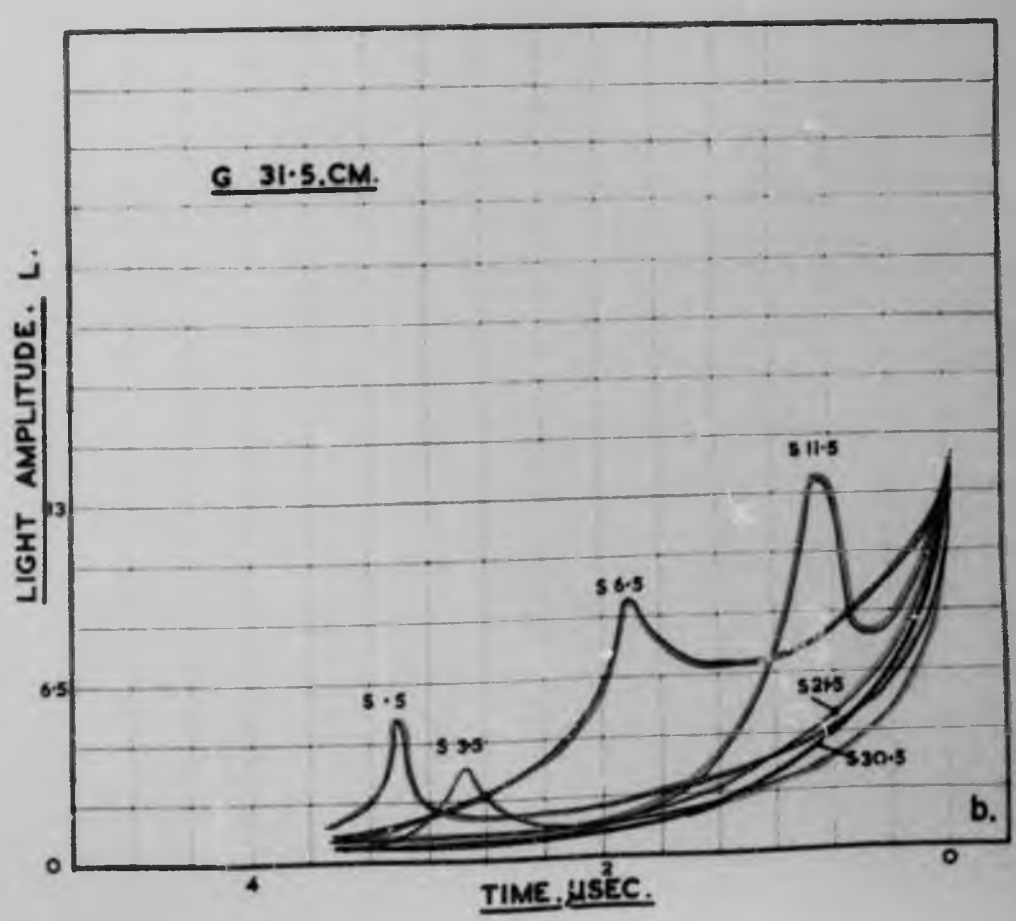
LIGHT AMPLITUDE VS. TIME BEFORE BREAKDOWN.



TIME. μSEC.

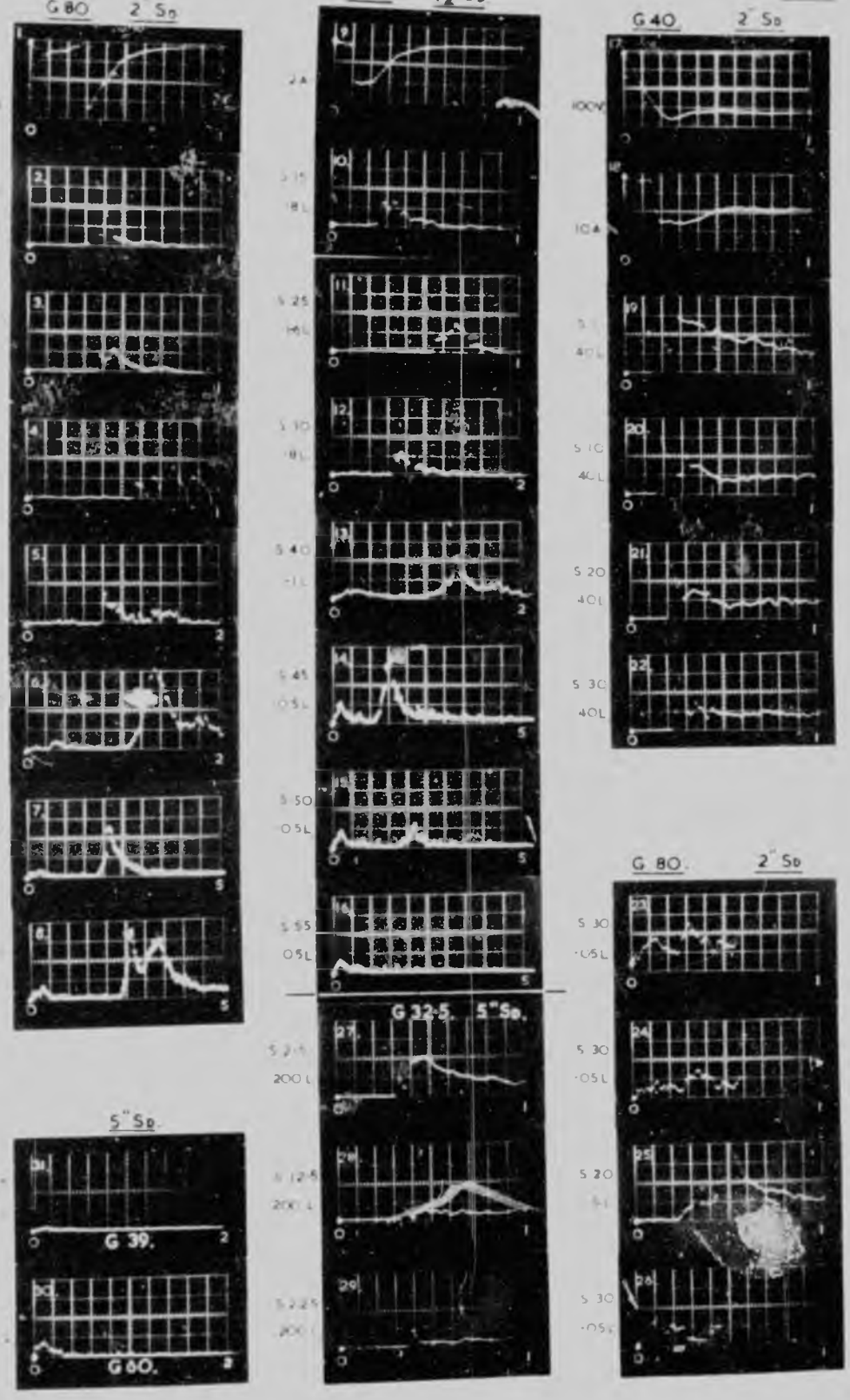
POSITIVE LEADER. G 18.



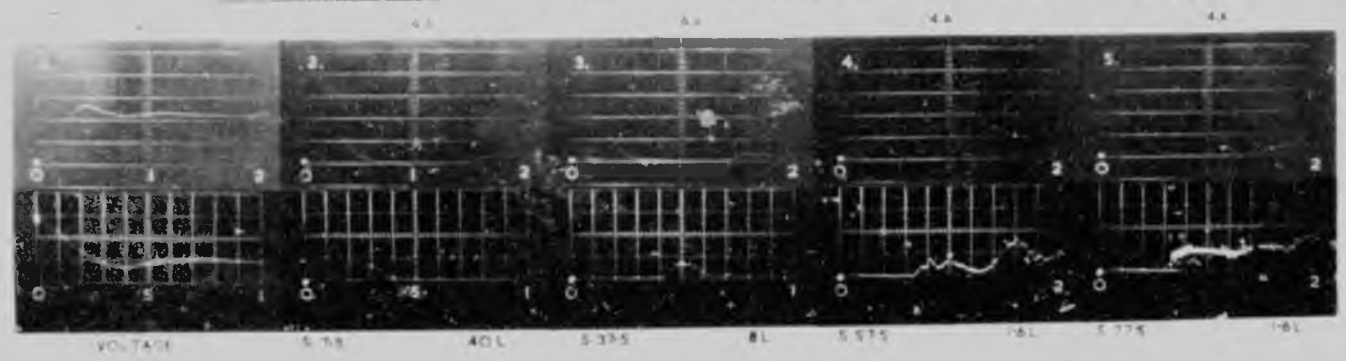


POSITIVE CORONA + 300 KV .25 μSEC RISE

PL 1



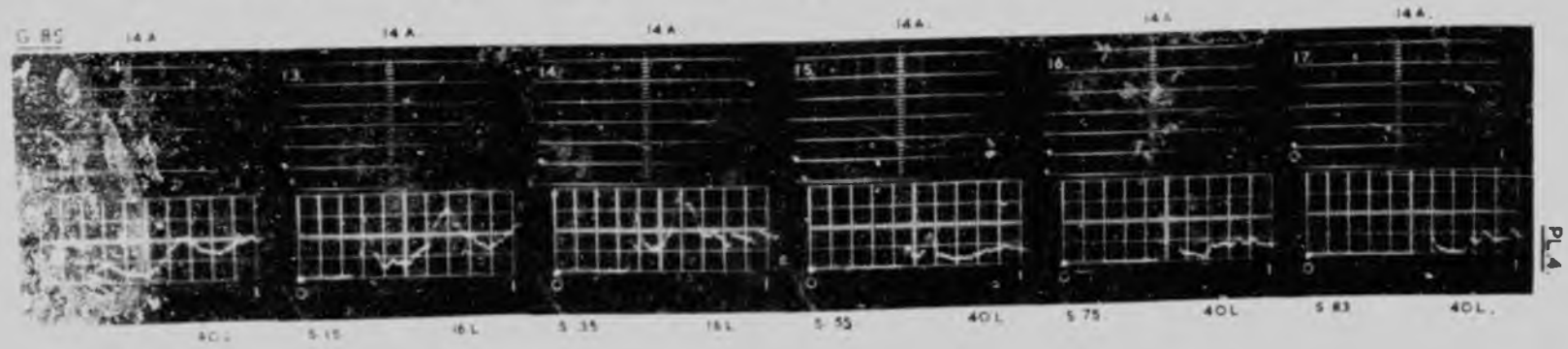
POSITIVE CORONA + 600 KV 25 μSEC RISE 2" SPHERE-PLANE (S).



G 120



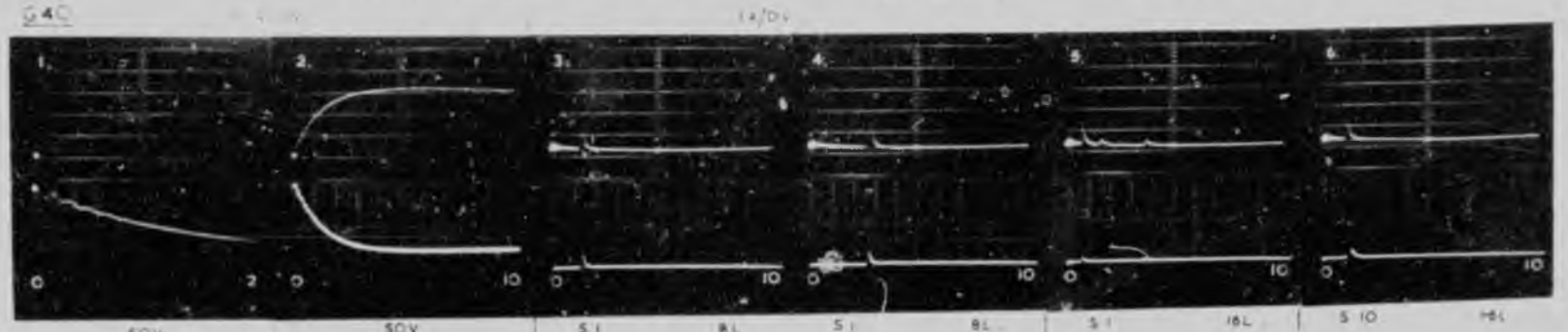
G 85



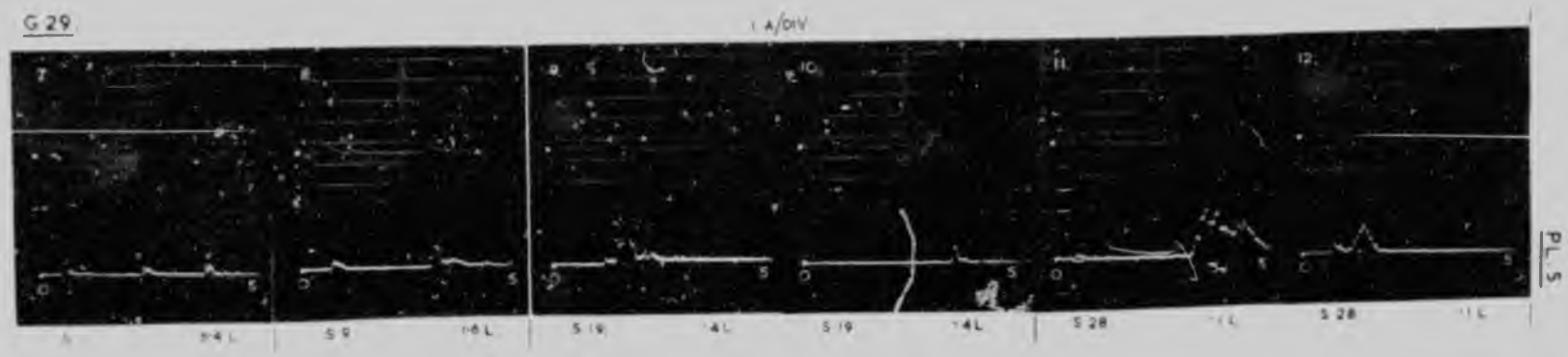
PL 4

POSITIVE CORONA +150 KV 3 μSEC RISE 1/2" SPHERE-PLANE

G 40

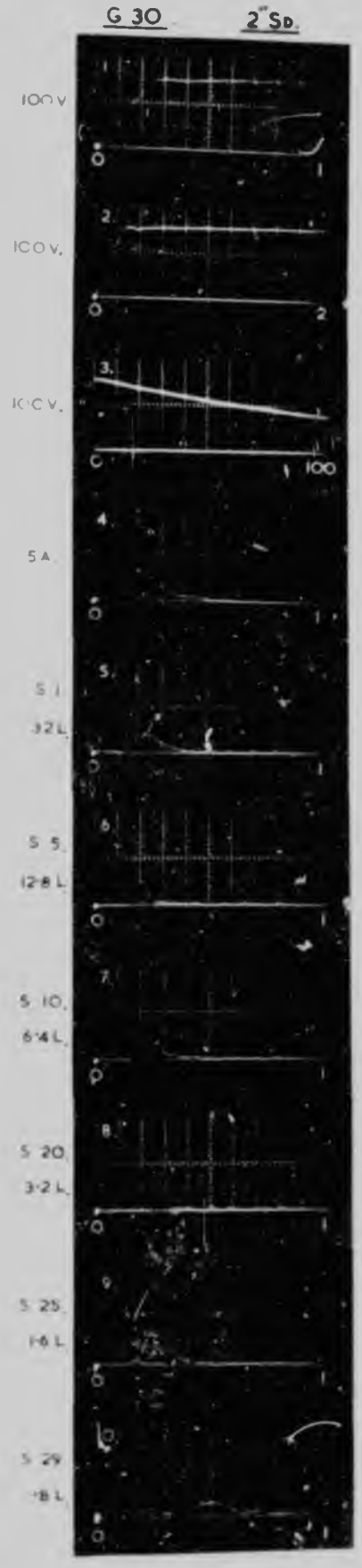


G 29



PL. 5

NEGATIVE CORONA — 300 KV ·25 μSEC. RISE

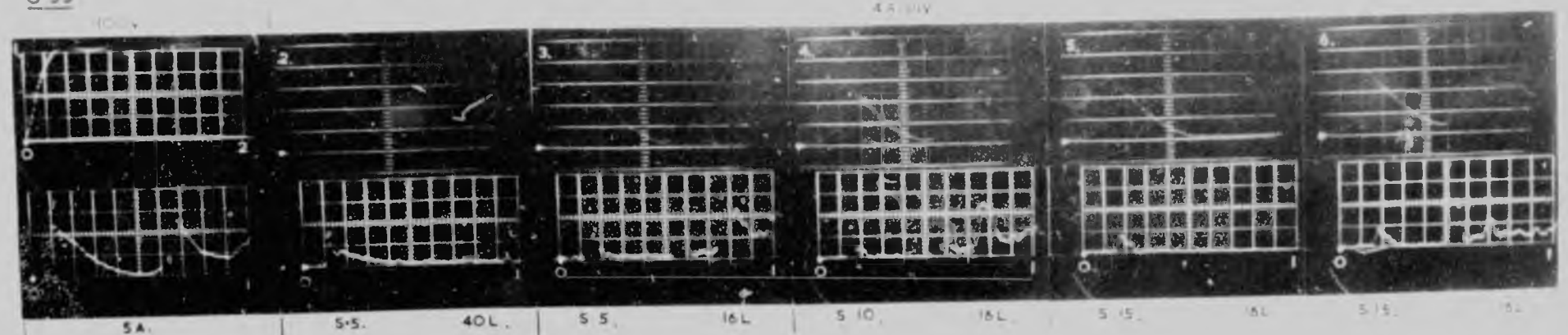


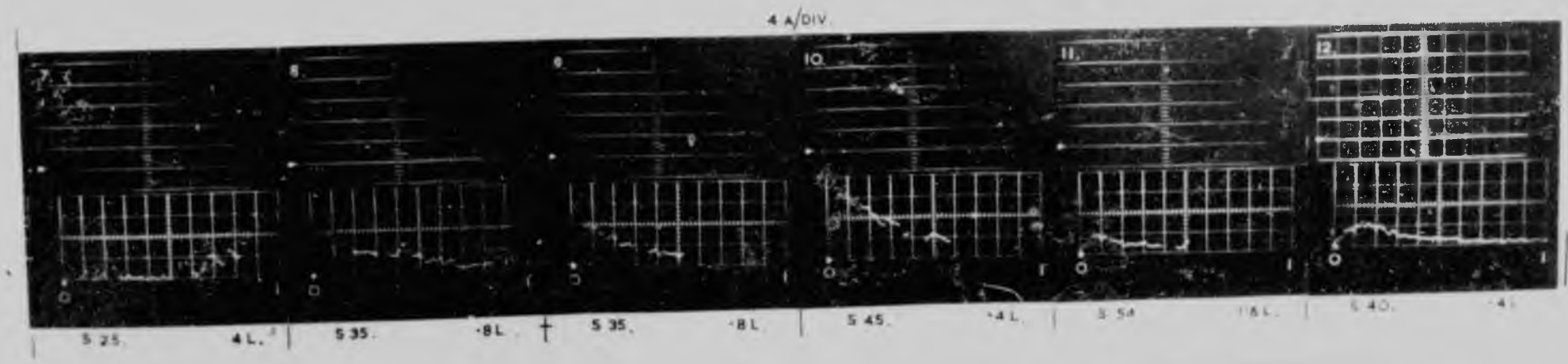




G 55

NEGATIVE CORONA — 600 KV. ·25 μSEC RISE 2" SPHERE–PLANE (5)

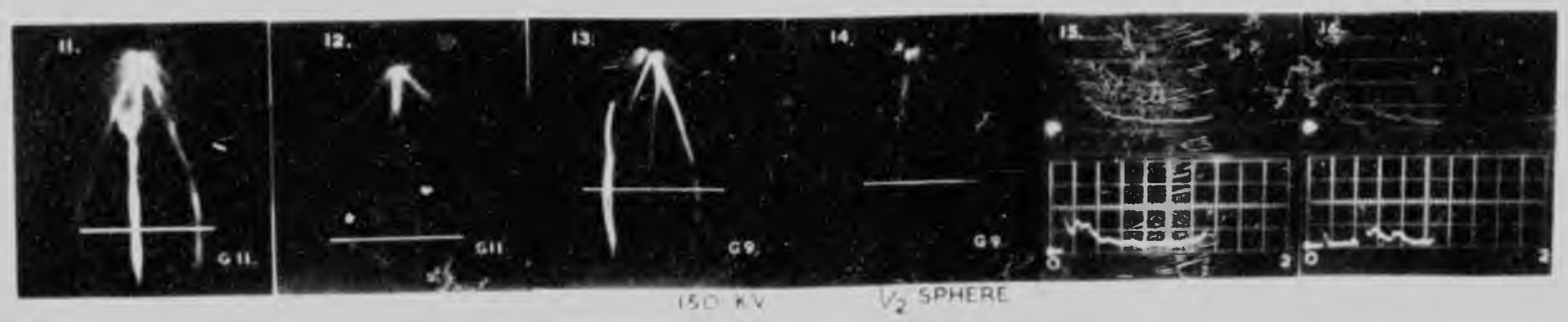




PL 7



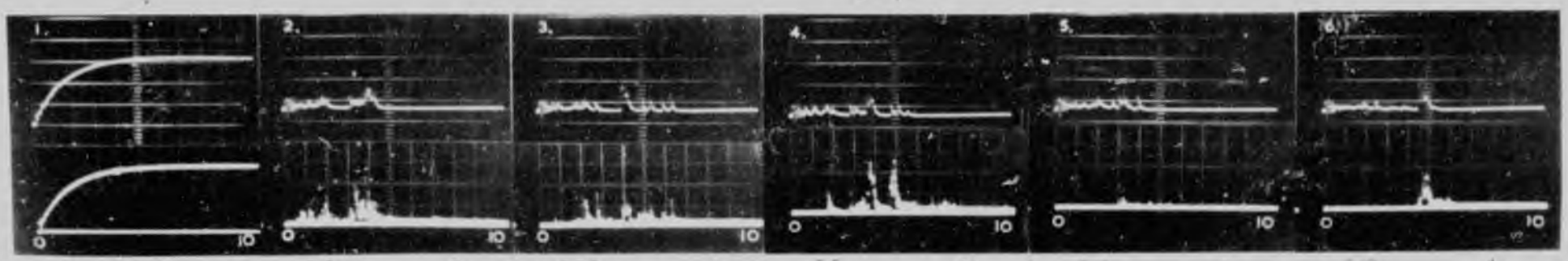


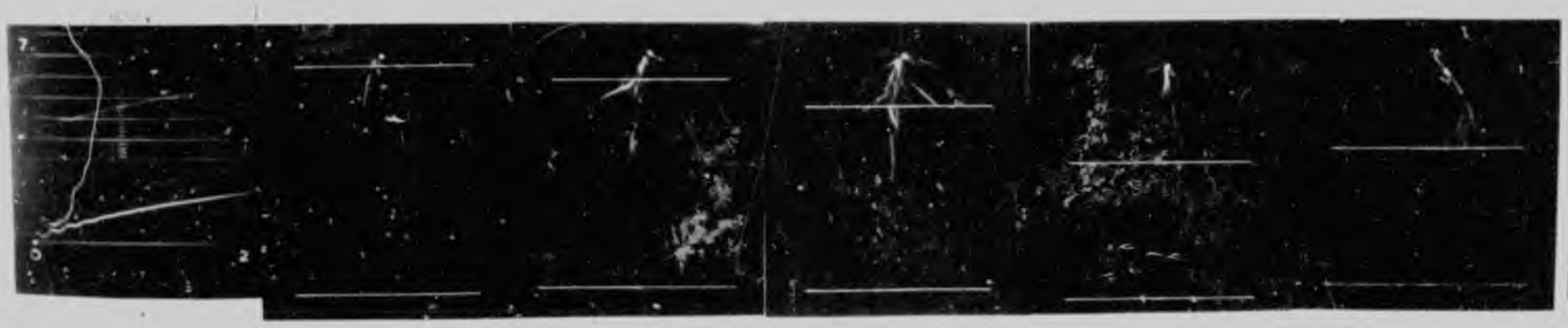


150 KV ½ SPHERE

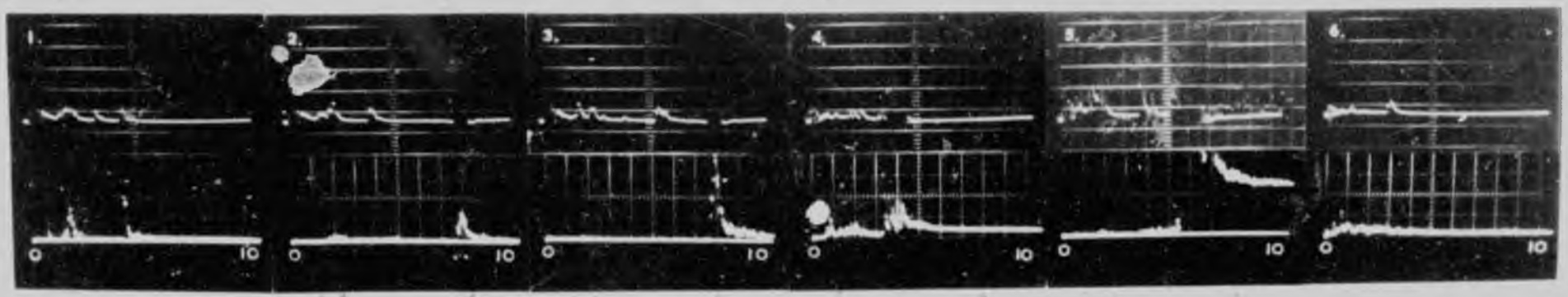
NEGATIVE CORONA — 300 KV 3 μSEC RISE 1/2 SPHERE — PLANE

G 25

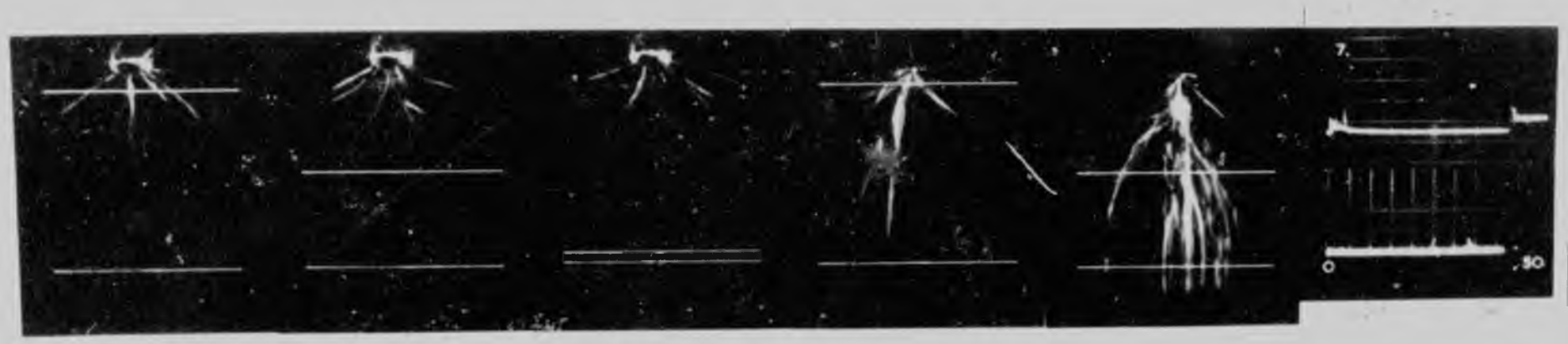




PL 9



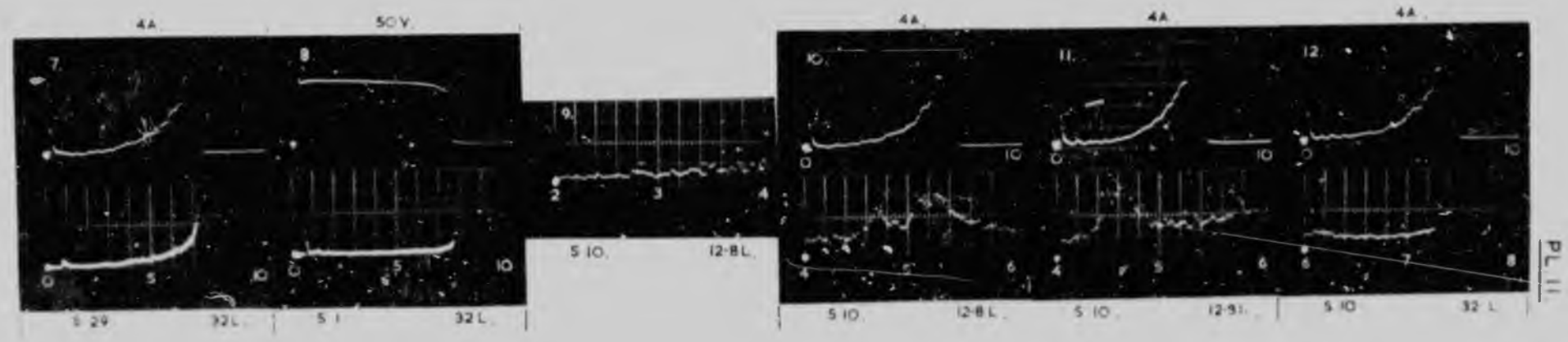
G 17-5



G 30

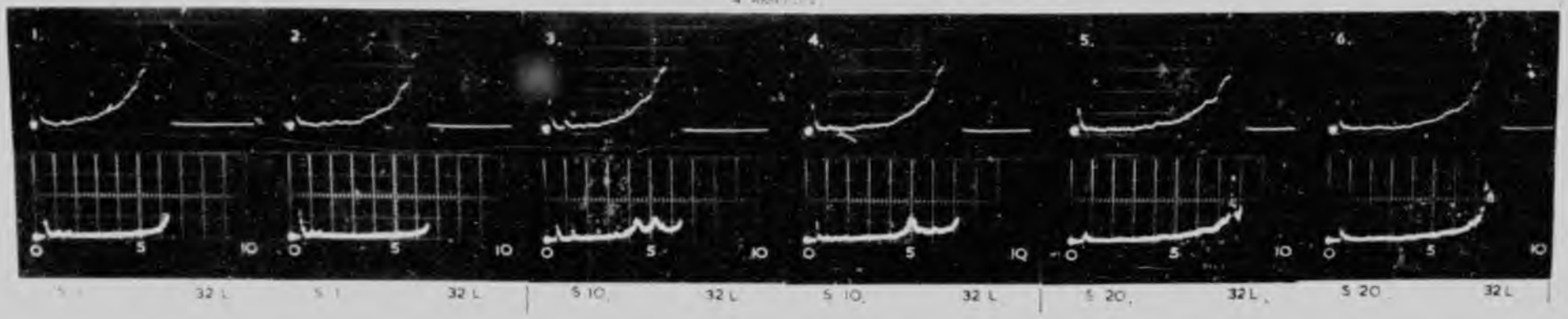
POSITIVE BREAKDOWN + 150 KV. ·22 μSEC RISE ½" SPHERE-PLANE

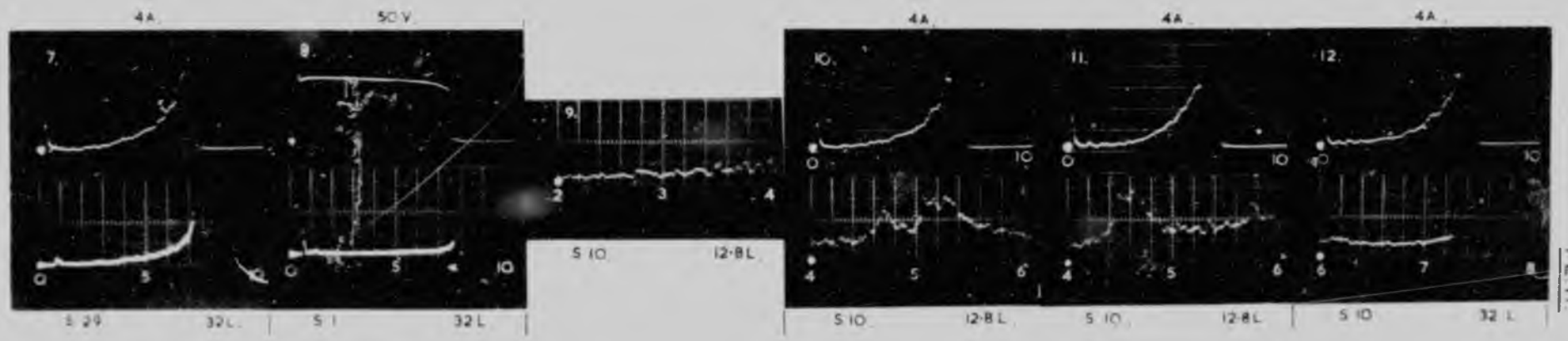




PL. 11

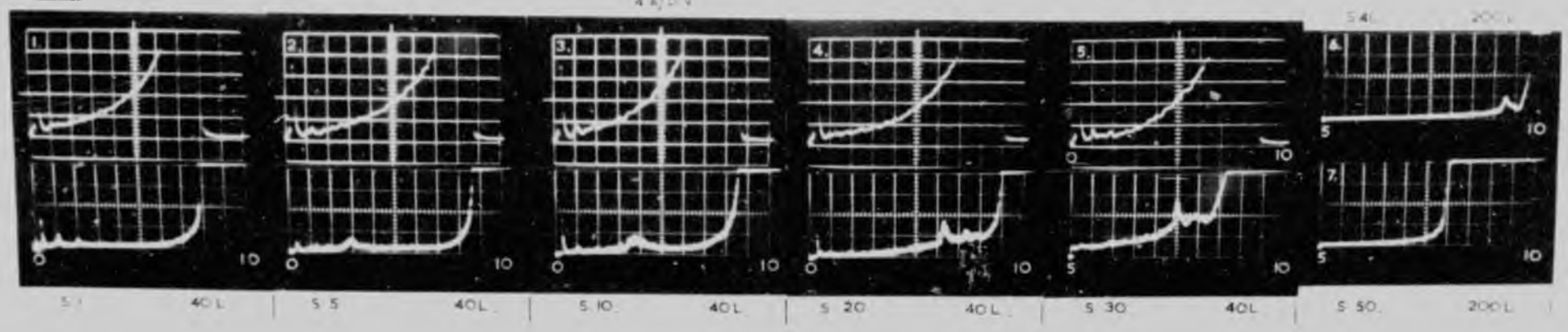
G 30 POSITIVE BREAKDOWN + 150 KV. ·22 μSEC RISE ½ SPHERE-PLANE

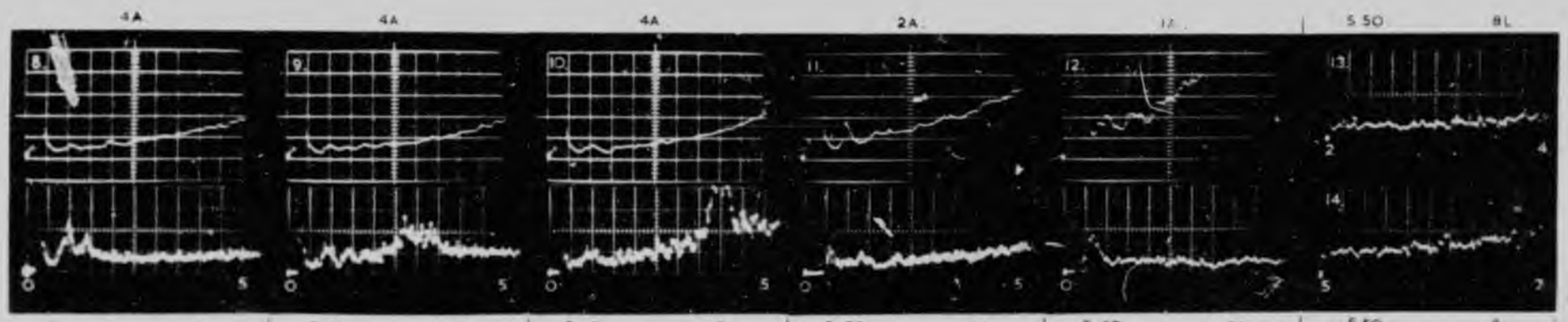




PL. 11.

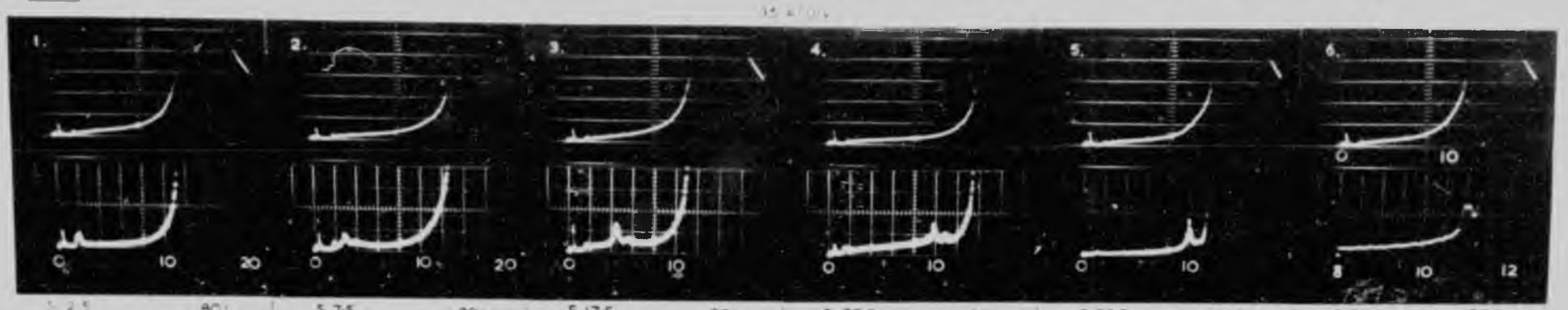
G60 POSITIVE BREAKDOWN. +300 KV. ·25 μSEC RISE. 2" SPHERE — PLANE.





PL 12

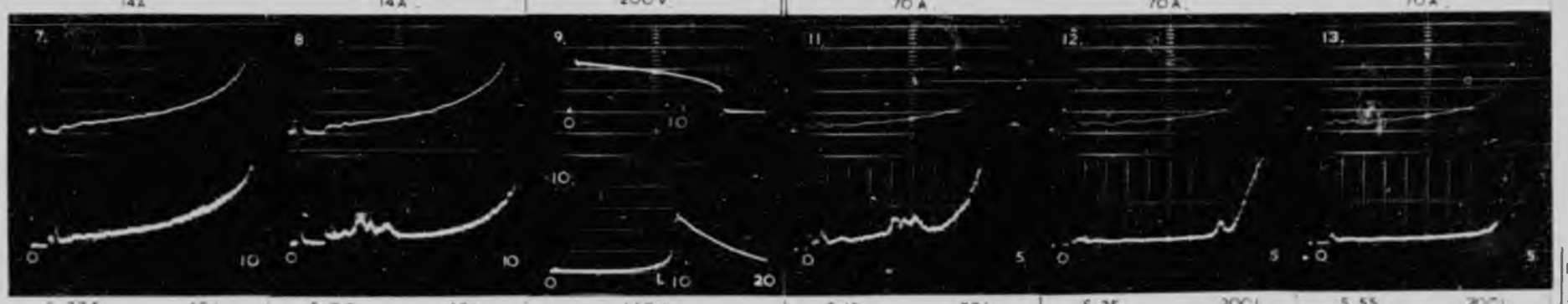
G 110 POSITIVE BREAKDOWN + 600 KV. ·25 μSEC RISE. 2" SPHERE-PLANE (S)



S 2·5 80L | S 7·5 80L | S 17·5 80L | S 37·5 80L | S 57·5 200L | S 77·5 200L

G 85.

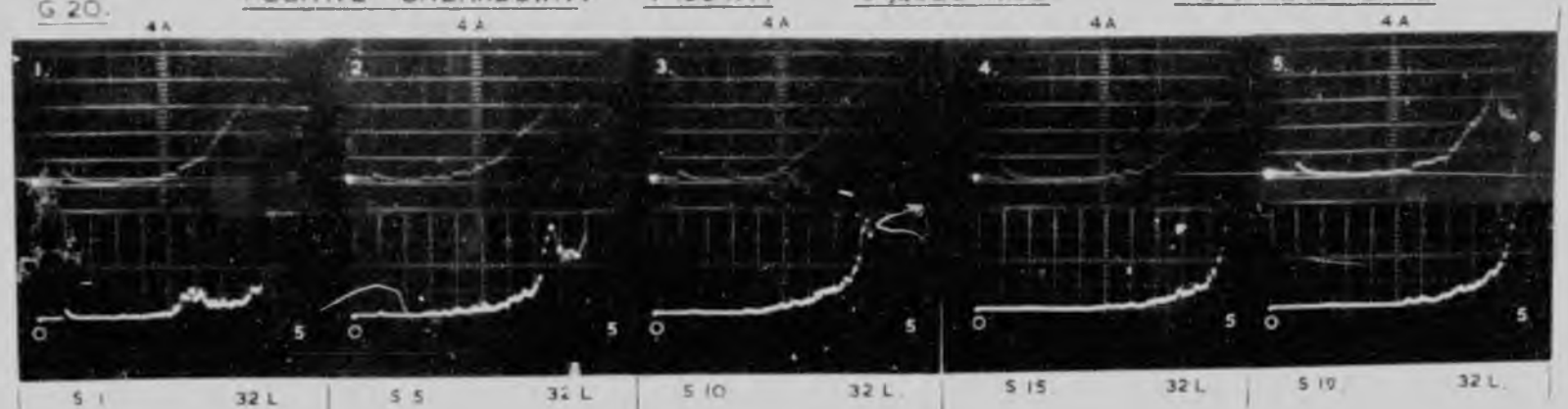
14A 14A 200V 70A 70A 70A



S 7·5 40L | S 7·5 40L | 140A. | S 15. 80L. | S 35. 200L. | S 55. 200L

PL 13

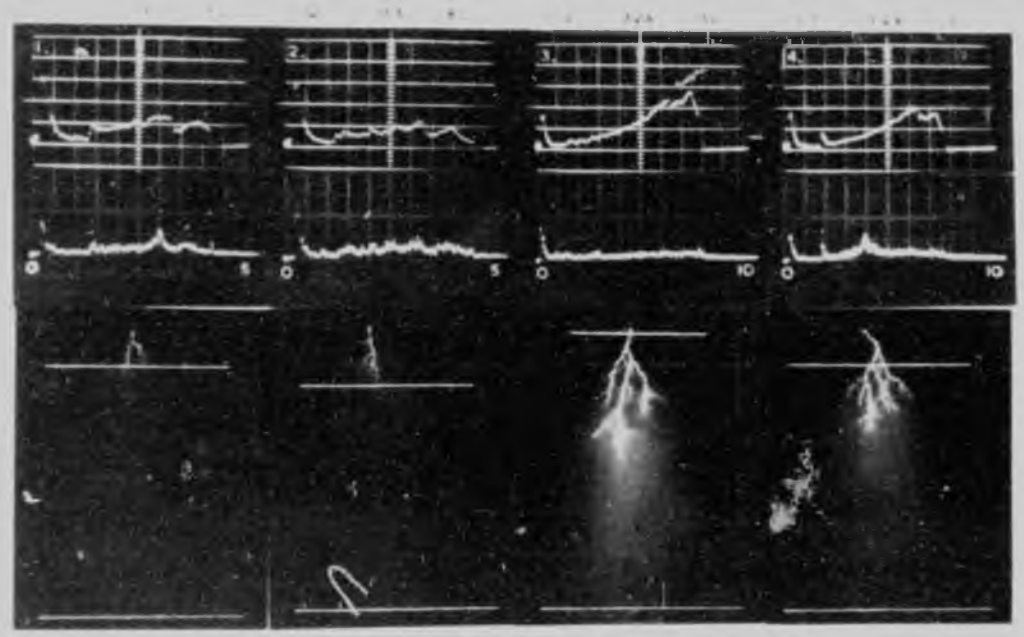
G 20. POSITIVE BREAKDOWN. + 150 KV. 3 μSEC RISE 1/2" SPHERE-PLANE

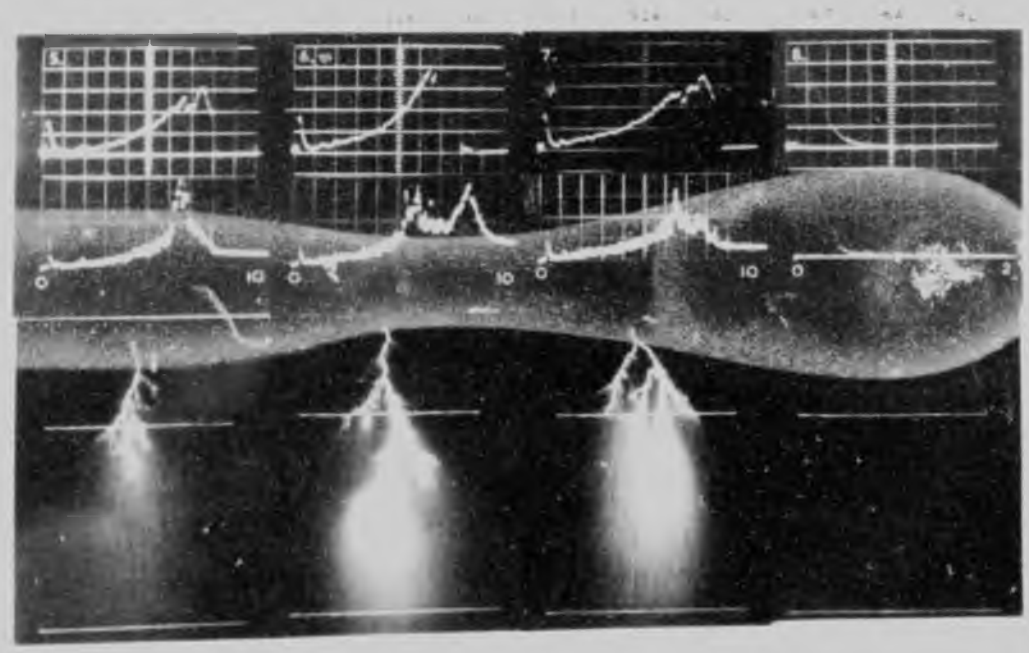




PL 14

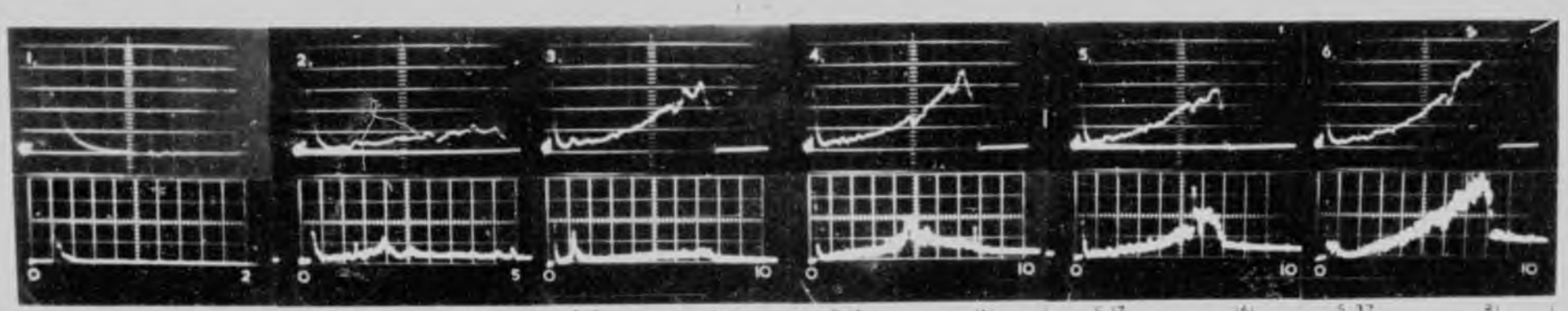
POSITIVE BREAKDOWN +300 KV .25 μSEC RISE 2" SPHERE - PLANE





RESIDUAL BREAKDOWN + 300 KV ·25 μSEC RISE 2" SPHERE PLANE

G 57.



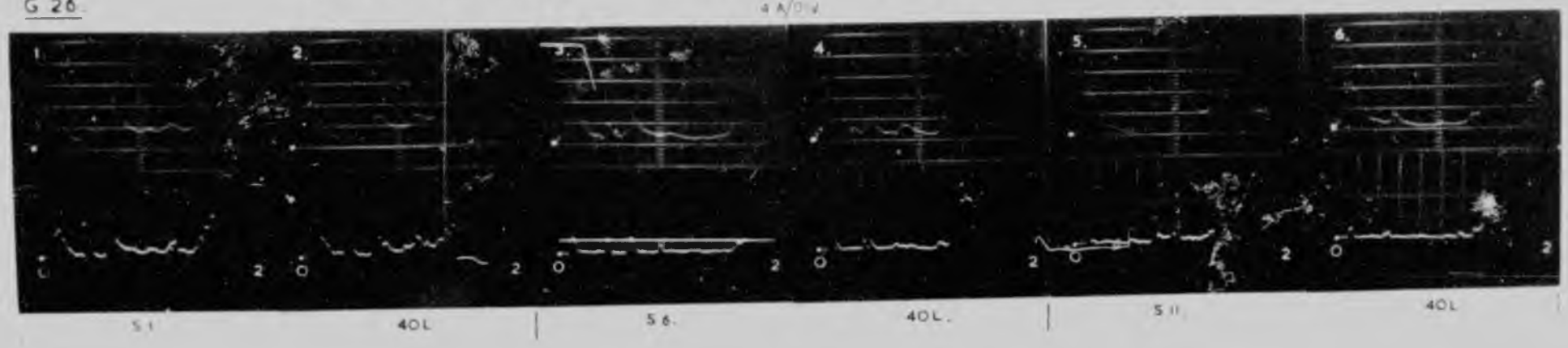


PL 16

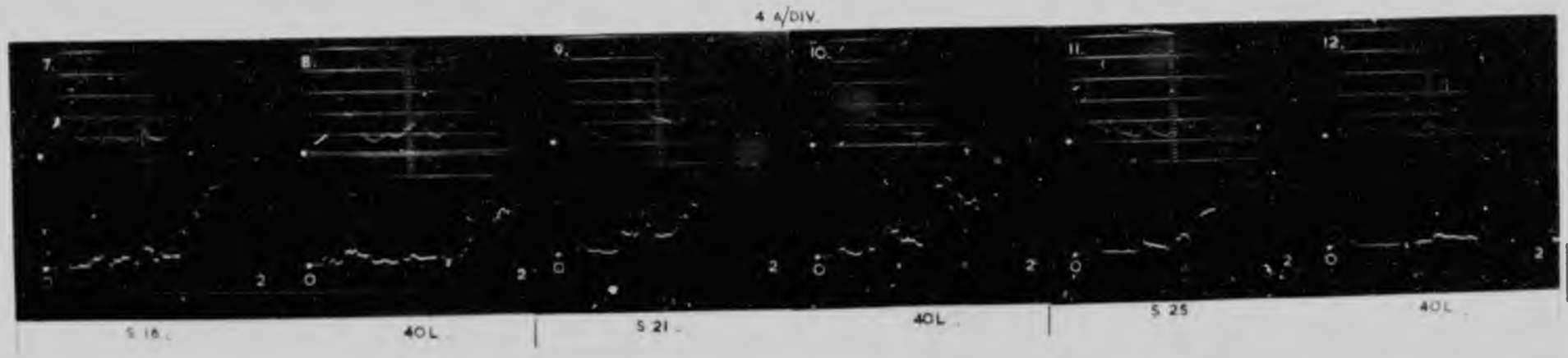
G 26.

NEGATIVE BREAKDOWN. — 300 KV. ·25 μSEC RISE. 2" SPHERE–PLANE.

4 A/DIV.



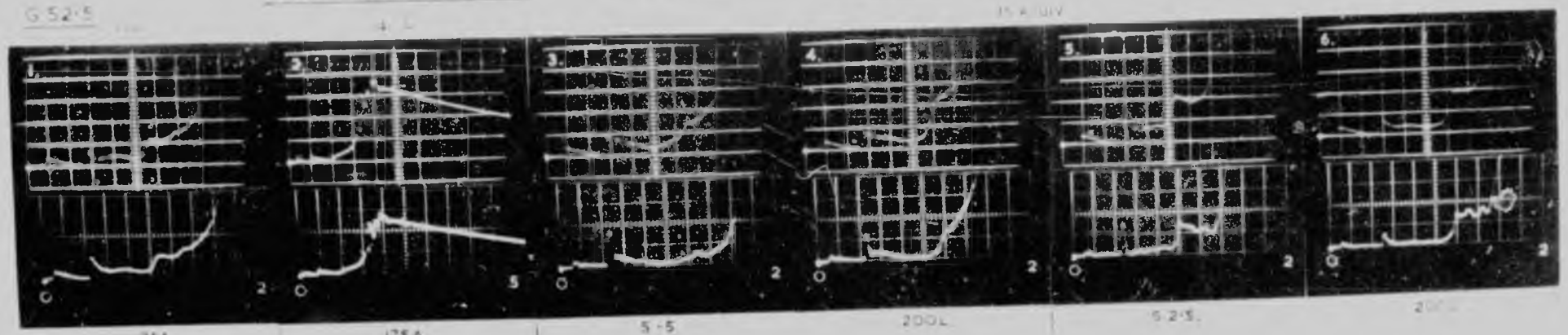
4 A/DIV.



PL 17

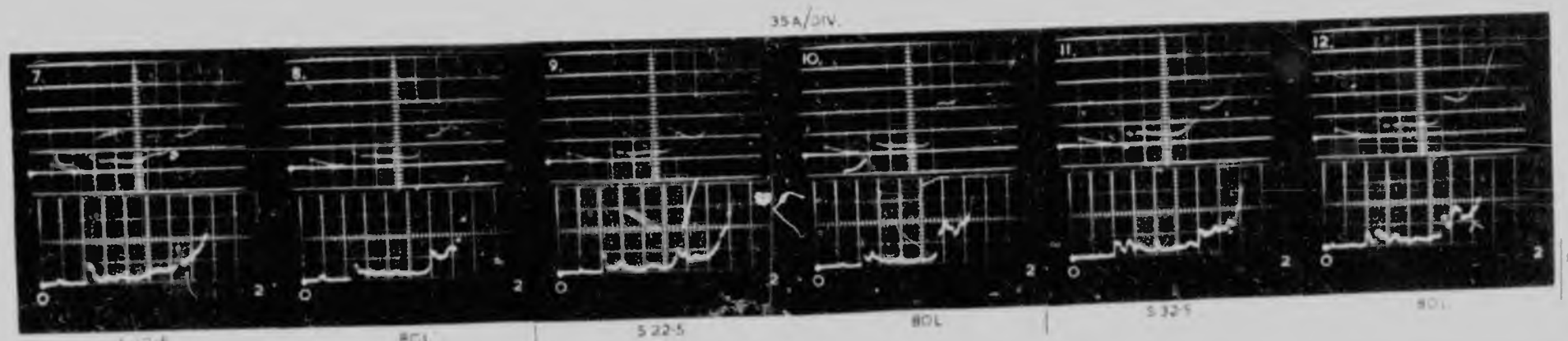
NEGATIVE BREAKDOWN — 600 KV ·25 μSEC RISE. 2" SPHERE – PLANE. (S)

G 52·5



35A 175A 5·5 200L 5 2·5 200

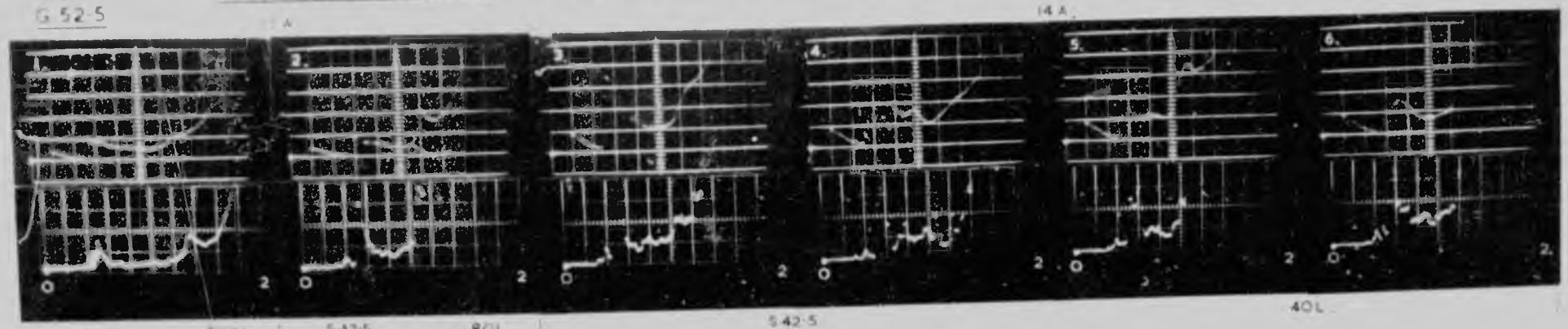
35A/DIV.

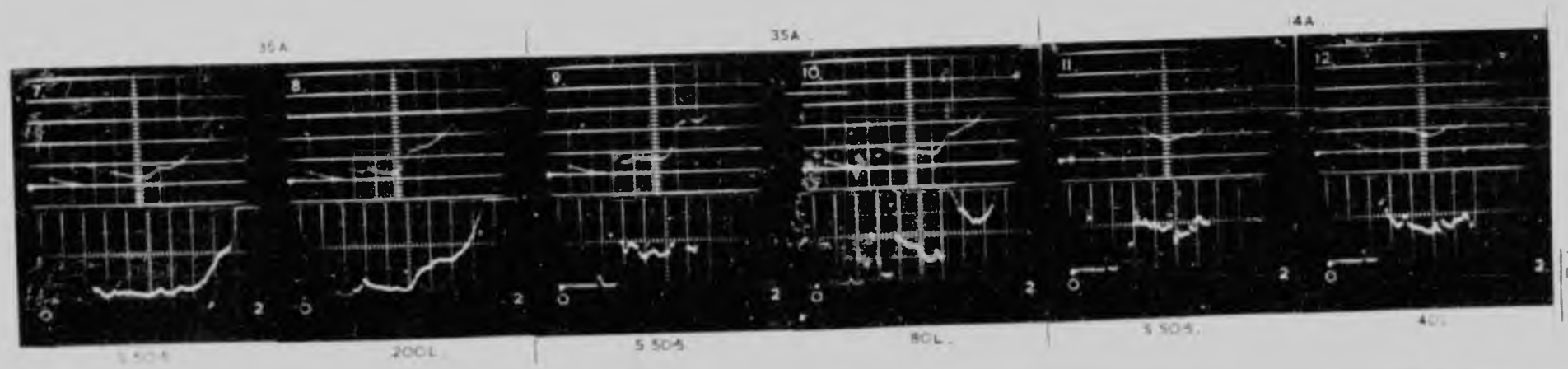


5 12·5 80L 5 22·5 80L 5 32·5 80L

P. 8

NEGATIVE BREAKDOWN — 600 KV .25 μSEC RISE 2" SPHERE — PLANE (S).

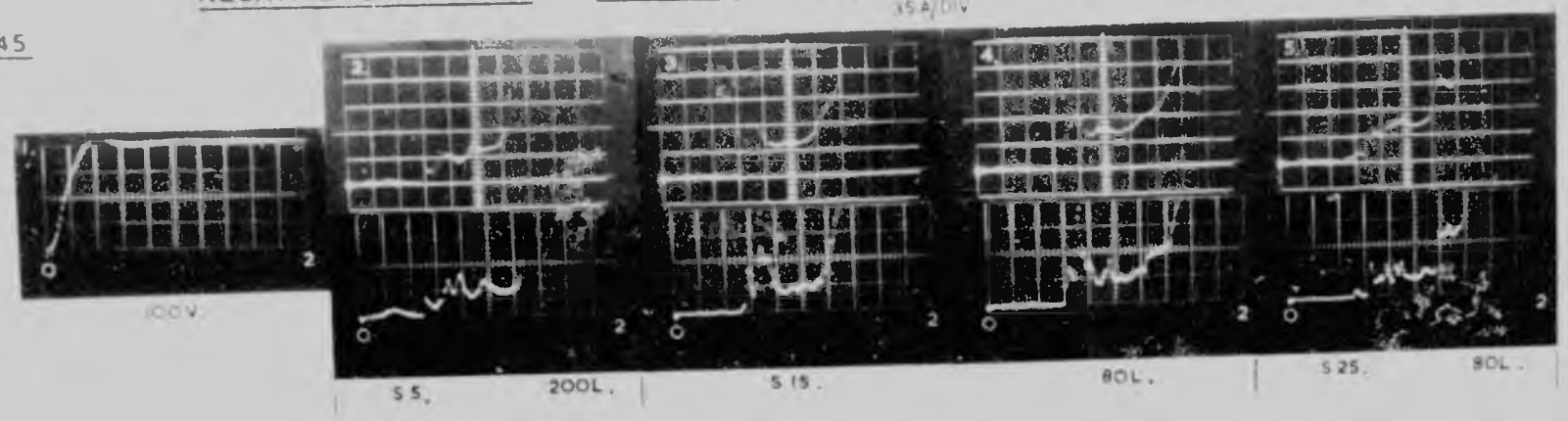


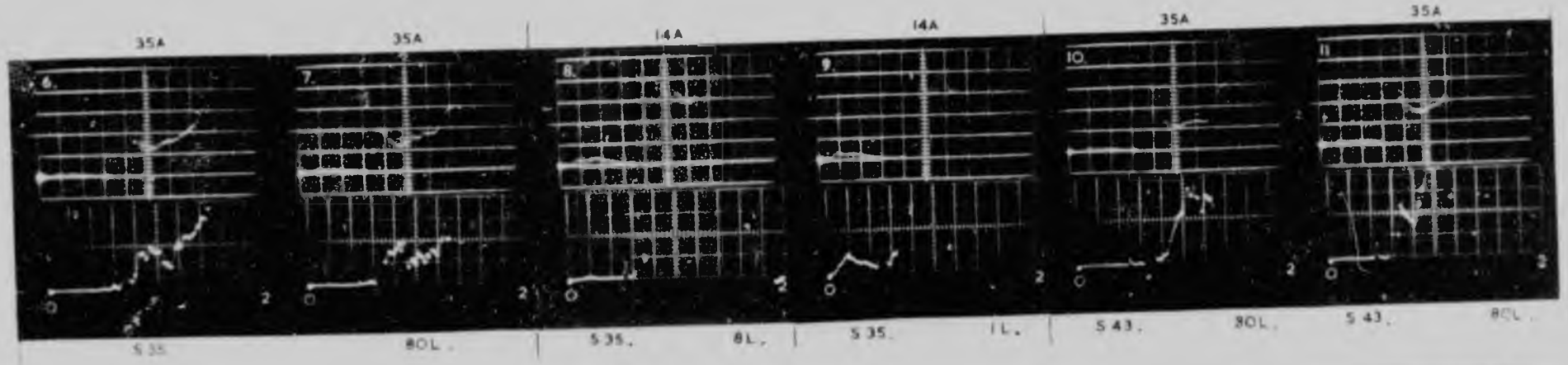


PL 19

NEGATIVE BREAKDOWN. — 600 KV. ·25 μSEC RISE. ½ SPHERE – PLANE (S).

G 45

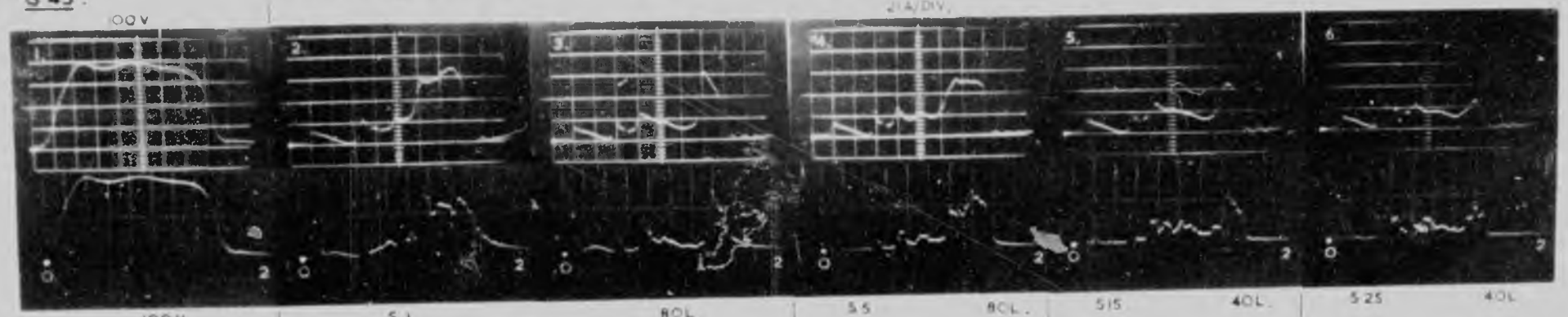




PL. 20.

G 45.

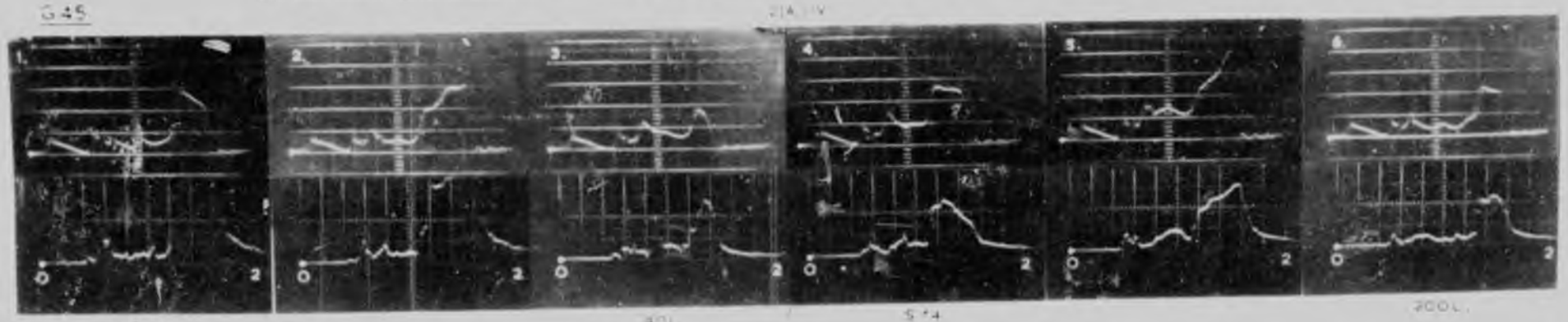
NEGATIVE BREAKDOWN. — 600KV. ·25 μSEC RISE 2" SPHERE — PLANE (S)

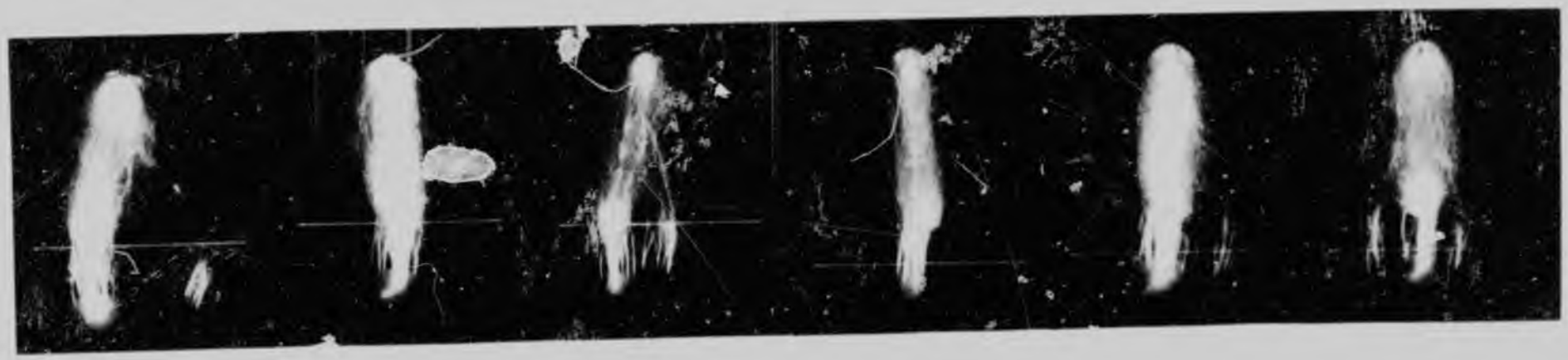




PL 21

NEGATIVE BREAKDOWN — 600 KV. ·25 μSEC RISE 2" SPHERE — PLANE (S)





PL 22

Author Kritzinger Johan Jacob
Name of thesis The Breadown Mechanism of long sparks in air 1960

PUBLISHER:
University of the Witwatersrand, Johannesburg
©2013

LEGAL NOTICES:

Copyright Notice: All materials on the University of the Witwatersrand, Johannesburg Library website are protected by South African copyright law and may not be distributed, transmitted, displayed, or otherwise published in any format, without the prior written permission of the copyright owner.

Disclaimer and Terms of Use: Provided that you maintain all copyright and other notices contained therein, you may download material (one machine readable copy and one print copy per page) for your personal and/or educational non-commercial use only.

The University of the Witwatersrand, Johannesburg, is not responsible for any errors or omissions and excludes any and all liability for any errors in or omissions from the information on the Library website.